Optimizing Infrastructure Resilience under Budgetary Constraint

By

Mohammad Najarian

A dissertation submitted to

the Department of Industrial Engineering

in partial fulfillment of the requirements for the degree of

Doctor of Philosophy

in Industrial Engineering

Chair of Committee: Gino J. Lim

Committee Member: Qianmei Feng

Committee Member: Ying Lin

Committee Member: Cumaraswamy Vipulanandan

Committee Member: Yunpeng Zhang

University of Houston

May 2020

DEDICATION

This dissertation is dedicated to my family for their unyielding love, support, and encouragement.

ACKNOWLEDGEMENT

I would like to thank many people who helped me to accomplish this research. Dr. Lim my advisor. I am thankful to Maryam Torabbeigi, Zahed Shahmoradi, and Arsalan Gharaveis who were a big help during my research. I would like to thank my parents, brothers, and sisters who supported me during my education. I also place on record, my sense of gratitude to all who, directly or indirectly, have lent their helping hand in this venture.

ABSTRACT

Natural and manmade disasters are low-probability, high-impact adverse events that incur extravagant cost and hardship on society. One way to mitigate the impact of these unfavorable events is to enhance the resilience of the system. Resilience is defined as the ability of a system to reduce the impact of an event and return it to its initial state in minimal time. The primary objective of this study is to develop methods for enhancing system resilience. To accomplish this goal, this study addresses: i) a quantification method for measuring resilience; ii) the suitability assessment of the developed resilience metric for various systems; iii) an optimization model for allocating a limited budget to components of a system to maximize improvement of the resilience; and iv) under the budget constraint, an optimal selection of multiple components of a system to minimize the total impact when those components are compromised.

The resilience metric (RM) is a quantitative measure that can help evaluate the effectiveness of investments on resilience enhancement. A good RM highlights the characteristics indicated in the associated resilience framework. We propose a new resilience metric and a methodology based on analysis of variance and experimental design to assess the suitability of a resilience metric. The numerical results show that our proposed metric performs better for a general system than the existing metrics found in the literature. In our metric, the three abilities of a resilient system (absorbability, adaptability, and rapid recovery) are statistically significant, whereas other metrics either lack one of these abilities or the importance of one ability is entirely neglected.

The proposed RM is used to formulate a mathematical programming model to maximize the resiliency of a system by allocating a limited budget to the system's components. Utility curves are introduced to build alternative component enhancement options that link between the cost of resilience improvement and the effect on the component functionality. Resilience-based component importance is then utilized to map the functionality of the component onto the functionality of the system. This approach provides insights as to which component needs to be enhanced and how much budget is required to do so.

To enhance the resilience of a network system, it is also essential to predict the potential action of the adversarial attacks on the network. This can be solved through the problem of finding a predetermined number of arcs whose failure have the highest impact on system functionality. This problem is computationally intensive; thus, we provide a mixed-integer formulation and a heuristic for initialization strategy to reduce the computational cost.

TABLE OF CONTENTS

LIST OF TABLES

LIST OF FIGURES

CHAPTER 1

I. INTRODUCTION

1.1. Background and Motivation

Society depends on infrastructures in order to maintain stability and regulate political, economic, and social issues and events. These infrastructures include electrical, water and wastewater, natural gas, transportation, banking and finance, railways, airways, telecommunication, etc. If these systems were to not function properly, major costs could be incurred, and lives could be endangered. Unfavorable events may disrupt these systems from being able to operate at an optimal level. An example of this can be seen from one of the most severe natural disasters Japan has ever seen, the magnitude-9.0 earthquake and accompanying tsunami that imposed $235 billion in repairs and restorations, as well as the 28,000 fatalities it caused. Another event was the September 11th terrorist attacks on the Twin Towers that resulted in 2,996 deaths and $10 billion just in infrastructure and building damage [1]. Adverse events effecting societal infrastructures are not limited exclusively to disasters imposed on physical systems. Cyber-physical attacks can exploit the vulnerabilities of the cyber side of systems in order to disrupt them. During the Cold War, Soviet Union used a software that was infected with a trojan horse to operate the pumps, turbines, and valves of their Siberian natural gas pipelines [2]. In 1982, this trojan horse caused an explosion which had a huge economic impact and other geopolitical consequences. Not all the manmade disasters are terroristic, some may be unintentional. The 2010 Deepwater Horizon oil spill, caused by an inadvertent explosion, resulted in

environmental destruction, health problems, severe regional economic damage, and inevitably caused $3.12 billion in damages.

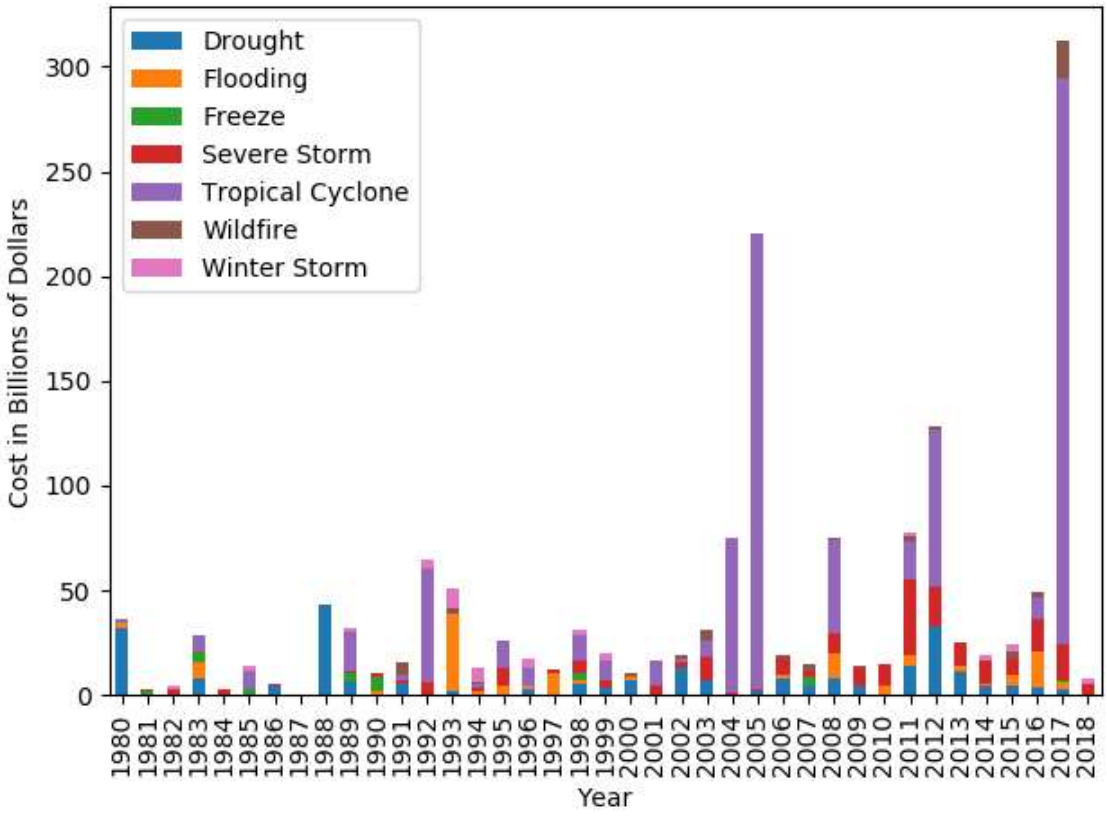

Figure I.1: Cost of billion-dollar natural disasters by year (CPI-Adjusted) [3]

Figure I.1 shows the annual cost of natural disasters in United States from 1980 to 2018. An immediate observation is that there seems to be no discernable pattern in the data, and, therefore, it doesn't seem feasible to be able to forecast the effect of these events in advance. In other words, these events are essentially unpredictable and unavoidable. Another common characteristic of these events is that, after disruption, it takes a long time for the system to recover. Seven years after Japan's 2011 Fukushima Daiichi nuclear disaster, there are still extravagant costs that are being incurred [4]. In December of 2016 the government of Japan estimated that the costs associated with decontamination,

compensation, decommissioning, and radioactive waste storage amounted to $187 billion. The 2017 hurricane Maria that devastated Dominica, St Croix, and Puerto Rico was another event that was accompanied by a long recovery period, in which one month after the hurricane, 85% of Puerto Rico still suffered from electrical outage. Two-and-a-half months after the disaster, only 53% of the population had electrical power.

These unfavorable events are inevitable; preventive strategies may not stop them from happening. But their consequences can be alleviated. There are several concepts that researchers and practitioners use to deal with these events. While these concepts are not mutually exclusive, they represent distinct conditions and situations.

Risk is the possibility of an undesired event and its associated loss [5]. Risk models (e.g., Kaplan model and Pressure and release model) consider the risk scenario, likelihood probability distribution function (PDF), and consequence of the risk. *Reliability* is the ability of a system or component to function under some previously stated conditions (operational and environmental) for a specified period of time [6], [7]. *Maintainability,* expressed as Mean Time to Repair (MTTR), is the ability of an item, under certain stated conditions of use, to be retained in, or restored to, a state in which it can perform its required function(s). This pertains to when maintenance is performed under the stated conditions, as well as to using prescribed procedures and resources. *Availability* is the probability that a system is available for use at a given time and is a function of reliability and maintainability. *Robustness* is the ability of a system to cope with a given set of disturbances and maintain its functionality [5]. *Stability* is the ability of a system to withstand long-term disruptions and continue its critical operations [8]. *Survivability* is the ability of a system to minimize the impact of a finite disturbance on value delivery to

alleviate the consequences of unfavorable events [9]. *Redundancy* is the extent to which other systems can replace the functionality or performance of another system without significant loss of either aspect [10]. *Resourcefulness* is the ability to identify and prioritize problems and to initiate solutions by identifying and monitoring all resources, including economic, technical, and social information.

These concepts are don't fully allow a way to study a system and improve it to reduce the negative impact of extreme events. Reliability only deals with a set of defined situations, which excludes some extreme event. Robustness considers the ability of a system at the time of a predetermined shock and it does not take in account recovery from the disaster. Risk does not consider the recovery time and it assumes a probability for the occurrence of an event. To cover these deficiencies, the concept of resiliency has been developed.

1.2. Resilience definition

Resilience (or *resiliency*comes from the Latin word "*resiliō*", which refers to the ability of an object to rebound or return to its original state after being stressed (e.g., bent, compressed, stretched, etc.). In 1973, Holling [11] noted the characteristics of a resilient ecological system to be bouncing back from a distress. Some years later the term resilience was described as a property of timber and used to explain why some types of wood were able to accommodate sudden and severe loads without breaking [12]. Gunderson et al. [13] recognized absorption as a characteristic of resiliency.

Researchers from different disciplines have proposed different definitions for resilience. However, a unified definition of resilience is still a work-in-progress. Below,

Table 1-1 summarizes definitions in different disciplines. All of these definitions maintain the idea of a system being able to reduce negative impact and rapidly recover to an acceptable estate.

Table I-1: Resilience definitions

Discipline	Definition of resilience
Dictionary	The power or ability to return to the original form, position, etc., after being bent, compressed, or stretched; elasticity. Resiliency is a quality in objects to hold or recover their shape, or in people to stay intact. This is a kind of strength [14]
Infrastructure Systems	The ability to reduce the magnitude and duration of disturbances. It depends on infrastructure and the system's ability to predict, absorb and adapt to disturbances and systems recover rapidly [15].
Economic Systems	The response to hazards that enables people and communities to avoid some economic losses at micro—macro market levels. It is the capacity for the enterprise to survive and adapt following market or environmental shocks [16].
Social Systems	The ability of a community to withstand stresses and disturbances caused by social, political and economic changes [17].
Organizational Systems	The ability of an organization to identify risks and to handle perturbations that affect its competencies, strategies and coordination [18].
Ecology	resilience determines the persistence of relationships within a system and is a measure of the ability of these systems to absorb change state variable, driving variables, and parameters and still persist [19].

As we mentioned earlier, there are overlapping concepts that may be confused with resilience. Figure I.2 illustrates the similarity and differences between resiliency and concepts of reliability, risk, and robustness:

Figure I.2: Overlapping concepts

Reliability vs resilience: Chandra et al. [20] sum up the differences between reliability and resiliency for a power grid. Resiliency is measured in response to an unfavorable event affecting the system, but reliability is measured generally in frequency, time, and duration of outage. Resilience may be computed before or after an event, however, reliability usually is computed over a certain time period. There are well defined measures for reliability, however there are no well-defined measures for resilience.

Risk vs. Resilience: Risk is the possibility of an undesired event and its associated loss [5]. There are two important models for risk analysis. The first model is Kaplan [21], which includes the risk scenario, likelihood PDF, and consequence of the risk. Given a set of possible hazards, risk is defined as

$$Risk_i = \{< S_i, f_i(\varsigma_i),\ g_i(\xi_i) >\},\ i = 1,2,\ \ldots$$

in which, ς is the hazard, ξ is the system capacity, S_i is the risk scenario i, $f_i(\varsigma_i)$ is the likelihood PDF of hazard i, and $g_i(\xi_i)$ is the consequence of the hazard i. The second risk model is pressure and release [22] which is defined as

$$Risk_i = f(\varsigma|i) \times g(\xi|i) \times Severity,$$

where, $(\varsigma|i) \times g(\xi|i)$ is the vulnerability for hazard i, $f(\varsigma|i)$ is the hazard potential impact ς relative to hazard i and $g(\xi|i)$ is the system capacity ξ relative to hazard i. An important difference between resilience and risk is that, unlike risk assessment, the probability of a disturbance is not a crucial factor in resilience.

Robustness vs. Resilience: Robustness has a lot in common with resilience and many papers [23] consider it as an important characteristic of a resilient system. However, robustness considers the strength of the system to withstand the degradation of the system's functionality, while resilience requires flexibility, adaptability, and agility on top of that. In robustness we know the threat and its impact, but in resilience the event is unprecedented.

These contrasts indicate that, while each concept is useful for applications, they cannot replace the resilience. In this dissertation we study the resilience of a system and how we can improve it.

1.3. Problem Description

Adverse events are unavoidable; however, their impact can be reduced by enhancing the resilience of the system. The widely used definition of system resilience is "the system's ability to prepare, absorb, adapt, and rapidly recover from a low-probability, high-

impact event" [24]. The primary objective of this dissertation is to provide decision makers with tools that enable them to get insight into the resilience level of a system and resilience enhancement. For this purpose, at first, a metric is developed to measure the resilience level of the system. Then, using this metric, a mathematical programming problem is formulated to maximize the resilience of the system for a given budget, the multi-arc disruption is utilized to find the vulnerable arcs, and finally, the resilience of interdependent natural gas and power systems is studied.

This dissertation will study how to quantitatively measure resilience of a system, which includes a method to develop a valid resilience metric. Having a quantitative metric is necessary to develop tools for improving system resilience. The first step is to define resilience, then develop the resilience metric, and finally assess the validity of resilience metric.

1.3.1. Resilience Quantification

Resilience quantification helps us to identify, justify, and prioritize any need for improvement, monitor changes, evaluate the effectiveness of the resilience strategies, or compare the cost-effective benefits of increasing resilience. Hosseini et al. [24] reviewed the resilience metrics and categorized them into two major groups by several criteria (Figure 1.3) . Qualitative metrics include conceptual frameworks and semi-quantitative indices. Conceptual frameworks describe the characteristics (e.g., redundancy, resourcefulness) of a resilient system, whereas semi-quantitative indices provide a subjective Likert scale (0-10) to different resilience-based system characteristics [24]. Quantitative metrics provide a quantitative means to assess resilience by measuring

performance of system, regardless of the structure of system. A quantitative metric is built on top of a conceptual frame work and provides a measure of the level to which a system has the resilience characteristics that are determined in the conceptual framework. A quantitative metric that can capture the stochasticity associated with system behavior is said to be *probabilistic* metric. Moreover, a *dynamic metric* accounts for time-dependent behavior [24]. There are metrics for specific systems that are categorized as *structural-based models.* They examine how the structure of a system impacts its resilience. In such methods, system behavior must be observed, and characteristics of a system must be modeled or simulated.

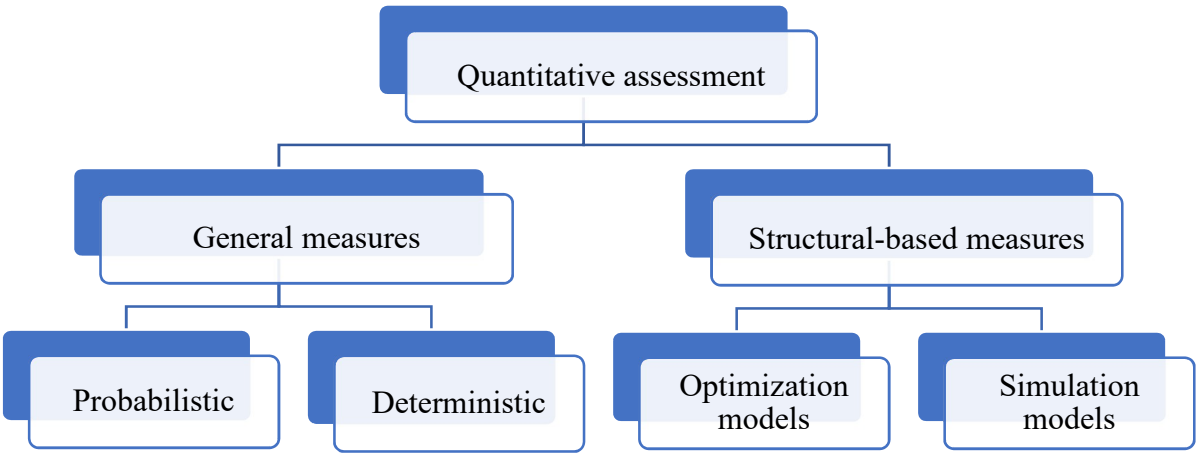

Figure I.3: Classification scheme of resilience assessment methodologies

Performance [25], [26] or functionality [27], [28] of a system refers to the requirements or objectives [25] of the system under study that indicates how well the system fulfills its intended goals [29]. It is measured as a dimensionless (percentage) function of time [27] which can be constant or vary with time [30]. For example, functionality of a natural gas network can be the combination of the normalized gas flow rate and the total length of the network [31]. For a power system, functionality can be the

percentage of energized transmission substations, critical facilities with power, or customers with power [26]. Choosing a performance or functionality depends on the system under study and the management need. General categories of performance measures used in metrics are technical, organizational, and economic. Technical metrics evaluate the behavior of technologies and of technology-dependent mission/business processes (e.g., cyber defense processes). Organizational metrics evaluate organizational processes for resilience. Economic metrics focus on the potential cost.

1.3.2. Resilience Metric Assessment

Several resilience metrics have been introduced in the literature, but the problem is how to choose the best metric for a general system. Unlike a well-defined concept like reliability, there is no agreement on the resilience measures [24]. Hence, we developed a methodology that uses experimental design to assess the quality of a resilience metric.

An experiment is an exercise designed to determine the effects of one or more variables (factors) on one or more characteristics (response variables) of some well-defined system (experimental unit) [32]. In our problem the experiment is measuring resilience. A treatment is a combination of factors at a specific level [32]. Experimental design concerns the validity and efficiency of the experiment [33]. A design includes, but is not limited to, factors to be included, their levels, the treatments for which the experiment should be run, the order which the treatments are run, randomized or non-randomized, replication, and blocking. The choice of an experimental design depends on the objective. For example, in a pharmaceutical factory, the variety screening trial does not need much replication to maximize accession number while variety release trial needs appropriate replication for a

high precision. After the design, we simulated the data for each treatment and analyzed them using analysis of variance (ANOVA) to determine which factors influence the response and which do not.

1.3.3. Investment Optimization

Resilience enhancement activities aim at mitigating the negative effect of adverse events. The extravagant cost and consequences of these events make investment on enhancing system resilience justifiable and appealing. But the resources are limited, and system wide hardening is not feasible; hence , the budget must be carefully allotted to maximize the effectiveness of the investments. As the complexity of the system increases, it becomes more difficult to decide which components to enhance. In the component importance approach [34], the influence of particular components on the overall resilience of the system is measured and the components with highest importance are enhanced. However, this method may not necessarily be optimal because as a result of component interactions, a less important component may have a higher effect on the resilience of the system than a more important component. Absorption and rapid recovery (Figure 1.4) are the two main capabilities of a component that we consider enhancing in this research. If the current absorption of a component is 60%, it means that after an adverse event the component functions at 60% of its normal functionality. A 20% improvement in the absorption means that the system will be improved to 80% of normal functionality. Time to recovery, *T*, is measured by unit of time. A 20% improvement in time to recovery means that the new time to recovery will be (1-20%)×T. Given the amount allocated to a

component, we may have different options to improve the absorbability or time to recovery (Figure I.5).

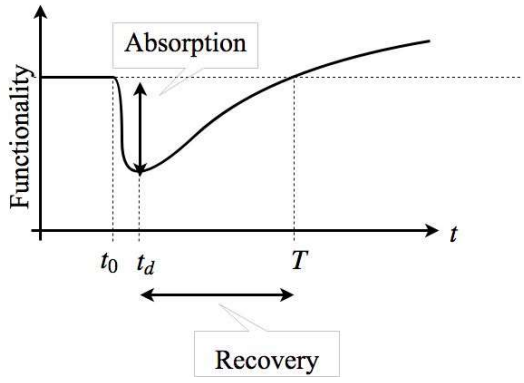

Figure I.4 Absorption and recovery capabilities

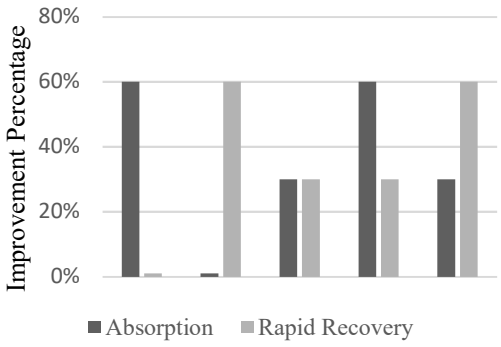

Figure I.5: Component improvement options

We formulate a mathematical programming model that maximizes the resilience of the system for a given budget. This model determines the amount that should be spent on each component and the aspects (absorption and time-to-recovery) of the component that must be enhanced within the allotted budget. For a system with three components, Figure I.6 shows the percentage of budget that is to be assigned to each of them. The first component receives 45% of the budget. Blue and green colors indicate the individual component absorption and time to recovery, respectively. So, for this component, there is more emphasis on reducing the recovery time than increasing the absorption.

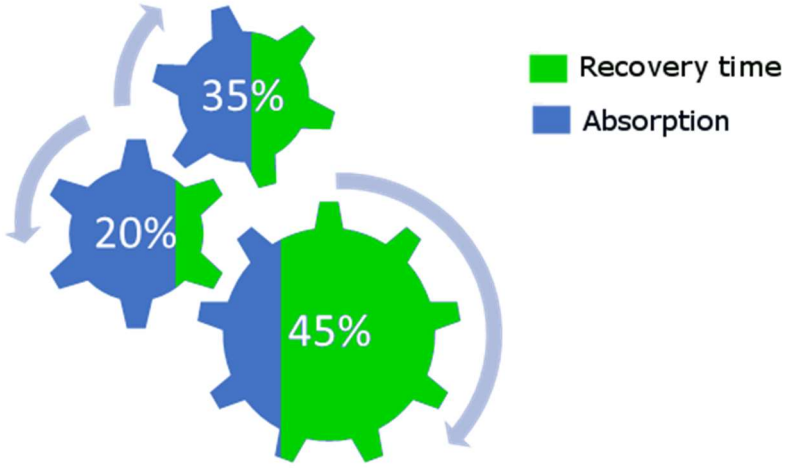

Figure I.6: Percent budget allocation and absorption and recovery options

1.3.4. Multiple-Arc Failure with Maximum Impact

In order to reduce the output of an adversary network, a limited budget is assigned to disrupt a predetermined number of network arcs. The multi-arc failure with maximum disruption problem (MADP) tries to find arcs in a way that the impact on the network flow is the most. The MADP problem has another application which is finding the arcs that are of interest of terrorists and try to protect them or change the network structure to make it more resilient.

1.3.5. Resilience of Interdependent Infrastructures

Infrastructures are interdependent, and, during and after an adverse event, cascading effects compound to the gravity of the consequences. So, the interdependence of potentially vulnerable infrastructures under disruption should be carefully considered for resilience enhancement activities. The critical infrastructures are complex systems and it is not easy to formulate interdependence in a single model. This dissertation introduces an applicable

statistical method to investigate the impact of the resilience of an infrastructure on the resilience of another infrastructure. Natural gas is a major resource for electricity generation and, at the time of a disaster, a disruption in natural gas system can affect the input to the gas fired generators. As a result, the functionality of a power system depends not only on itself, but also on the resilience of the natural gas system. The approach of finding the statistical significance of the natural gas system resilience on the power system resilience can be applied to other systems, including cyber-physical systems.

1.4. Contributions

This dissertation is directed towards resilience enhancement of cyber-physical systems. It addresses three main problems of resilience level evaluation, budget assignment, and vulnerability detection. We present a new methodology to check the consistency of resilience metrics with their underlying framework (the validity of the metric). One of the shortcomings of existing metrics is that they cannot evaluate the resilience of a system, as the underlying conceptual framework suggests, as they intended. We propose a new metric that covers this gap. We also investigate the impact of resilience of an infrastructure on another infrastructure.

Due to the complexity of the system, it is not easy to find the collective effect of investment on the components on system resilience. We introduce a method to tackle this complexity buy incorporating the component importance and mapping the component's functionality to system functionality. In our approach a new formulation is presented that maximizes system resilience under budgetary constraint. We introduce utility function into component enhancement, and a resilience-based component importance to map between

an individual component functionality and system functionality. The proposed method considers a set of possible events, their effects on the component functionality, and the component's enhancement alternatives. The alternatives employ a utility function to construct the set of alternatives for component enhancement. In the final step of the method, a mathematical programming model is introduced that maximizes the system resilience for a given budget.

The problem of finding multiple arc whose disruption has the maximum impact on the network is known to be computationally intensive. To tackle this problem, we introduce a heuristic that finds an initial solution for warm start. For this heuristic, a new betweenness centrality metric is introduced. This initial solution reduces the computation time drastically. Moreover, a pattern generation algorithm is introduced that solves the problem in a shorter time with an objective close to optimal objective.

1.5. Outcomes

Journal Publications

- M. Najjarian and G. J. Lim, "Design and assessment methodology for system resilience metrics," Risk Analysis, 39(9), pp1885-1898, September 2019
- M. Najarian and G. J. Lim, Optimizing Infrastructure Resilience under Budgetary Constraint, *Reliability Engineering and System Safety* (198), June 2020.
- M. Najarian, G. J. Lim, and M. Barati, Levelized Resiliency Assessment of Interdependent Natural Gas and Electric Power Systems, *Proceedings of the 2018 IISE Annual Conference*, May 2018.
- M. Najarian and G. J. Lim, Multiple-Arc Failure with maximum Impact on Network Flow.

Conference Presentation

- M. Najarian, G. J. Lim, and M. Barati, Resilience Assessment of Interdependent Gas Network and Electrical Power System Infrastructures: A Quantitative Approach. *2017 INFORMS Annual Meeting*, October 22-25, 2017.

- M. Najarian, G. J. Lim, and M. Barati, Levelized Resiliency Assessment of Interdependent Natural Gas and Electric Power Systems, *IISE Annual Conference and Expo 2018*, May 19-22, 2018.

- M. Najarian, G. J. Lim, A Methodology for Infrastructure Resilience Metric Assessment, *2018 INFORMS Annual Meeting*, November 4-7, 2018.

- M. Najarian, G. J. Lim, A Flow-Based Network Resilience Metric, *2019 INFORMS Annual Meeting*, October 20-23, 2019.

1.6. Organization

The remainder of this dissertation is organized as follows. Chapter 2 reviews the relevant literature on resilience measurement, budget allocation, and interdependency. In Chapter 3, the proposed methodology is presented to assess a resilience metric followed by newly proposed resilience metric. The proposed metric is compared to other existing metrics. Chapter 4 describes our mathematical programming model to optimize the system resilience within a given budget. In Chapter 5, a solution approach for the multi-arc failure with maximum impact on network flow is presented. In Chapter 6, an approach is suggested to measure the effect of the resilience of a system on the resilience of an interdependent system. We discuss conclusions and highlight future research directions in Chapter 7.

CHAPTER 2

II. LITERATURE REVIEW

In 2017, Hurricanes Harvey, Irma, and Maria happened within the short period of time from August to October. They affected the coastal and inner regions of Texas, Florida, and Puerto Rico, respectively. These three hurricanes were all Category 5 storms; however, each one affected the power system outages in Texas, Florida, and Puerto Rico in distinctly different ways (Figure II.1). The outages that occurred in Texas and Florida were at 2%, and were able to recover to their initial states in less than a month [35]. However, in Puerto Rico, the power outage was at 96%, and after one month, it only recovered by 22%. Even 8 months after Hurricane Maria, Puerto Rico's power system wasn't fully recovered, and the outage was around 10% [36].

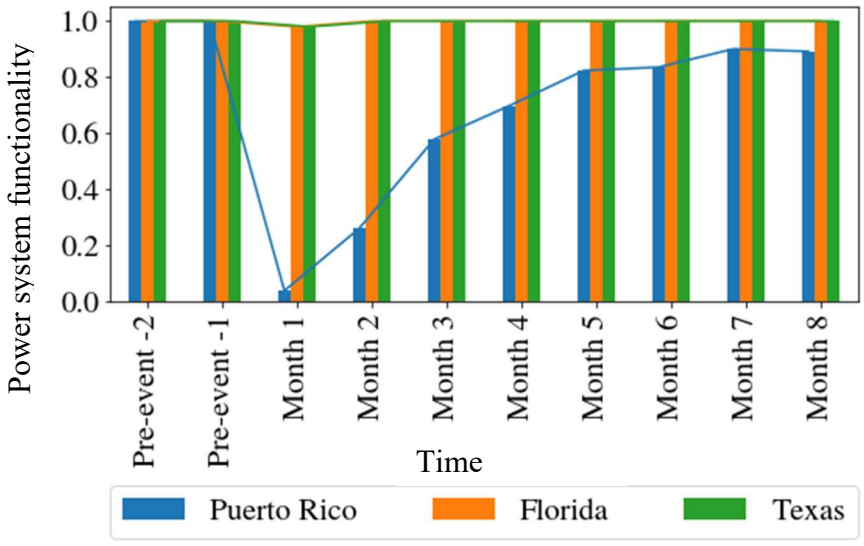

Figure II.1: Hurricanes Harvey, Irma, and Maria statistics [37]

The differences in how the power systems were affected in these three separate regions were caused by the differences in their power grid resilience levels. Resilience is

the ability to reduce the magnitude and duration of disturbances [24]. The level of resilience depends on the particular infrastructure involved and the system's ability to anticipate, absorb and adapt to disturbances, as well as rapidly recover to an acceptable and stable state [15], [25], [28], [38]–[42] (Figure II.2). *Anticipation* is the ability of the system to predict and prepare for a disruption; it is aimed at avoiding and withstanding potential disruption. The plans and designs in the anticipation phase can help to minimize potential impacts on availability, accessibility, affordability, and acceptability of the system output [24]. It may not be possible for a system and its associated components to evade disruption. However, a proper configuration system will allow for better *absorption,* which reduces the deterioration in a system's functionality and the cascading effects. *Adaptation* is the utilization of existing resources to increase the performance of the system shortly after disruption [24]. *Rapid recovery* is the ability of the system to respond to the event rapidly and reinstate all system operations and service availabilities to their pre-event capacity and efficiency [43]. Each of these capabilities can be improved upon through their specific set of principles. Resourcefulness, coordination, collaboration, and creativity can boost anticipation. Robustness, stability, flexibility, diversity, and efficiency can improve absorbability. Resourcefulness, coordination, and redundancy can increase the adaptation. Finally, agility, collaboration, flexibility, resourcefulness, and redundancy can reduce the recovery time [43].

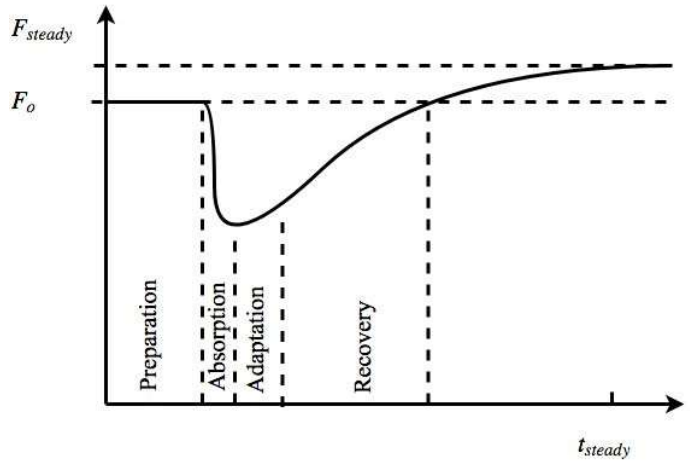

Figure II.2: Abilities of a resilient system

The resilience metric is a basic tool for the quantitative study and analysis of the system's resilience. It is used for identifying and prioritizing any need for improvement and evaluating the effectiveness of the resilience strategies [44]. Studies done on resilience-based component importance [34] and investment [45], [46] rely on resilience metrics. When a resilience metric is available, the resilience of the system can be assessed against baseline conditions, thresholds that reflect program objectives, principles of good resilience, or peers (benchmarking) [47]. Several metrics have been proposed in certain literature [24]. A structural-based metric is utilized to consider the impact of the system's structure on its resilience [24]. In contrast to a general metric, a structural-based metric can be used for the system it is developed for. To develop a general metric, functionality (performance) of the system should be measured. Performance of the system can vary based on the context and objective. For example, for a power network, performance can be the number of customers that are served [48], the load served [49], [50], or the time that system is up and running [51]. After developing a list of metrics, the next issue that should be addressed is how a particular metric – that is, the metric that fits the system under study - should be selected.

The National Mitigation Investment Strategy provides an approach to investments in mitigation activities and risk management across the United States for federal departments and agencies. These include state, territorial, tribal, and local governments (SLTTs) and private and non-profit sector entities such as businesses, philanthropies, foundations, universities, and other non-governmental organizations [52]. The investment decisions on cyber-physical systems, especially those with certain social impacts on critical infrastructures, can be viewed from political [53], social, environmental, economic, financial [54], and engineering prospects [53], [55]. One of the goals of the engineering prospect is to determine how to allocate the budget to specific components of the system in order to maximize the resilience.

An integrated risk-based decision support system is recommended to alert the utilities about the probable losses due to lack of investment [56]. To establish a relationship between structural features and performance, a link-node representation of water distribution is studied by network metrics. These metrics include link density, average node-degree, diameter, average path-length, clustering coefficient, meshed-ness coefficient, central-point dominance, density of articulation points, density of bridges spectral gap, and algebraic connectivity. Using these metrics, properties like redundancy and fault tolerance are quantified [55]. When a better tool is not available, a rapid risk analysis for a flood can be utilized to support risk-based investment prioritization at the community level [57]. In the planner-attacker-defender model presented in [58], small investments are made in switch installation to enhance resilience in response to an attack.

An important factor in investment decisions made regarding system resilience is the resource allocation. A resilience-based component importance (RCI) metric measures the

extent to which an individual component contributes to the resilience of the system [34], [59]–[61]. Using this measure, the components can be ranked based on their importance, and the budget is allocated in order of said importance. At the component level, the allocated budget is used to improve a combination of component absorption and recovery time factors. The collective enhancements in these individual components determine the change in the resilience of the system. Hence, at the time of resource allocation, a decision on component level enhancement should also be made.

When an adverse event happens (e.g., hurricane, cyber-physical attack, etc.), it can damage interdependent infrastructures. For example, gas-fired electricity generation plants rely on gas, and gas transmission pumps need electricity to pump gas through the transmission pipelines. An adverse event may disrupt the gas network, and, as a result, the gas-fired generators won't be able to produce electricity required. Therefore, the resiliency of the natural gas systems may, in turn, affect the resilience of the power system. Rinaldi et al. [62] highlight different types of interdependencies associated with urban infrastructure, including physical, cyber, and geographic. Two infrastructures are physically interdependent if the state of each one is dependent on the material output(s) of the other. Interdependence is cyber when the state of the infrastructure is dependent on the information transmitted through the communications infrastructure. In a geographical interdependence, a change of the local environment can create change in multiple systems. Dependencies and interdependencies can cause cascading or escalating effects [62]. A preparedness decision making framework is proposed in [16] to promote interdependent economic resilience estimation. A protection plan is formulated as a multi-objective model in [63] in which the protected nodes cannot be attacked. The objectives are to minimize the

maximum percentage of infected nodes, the cost of implementing the protection plan, and total time of the attack diffusion. The algorithm presented in [64] identifies vulnerabilities due to interdependencies in the current and proposed designs. A coupled model of natural gas and power systems is provided by [65] in which the relationship between profit and production in the electricity model is introduced into the objective function of the gas model, which minimizes the system's cost.

CHAPTER 3

III. DESIGN AND ASSESSMENT METHODOLOGY FOR SYSTEM RESILIENCE METRICS

3.1. Introduction

Natural or human-made disasters may impose costs, disrupt routine activities, and threaten human life. From 1980 to 2011, more than 130 extreme events resulted in 881 billion dollars in damages in the United States [66]. Hurricane Katrina caused 108 billion dollars and 1,833 fatalities in 2005.[67] Hurricane Harvey in 2017 and Sandy in 2012 cost $125 [68] and $70 billion [69], respectively. To improve understanding of unfavorable events and alleviate the resulting consequences, researchers and practitioners have developed several concepts such as risk, robustness, stability, survivability, and reliability. Risk is the possibility of an undesired event and its sequenced loss [70], robustness is the system's ability to tolerate short-term adverse conditions,[70] stability is the ability of a system to withstand long-term disruptions and continue its critical operations,[8] survivability is the ability of a system to minimize the impact of a finite disturbance on value delivery to alleviate the consequences of unfavorable events,[9] and reliability is the ability of a system or component to function under stated conditions (operational and environmental) for a specified period of time.[6], [7] However, in the face of the extreme events, like catastrophic hurricanes or earthquakes, some aspects are not covered by these concepts which led to the development of another concept: resilience.

Resilience (or resiliency) comes from the Latin word "*resiliō*," which means "to bounce" [71]. Disciplines like social systems [72], organizational systems,[18] economic systems [73], psychology [74], ecology[11], and engineering [75], [76] have been studying resilience. However, each discipline considers it from its point of view; hence, the definitions may vary. The common elements of resilience among them are disruption and returning to the normal situation. Compared to the other fields, not only the number of resilience studies in the realm of engineering are limited [24], but also there is not unanimity on its definition. We divided the literature review into two sections: 1) resilience conceptual framework that includes the studies on the concepts and fundamentals of resilient systems, and 2) resilience quantification which reviews the studies on the RMs.

3.1.1. Resilience Conceptual Framework

Theoretical frameworks mainly discuss the characteristics of a resilient system and steps to enhance the system's resilience. Hoffman and Nilchiani [10] characterized the disaster resilience's goals to include reduced failure probabilities, reduced consequences from failures, and reduced time-to-recovery. The resilience of a network is a multidimensional, dynamic concept [77] that addresses its ability to absorb and recover from an external, high-impact, low-probability event.[78] Both pre-disaster (preparedness) and post-disaster (recovery) activities are necessary for a resilient system [79].

Performance [25], [26] or functionality [27], [28] of a system refers to the requirements or objectives [25] of the system under study that indicates how well the system fulfills its intended goals [29]. It is measured as a dimensionless (percentage) function of time [27], [28]. For example, for a natural gas network it can be the combination

of the normalized gas flow rate and the total length of the network[31]. For a power system, it can be the percentage of energized transmission substations, the percentage of critical facilities with power, or the percentage of customers with power [26].

Four abilities of a resilient system are anticipation, absorption, adaptation, and rapid recovery [25], [28], [38]–[42], [80]. We merged the resilience profile from Francis and Bekera [38] and Ganin *et al*. [28] to obtain four phases as seen in Figure III.1. While the former does not assume separate phases for anticipation and absorption, the latter does not include the slack time (δ). *Anticipation* is tshe phase before anything happens ($t \leq t_o$) to the system while preparing for a hazard. This can include forecasting the adverse event, its severity, list of the components prone to failure, the plans for different scenarios, etc. In this phase, the functionality is in normal state (F_o). *Absorption* is the phase in which the system absorbs the impact of the hazard and reduces the severity of consequences when a disaster strikes the system ($t_o \leq t \leq t_d$). As a result, the system functionality drops to F_d. The value of F_d is closer to one as the system becomes more resilient. *Adaptation* is the phase after a disaster and just before the recovery phase ($t_d \leq t \leq t_r^*$). During this time, the system can utilize its current resources to improve the functionality of the system from F_d to F_r^*. This phase may include temporal repair, utilizing the redundant components, prioritizing and addressing the more critical demands. Francis and Bekera [38] assumed initial recovery actions that take place at slack time (t_δ) to improve the functionality to F_r^*. These initial recovery actions are not final and are prone to change by the next phase. The final phase is *recovery* ($t_r^* \leq t \leq T$) in which the system gradually returns to its initial state, or to a stable state. These phases are not mutually exclusive. For example, the recovery phase may start in the middle of adapt phase.

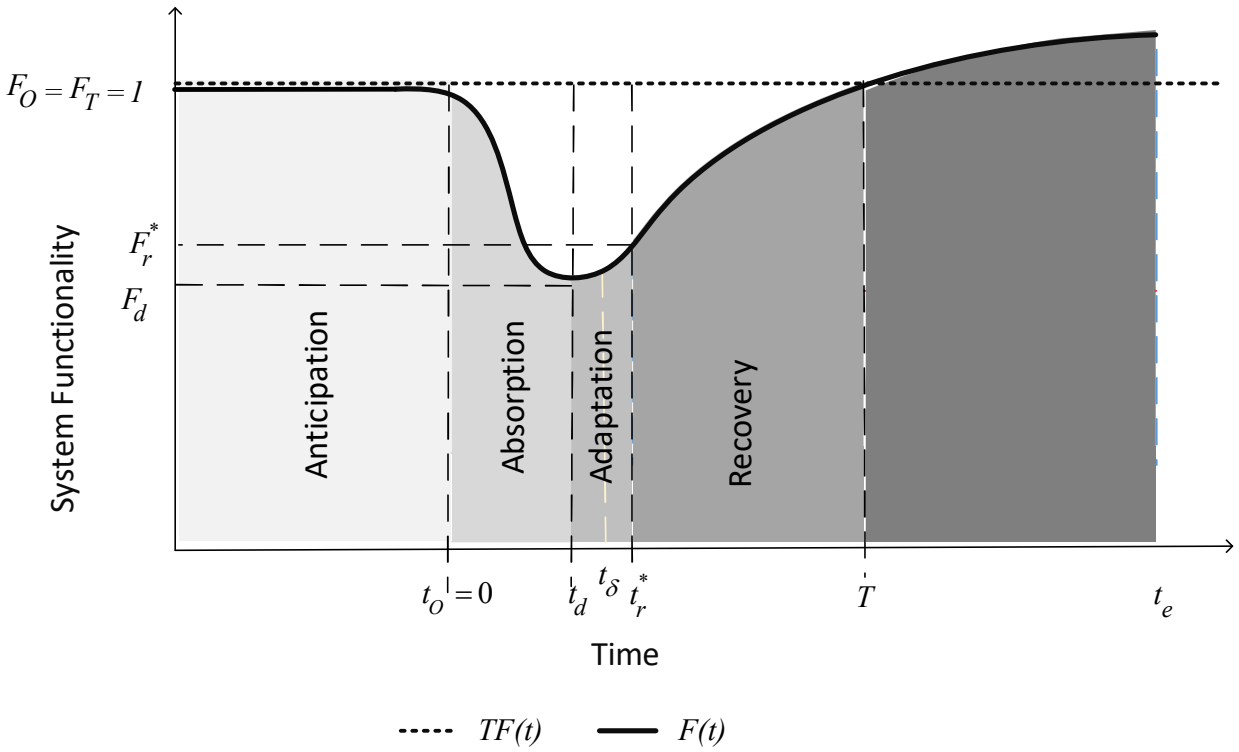

Figure III.1: Resilience functionality phases

3.1.2. Resilience Quantification

The extravagant cost of disasters justifies the investment to improve the system's resilience. Quantification is an essential tool to achieve this goal. This tool can be utilized to identify, justify, and prioritize any need for improvement [44]. Some other applications include monitoring changes in the resilience level, evaluating the effectiveness of the resilience strategies, or comparing the cost-effective benefits of improving resilience [44]. RMs must reflect the abilities of a resilient system, and thus must serve the following goals [81], [82]:

- To provide objective evaluations of the system's current state of resilience.

- To provide a mean for identification of potential infrastructure vulnerabilities.
- To enable the evaluation of the changes in the resilience resulted from of the resilience enhancement activities.

There are different approaches to assess resilience. Hosseini *et al*. [24] categorized the quantitative measures into two groups: general and structural. *General* measures can be applied to any domain. They include deterministic and probabilistic, and static and dynamic models. In contrast, *structural* based measures are domain-specific representations of the components of resilience. Optimization, simulation, and fuzzy logic models are utilized in these models.

Willis and Loa [83] classified the metrics by three characteristics: resolution, type, and maturity. *Resolution* refers to the scale of the system being described; *type* refers to where the metrics fit; and *maturity* relates to the suitability, systematically collection, and organization of the metrics. Moreover, an RM should not be difficult to implement [51], [84], and it must produce the same result when the assessment is repeated [84].

While some papers assume that RM can be greater than one [38], [85], Ayyub [25] defines the RM to be a function that maps a set of possible situations, to the interval [0,1]

$$RM : C \rightarrow [0, 1], \tag{1}$$

in which C is an algebra.

The network structure and components [23], [86]–[90] can also improve the resilience of a system, and network measures can be included in an RM. Abbasi *et al.* [86] presented a resilience vector for a power grid which comprised of five sub-indices: load

shedding cost savings, restoration cost savings, adaptability, weighted algebraic connectivity, and weighted betweenness centrality. The last two sub-indices are extracted from the network structure. Zhang and Wang [87] introduced a network-based RM that does not consider the performance of the system. However, performance must be incorporated into a metric [29] because it reflects how well the system delivers on its intended purpose during and after an event [29].

Some researchers used the ratio of the area of real performance region to the area of target performance as an RM [91]–[94]. Others divided the previous metric by the recovery time to take into account the time-to-recovery [59], [95]–[97]. The metric offered by Francis and Bekera [38] is based on the few data points $((t_o, F_0), (t_d, F_d), (t_{r^*}, F_{r^*}), (t_e, F_e))$ on the functionality curve (Figure III.1), which does not consider the whole functionality curve that indicates how the process degrades and recovers. Kwasinski [51] used a metric from reliability as an indicator of resilience. Ayyub [25] used a weighted sum of normalized ratio of areas in two intervals, one from t_o to t_d, and the other from t_d to T.

Definition. Valid Resilience Metric

A valid RM associated with a conceptual framework is a metric that

i. Reveals if a system has the abilities suggested by the associated conceptual framework, and

ii. Is not biased towards any of these abilities, i.e., it must not overemphasize or underemphasize the importance of any of these abilities.

Systems with different abilities' settings can have the same resilience measure against the same incident (Figure III.2), but it may be different for a biased metric. For example, consider System 2 in Figure III.2 with a weak absorption but a rapid recovery, and System 3 with a better absorption but a tardy recovery compared to System 2; for an unbiased RM System 2 and System 3 have the same resilience value, but for a biased metric which overemphasizes the rapid recovery, System 2 shows a better resilience.

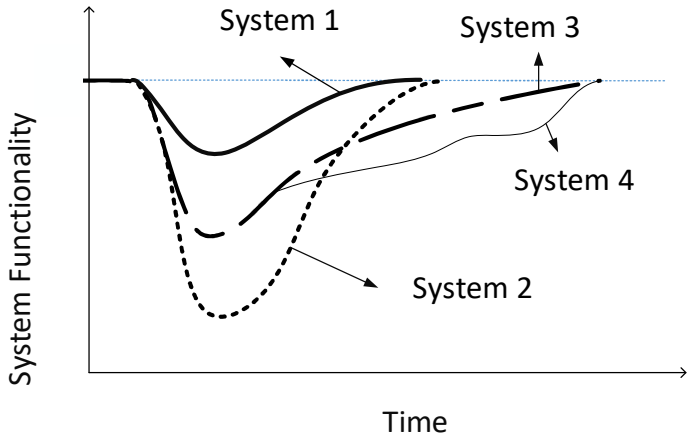

Figure III.2: Different resilience abilities, systems different settings of abilities: System 1 has a higher absorption and shorter recovery period comparing to other two systems. While System 2 has a shorter recovery and poorer absorption comparing to System 3, both have the same resilience measure

Now that we defined a valid RM, the question that arises is *"how can we validate an RM?"* In the subsequent sections of this study, we present our proposed RM and a methodology to examine the validity of RMs. We provide numerical results, analyze our proposed metric, and compare it to other performance-based metrics. Throughout this document, we use RM and resilience index interchangeably.

3.2. Existing resilience metrics

So far, several RMs have been developed for the systems which are categorized as general or structural [24]. In this section, we present the existing metrics and their limitations. We use the following notation in the rest of this document. We name the existing metrics as $Index_i, i = 1 \dots 6$. The pair (t, F) indicate the time and functionality of the system at that time (Figure III.1). The point (t_O, F_O) on the curve corresponds to the normal or initial state when an incident occurs, at (t_d, F_d) system has degraded to its lowest functionality, t_δ is the time that the initial recovery actions are started, $(t_r^*,\ F_r^*)$ is the end of adaptation, where initial recovery actions end, and $(T,\ F_T)$ corresponds to the point that recovery is achieved.

A normalized metric ($Index_1$) indicates the percentage of the targeted functionality (TF) that has been satisfied [91]–[94]. It is

$$Index_1 = \frac{\int_0^T F(t)dt}{\int_0^T TFdt}. \tag{2}$$

The area $\int_0^T TF(t)dt$ is a normalizing factor which helps to compare resilience of different systems and different performance magnitudes together. However, $Index_1$ does not show the importance of rapid recovery ability as we have elaborated in the discussion section.

Kwasinski [51] presented $Index_2$ for power systems, which is similar to availability index[98] which is

$$Index_2 = \frac{T_u}{T_u + T_d}, \tag{3}$$

where T_u and T_d are the summations of the up and down times of the system's components. An obvious weakness of this metric is that if we have two components with huge capacity differences, and $Index_2$ cannot distinguish the differences between their impacts on the resilience measure.

In $Index_3$ [20], [34] the minimum functionality is subtracted from the numerator and denominator of $Index_1$ to focus more on the after event activities (adaptability and recovery). However, their metric still has the same flaw as $Index_1$.

$$Index_3 = \frac{\int_0^T [F(t) - \min\{F(t)\}]dt}{\int_0^T [TF - \min\{F(t)\}]dt}. \quad (4)$$

Francis and Bekera [38] proposed an index that includes absorptive capacity (F_d/F_0) which shows the ability of the system to absorb shocks without recovery action, adaptive capacity (F_R/F_0) which relates to those post-disaster activities taken after the disruption, and speed of recovery S_p which is:

$$S_p = \begin{cases} \frac{t_\delta}{t_r^*} e^{-a(t_r - t_r^*)} & t_r \geq t_r^* \\ \frac{t_\delta}{t_r^*} & otherwise, \end{cases}$$

and

$$Index_4 = S_p \frac{F_R}{F_0} \frac{F_d}{F_0}. \quad (5)$$

Although it includes sub-metrics for the abilities of the system, this metric just used few functionality points, and it cannot demonstrate how the functionality changes along the functionality curve (e.g., Systems 3 and 4 in Figure III.2).

Ayyub [25] introduced $Index_5$ as

$$Index_5 = \frac{t_0+F\Delta T_d+R\Delta T_R}{t_0+\Delta T_d+\Delta T_r}, \tag{6}$$

where $\Delta T_d = t_d - t_0$, F is the failure profile, $F = \frac{\int_{t_i}^{t_d} F(t)dt}{\int_{t_i}^{t_d} TFdt}$, $\Delta T_R = t_R - t_d$, R is the recovery profile, $R = \frac{\int_{t_d}^{t_r} F(t)dt}{\int_{t_d}^{t_{Rr}} TFdt}$, and $t_0 = 0$.

Kadri and Chaabane [95] divided the value of $Index_1$ by T to incorporate rapid recovery into the RM. $Index\ 6$ is

$$Index\ 6 = \frac{\frac{\int_0^T F(t)dt}{\int_0^T TF(t)dt}}{T}. \tag{7}$$

These two last indices put a high weight on the recovery time, while a valid metric must be unbiased towards any of the abilities.

3.3. Proposed resilience metric

As an attempt to overcome the shortcoming of the existing metrics, we develop a performance-based valid RM that can be used in a variety of areas and is more consistent with various conceptual frameworks. This metric includes parameters that should be determined by the decision makers; hence, it is flexible to any application at hand. Our proposed RM is based on three post-disaster related abilities (absorption, adaptation, and recovery) because it is commonly reported in the literature. Although adding the anticipation ability (a pre-disasters component) can help improve the system resiliency, it is beyond the scope of this paper.

The first component is *absorption* (r_1). This component measures how well the system can maintain its functionality in the face of an unfavorable event, and how much the negative effects will be prevented. The formula for $r_1$is:

$$r_1 = \frac{\int_{t_o}^{t_d} F(t)dt}{\int_{t_o}^{t_d} TF(t)dt}, \tag{8}$$

in which, *F*(*t*) is the functionality of the system at time *t,* and *TF*(*t*) is the required functionality or demand at time *t*. Since the functionality of a system cannot be negative (e.g., 0 indicates non-functional system), both functions map the time to R_+, the non-negative real numbers. Also, for $t \in [0, t_d)$, the following inequality holds true, $F(t) \leq TF(t)$; hence $0 \leq r_1 \leq 1$.

The second component is *adaptation* (r_2). This component shows how well we assigned and utilized the existing resources to mitigate the consequences of the event, which can be measured by the loss of functionality after degradation until recovery over the target functionality. The recovery actions may result in two situations for the functionality. If the system recovers to a steady state at the same level or below the initial state ($F_R \leq F_o$), then we use $T = t_R$. Otherwise ($i.e., F_R > F_o$), we choose T to be the time that the functionality recovers to its initial state ($T = F^{-1}(F_o)$ and $T > t_o$, where F^{-1} is the inverse of functionality function). Because the goal of recovery is to bring the system back to the initial state, any efforts made beyond the initial state falls under *capacity enhancement*[99]. Using this *T*, the formula for r_2 is as follows:

$$r_2 = \frac{\int_{t_d}^{T} F(t)dt}{\int_{t_d}^{T} TF(t)dt}, \tag{9}$$

where

$$T = \begin{cases} t_R & F_R \leq F_o \\ F^{-1}(F_o) & F_R > F_o \text{ and } t > t_o \end{cases}.$$

With a reasoning like the previous part, we will have $0 \leq r_2 \leq 1$.

The third component is time-to-recovery (r_3). Each system has a favorite time-to-recovery (T_0) which can be determined in several ways, such as expert opinion. Having T_0 we calculate r_3 using formula (4).

$$r_3 = f(T) = \begin{cases} 1 & T \leq T_0 \\ \frac{T_0}{T} & otherwise, \end{cases} \quad (10)$$

when $r_3 = 1$, it tells us that the time-to-recovery is shorter than the favorable time and if the recovery time is terrible ($T \to \infty$) then the corresponding component is very small ($r_3 \to 0$). The function $f(T)$ can be replaced by the function that best suits the system. Also, it holds that $0 \leq r_3 \leq 1$. Our proposed RM is a convex combination of the three components

$$r = \alpha_1 r_1 + \alpha_2 r_2 + \alpha_3 r_3, \quad (11)$$

$$\sum_{i=1}^{3} \alpha_i = 1 \text{ and } \alpha_i \geq 0 \text{ for } i=1,2, \text{ and } 3,$$

where r_1, r_2, and r_3 are values of absorption, adaptation, and recovery components, respectively. The weight parameters $(\alpha_1, \alpha_2, \alpha_3)$ can be obtained using any priority ranking method among those three abilities such as analytic hierarchical process (AHP) [100].

3.4. A resilience metric assessment methodology

When we talk about a valid RM, the question arises: “how can we assess its validity”. In this section, we introduce a methodology that can be used for this purpose. This methodology is not just for a particular case or domain and can be applied to any performance-based RM. Our methodology utilizes experimental design [32] and statistical analysis.

“An experiment is a test or a series of tests in which purposeful changes are made to the input variables of a process or a system so that we may observe and identify the reasons for changes that may be noticed in the output response” [32]. Experimental design is an efficient procedure for planning experiments so that the data obtained can be analyzed to yield valid and objective conclusions [101]. It is used to choose between alternatives, select the key factors affecting a response, model a process, "fine tune" a process, and optimize a process output [32], [101].

We use the experimental design method to assess the validity of a metric. The steps of the proposed methodology are as follows.

Step 1: Select factors and their levels. We must have a factor for each of the items we want to study, which in our case they are abilities of the system. Each factor can be a function of sub-factors. Combinations of factor levels are called treatments. The **response** variable is the RM value.

Step 2: Obtain the performance measure for each treatment. The probability of occurrence of extreme events is minimal, and it is not feasible to get the real data for

experiments. Hence, we use simulation to obtain the data. The output of a simulation is the functionality of the system which will be used in calculating the resilience.

Step 3: Calculate RM. In this step, we use the performance data in the previous step to calculate the resilience for each treatment.

Step 4: Analyze the results. Now use analysis of variance (ANOVA) to test the statistical significance of factors' effects on the resilience of the system. The output of ANOVA includes the *p*-values for the factors. In statistics, we compare this *p*-value with a significance level. The smaller the *p*-value, the more significant it is. If *p*-value for a factor is significant, it signals that changing the value or level of that factor (ability) will not change the resilience; hence we can say that that metric is not valid. For example, if a factor associated with absorption has a p-value of 0.1, then it shows that this factor is not significant, and that means that absorption has no significant effect on the resilience of the system. However, from the conceptual framework, we know that it is one of the key abilities of a resilient system.

3.5. Numerical studies

In this section, we will examine our proposed RM by the methodology that we presented in Section 4. For this, we need a system to simulate the events (i.e., feed input factors for each treatment and extract response and calculate the output of the proposed RM). We adopted security constrained unit commitment (SCUC) which models electrical power systems [102], [103]. The SUSC model and description can be found in Appendix I

For simplicity, without loss of generality, we assumed that the disruption just affects the nodes (generators), however, it can be extended to include links and other components

as well. We applied SCUC on a modified 57-bus test case which consists of 57 buses, seven units, and 80 lines [104]. The data can be found in Appendix II. Now we go through the steps of our methodology for metric assessment.

a. Metric assessment

The following steps are followed to assess the proposed resilience metric and check if it is a valid RM for the power system example.

Step 1: Select factors and levels. Let labels A, B, and C stand for the three design factors (absorption, adaptation, and recovery, respectively). The factors should be extracted from the primary items that influence the resiliency of the power system units. These items are time-to-recovery, generation capacity, ramp up, ramp down [102], and severity, where severity is the number of generators that are inoperable. In 57-bus test case data, there is a high correlation among the generation capacity, ramp up, and ramp down. Due to this correlation we arbiterarily choose one of them, e.g., generation capacity. During an adverse event, a better absorption can result in fewer inoperable generators. Hence we use severity as a measure of A. Generation capacity can be used for B. This is because, after an adverse event, the high capacity generators can inject more spinning and non-spinning reserves into the system and satisfy more demand [105], [106]. Factor C is time-to-recovery.

For factors A and B, we selected two levels using the Pareto rule in a way that the distance between two levels is 80% of the range of data. In a severe situation, the number of inoperable generators will increase. In the 57-bus test case, there are seven generators with generation capacities of 20, 30, 50, and 80 Megawatts. Since we have seven generators, at its lowest level, B assumes 1, which means that only one generator will

become inoperable and the rest of generators will continue their regular production. At its highest level, four generators will become inoperable. For factor C, which is the time-to-recovery, we used the time-to-repair (TTR). Researchers use lognormal and exponential probability distributions for TTR [107]. We collected the mean time-to-repair (MTTR) of each generator (unit) [108]–[111], and we fit an exponential probability distribution for the TTR. We assume that generator is operable after this TTR. The time horizon for usual SCUC is 24 hours, however, since the MTTR for some generators was more than 24, we considered a 96 hours horizon. Let *g(t)* be the exponential probability distribution function of time-to-repair, *t*, and *G(t)* is its cumulative distributin function. Therefore, the TTR corresponding to a probability p is calcuated as $G^{-1}(p)$. We expect a complicated relationship between time-to-recovery and the RM value. Hence, five levels[112] are selected to reflect the actual effect of recovery time on the RM. The first four levels are $G^{-1}(0.25)$, $G^{-1}(0.5)$, $G^{-1}(0.63)$, and $G^{-1}(0.75)$. The last level (T) is the minimum of the time horizon (96) and $G^{-1}(0.99)$ for the selected generator.

Table III-1: Factor and levels for metric assessment. For recovery time f is the exponential probability density function

Factor Name	Factor ID	Levels
Generating capacity (MW)	A	Low (-) = 20, High (+) = 80
Severity (#of inoperable generators)	B	Low (-) = 1, High (+) = 4
Time-to-recovery (Hours)	C	$G^{-1}(0.25)$, $G^{-1}(0.5)$, $G^{-1}(0.63)$, $G^{-1}(0.75)$, T

Figure III.3 shows the treatments resulted from experimental design. The name of each treatment consists of the AB treatment label (i.e., *1, a, b, ab*), an underscore, and probability of factor C. For example, case a_0.25 corresponds to the TTR for the probability of 0.25 and AB at *a* (i.e., factors A is at its high level (+) with a value of 80 and B is at its low level (–) with a value of 1.) For each treatment, we generated the data for inoperable generators.

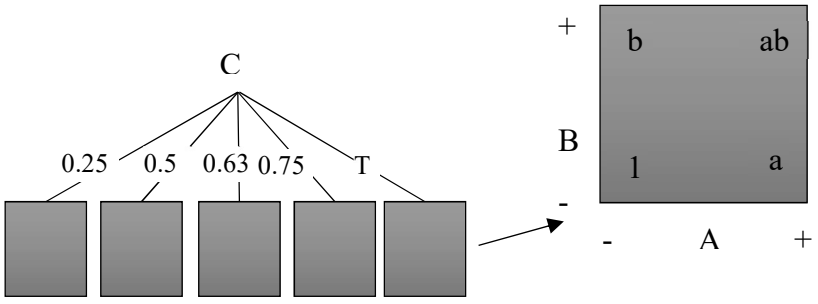

Figure III.3: Design of the experiment for analysis of metrics

Step 2: Obtain the performance measures. For this step, we coded the SCUC in Java and used Java API of IBM CPLEX Studio 12.6 for optimization[113]. For each of the treatments, we fed the input data into the SCUC, extracted load shedding, and calculated

the demand served (demand served equals actual demand minus load shedding). Figure III.4 plots the demand served and actual demand.

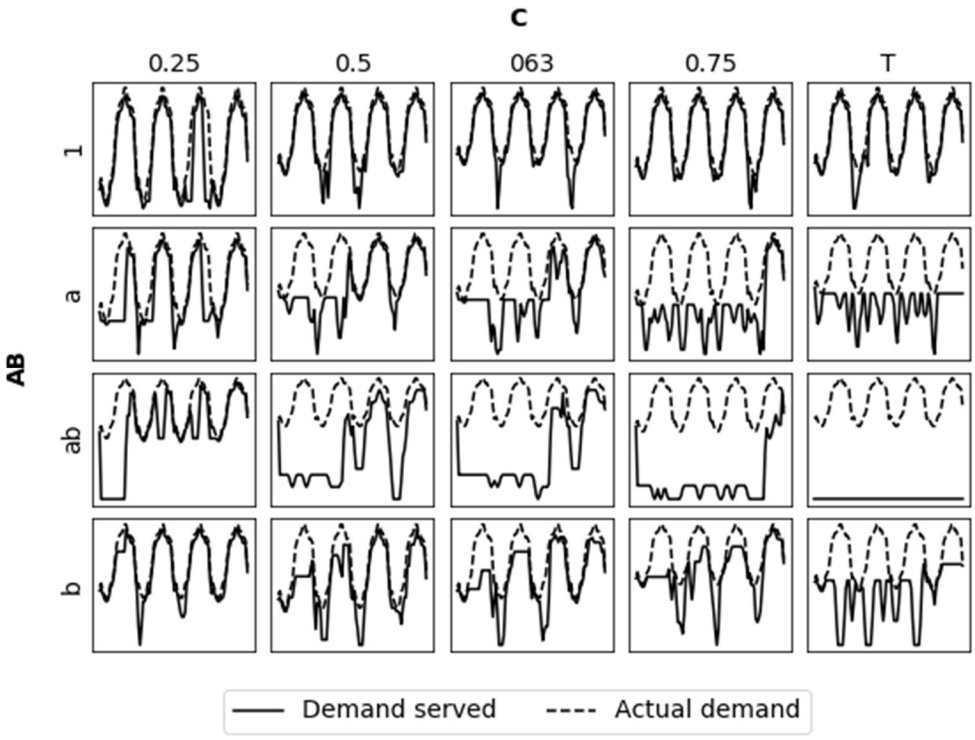

Figure III.4: Demand vs. supply for each treatment. The columns correspond to levels of factor C, and the rows correspond to level combinations of AB.

Step 3: Calculate RM. For our proposed metric, we first calculated the metric components (Figure III.5). Then, to study the effect of the choice of α_is on the resilience, we devised different combinations of α_is (Appendix III). The name of each combination is derived from the values of the α_is (e.g., m145 is for $\alpha_1 = 0.1, \alpha_2 = 0.4, \text{and } \alpha_3 = 0.5$; and m25255 is for $\alpha_1 = 0.25, \alpha_2 = 0.25, \text{and } \alpha_3 = 0.5$). Finally, we calculated the resilience for each treatment and each combination of α_is.

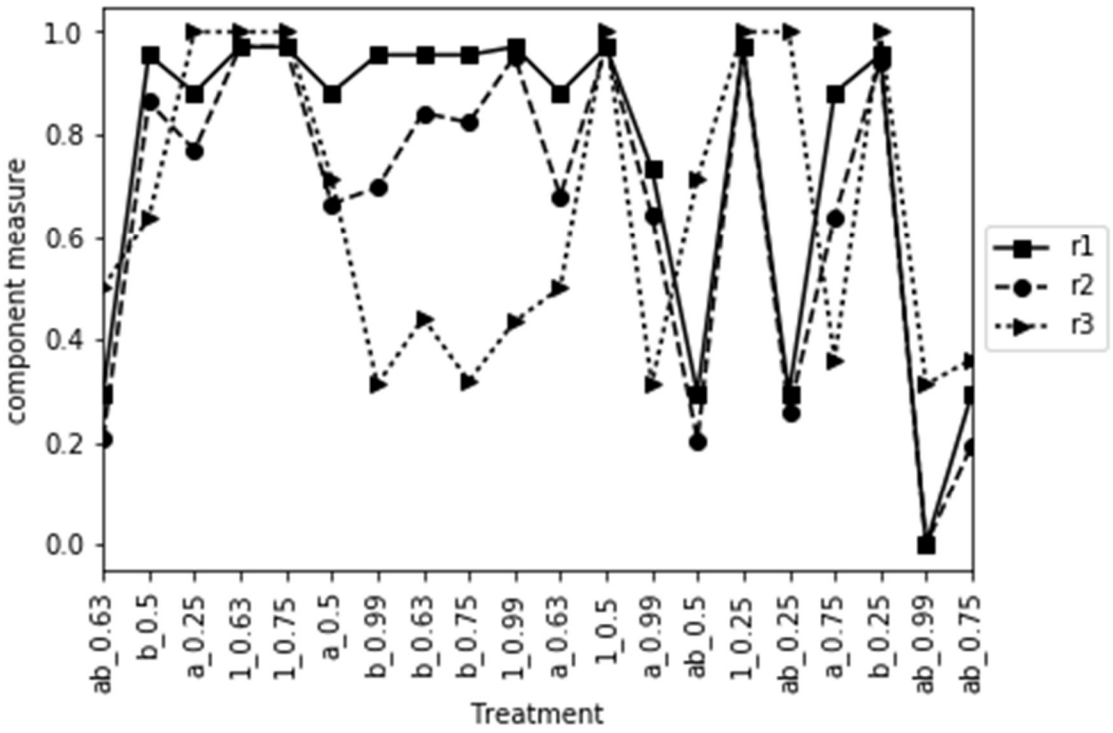

Figure III.5: Resilience metric components

Step 4: Analyze the results: First we determined the effect model using the experimental design techniques, and then calculated the ANOVA table. To see if there are interactions among the factors we drew interaction plots (Appendix IV). Since there were no interactions (interaction lines does not cross each other) we used the following linear model:

$$Y = \mu_0 + \mu_1 X_1 + \mu_2 X_2 + \mu_3 X_3 + \epsilon \tag{12}$$

in which the variables X_1, $X_2, and\, X_3$ correspond to the factors A, B, and C. μ_i are parameters and ϵ is the error term. Table II contains the ANOVA table for the metric corresponding to vector $\alpha = (\alpha_1, \alpha_2, \alpha_3) = (0.25,0.25,0.5)$.

Table III-2: ANOVA table for $\lambda = (0.25,0.25,0.5)$

	df	sum_sq	mean_sq	F	PR(>F)
A	1	0.4258	0.4258	101	2.40E-08
B	1	0.3008	0.3008	72	2.60E-07
C	1	0.3501	0.3501	84	9.20E-08
Residual	16	0.0668	0.0042	nan	nan

We calculated ANOVA for all λ vectors (Table III). Among these combinations, for cases m451 and m541 the factor A is not significant at 0.01 significance level. Thus, we will exclude these two from the possible $\alpha_i s$. All other combinations are validated through our model. For application, one can choose one of these α_i combinations using AHP.

Table III-3: *P*-values extracted from ANOVA for some combinations of α_is

	m145	m235	m25255	m325	m415	m154	m253	m25525
A	1.40E-08	1.90E-08	2.40E-08	3.20E-08	6.80E-08	2.00E-09	6.50E-09	2.00E-08
B	2.20E-07	2.30E-07	2.60E-07	3.00E-07	4.80E-07	6.70E-08	2.90E-07	9.60E-07
C	6.20E-08	7.60E-08	9.20E-08	1.20E-07	2.30E-07	2.60E-07	1.70E-05	0.00018

	m352	m451	m514	m523	m52525	m532	m541
A	6.70E-08	5.90E-07	1.10E-07	1.90E-07	3.10E-07	5.20E-07	1.40E-06
B	3.30E-06	2.80E-05	1.20E-06	3.80E-06	7.50E-06	1.50E-05	5.20E-05
C	0.0015	0.035	8.40E-06	0.00025	0.0013	0.0053	0.05

3.6. Discussion

The presented methodology enables us to study various resilience metrics quantitatively. Since we are looking for a general metric to quantify the system resilience,

all metrics are compared based on the conceptual framework of a resilient system (Section 1.1). If two out of three resilience abilities are fixed as constant and leave the other one to change, we must be able to identify the change in a resilient metric. If it does not show that the altered ability have a significant effect on the metric, and the resulting metric is not valid.

We now examine the performance of the existing resilience metrics using the proposed assessment methodology for the power network system discussed in Section 5. For this specific example, the results of Step 1 and Step 2 are the same as those presented in Section 5. Hence, we will perform the remaining two steps for each of the metrics in this section. The result of Step 3 is summarized in Figure III.6. As we expected, $Index_2$ is less sensitive to the generation capacity in a way that when we have four high capacity inoperable generators (case ab_0.99), the rest of the indices are close to 0. $Index_6$ has the least correlation with other metrics, and it shows less variability compared to other RMs. One can see that when we have a long time-to-recovery and more significant severity (cases ab_0.99 and case b_0.99), $Index_3$ drops dramatically. Also for case 1_0.25 which is the least severe case, $Index_3$ has an unfavorable result, and we have weaker resilience than case 1_0.63, which has the same treatment setting except for time-to-recovery.

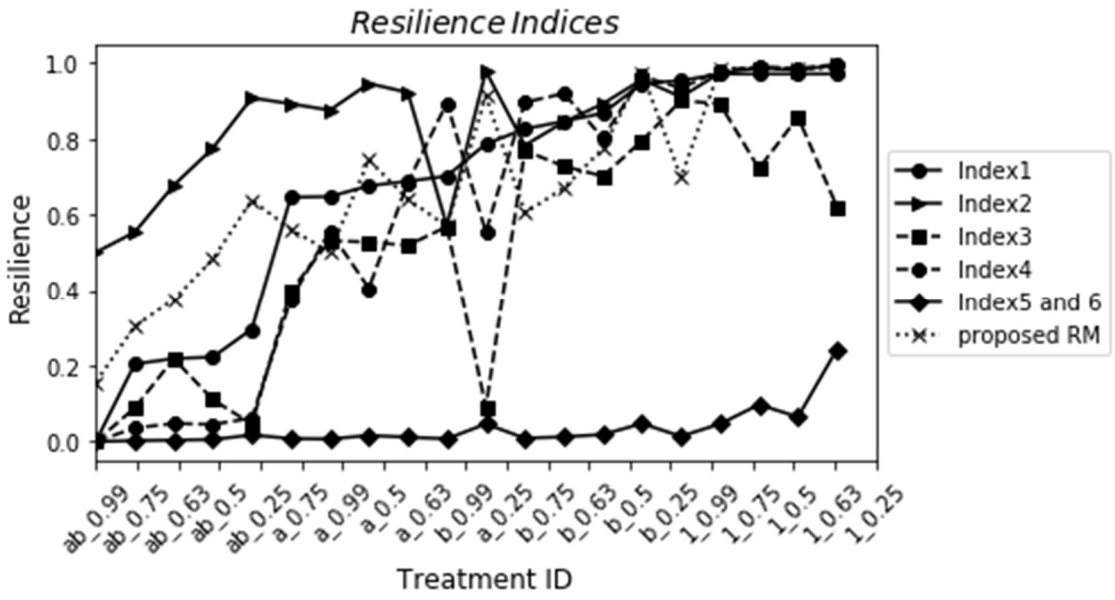

Figure III.6: Chart of RM values for experimental design treatments

Analysis of variance will demonstrate which factors have a significant effect on the metrics. The *p*-values from ANOVA tables for these metrics are summarized in Table III-4.

Table III-4: The p-values extracted from ANOVA analysis

	$Index_1$	$Index_2$	$Index_3$	$Index_4$	$Index_5$	$Index_6$	**Our proposed Metric***
A	9.6e-08	0.013	4.2e-07	5.1e-09	0.024	0.024	2.4e-08
B	1.3e-05	7.9e-06	0.0044	0.00021	0.027	0.027	2.4e-08
C	0.048	6e-05	0.25	0.66	0.0087	0.0087	2.4e-08

*Results are based on $\lambda = (0.25, 0.25, 0.5)$

The p-value is a good way to assess statistical significance of a factor on resilience. $Index_1$ shows that at a significance level of 5%, recovery time is not a statistically significant factor for resilience, while the other two factors are significant. Resilience frameworks emphasize that time-to-recovery is one of the important abilities of a resilient system. Based on this perspective, $Index_1$ is not valid. Likewise, $Index_2$ underrates the effect of factor A. $Index_3$ and $Index_4$ also do not show the significance of time-to-recovery (their

p-value is larger than 0.05). $Index_6$ underrates the effect of factors A and B which account for absorption and adaptation. Table 4 summarizes the pros and cons of the existing metrics.

Table III-5: Pros and cons of the current RMs derived from the ANOVA analysis

	Pros	**Cons**
$\boldsymbol{Index_1}$	Considers the absorption and adaptation (implicitly)	Does not reflect recovery time
$\boldsymbol{Index_2}$	Considers adaptation and time-to-recovery	Undervalues the significance of absorption
$\boldsymbol{Index_3}$	It is Similar to metric 1, but it better shows the adaptation and recovery actions	Does not reflect recovery time
$\boldsymbol{Index_4}$	Considers absorption and time-to-recovery	It is more sensitive to the generator capacity than to the time.
$\boldsymbol{Index_5}$ ***and*** $\boldsymbol{Index_6}$	Considers the absorption and adaptation (implicitly) moreover, time-to-recovery	It is too sensitive to time-to-recovery and underrates the effect of the other abilities.

Overall, the p-values of all factors in our proposed metric are close to 0 as seen in Table III-5; hence, they are all significant. Furthermore, the proposed metric is not biased toward any of the three factors. Therefore, our proposed metric is a valid resilience metric.

3.7. Conclusion

Building a resilient system or community cannot be overemphasized against disasters. There have been several approaches reported in the literature to quantify resilience of a system. However, they were often designed to work for a specific application and there is a large variability on the performance of resilient metrics. Therefore, we have developed a statistical assessment method for a resilient metric to be valid according to the concept of resilience. The design of experiments and ANOVA are utilized. We have tested well-known resilience metrics to compare performance using a power network system. Because those metrics exhibited a large variation in performance, a new resilience metric was developed. Using the proposed assessment methodology, the new resilience metric was evaluated and compared with the existing metrics. The results showed that the proposed metric is a valid resilience metric, which is not biased towards any of the abilities of a resilient system. As an extension to this work, one can include pre-disaster information for the resilience metric, i.e., "anticipation" ability. Such a metric may be able to capture the resilience of a system more accurately.

CHAPTER 4

IV. OPTIMIZING THE INFRASTRUCTURE RESILIENCE UNDER BUDGETARY CONSTRAINT

Communities located in regions prone to natural and man-made disasters endure hardship and financial loss in the face of these events. Investment to enhance infrastructure resilience is vital to reduce the consequences of these low probability high-impact events. Budget and resources are limited, and they must be allocated wisely to infrastructure components to build a resilient community. The complexity of infrastructure makes it difficult to show the effects of component enhancements on system resilience. This paper proposes a mathematical programming model aimed at optimizing infrastructure resilience against a set of adverse events by optimally allocating budget to the infrastructure components. Investment, component enhancement, and corresponding functionality are combined with the resilience-based component importance to tackle the system complexity. Three utility functions are presented to determine the possible component enhancement alternatives for an allocated budget and to choose the optimal alternative. A resilience-based component importance metric is introduced, which is used in the budget allocation optimization problem. This approach establishes a relationship between amount allocated to a component and changes in its absorption and recovery, and the aggregate of all such changes on the components on the system functionality. The results show that the utility function of a component impacts the resilience enhancement of the system

4.1. Introduction

Adverse events like natural disasters (e.g., earthquake, tropical cyclone, severe storm, flooding, freeze, wildfire, winter storm, etc.) or man-made disasters (terrorist and non-terrorist) can disrupt the community infrastructures. These adverse events have two traits in common. First, their occurrence probability is low; the expected number of hurricanes in 100 years in Texas is 7.1 and the expected number of major hurricanes is 2.2 [114]. Second, their impact in terms of cost and hardship is tremendous. During the past 37 years, 40 cyclones have caused a combined $870.2 billion in total damages with an average of $21.8 billion per event. Hurricane Harvey in 2017 alone accounts for $125 billion of this amount [3]. Resilience is a concept that addresses the ability of a system to continue its functionality during and after an extreme event with low functionality degradation and a rapid return to normalcy. Anticipation, absorption, adaptation, and rapid recovery are the main characteristics of a resilient system [24]. The United States Government Accountability Office (GAO) expressed the necessity of an investment strategy for resilience enhancement that reduces the nation's losses from future disasters. The investment decisions on cyber-physical systems (CPSs), especially those with a social impact like critical infrastructures, can be viewed from political [53], social, environmental [115], economic [116], financial [54], and engineering [53], [55] perspectives. While the benefits of these investments are generally difficult to monetize [117], an early investment in community resilience will pay back when disasters inevitably strike [44], and a lack of investment will possibly result in an overall higher cost [56]. Considering this importance, the Federal Emergency Management Agency (FEMA) is working on the National Mitigation Investment Strategy ("Investment Strategy") which provides a national

approach to invest in mitigation activities and risk management across the United States [52].

The problem of investing in urban infrastructure resilience can be considered at three levels: macro, meso, and micro. At the macro level, the problem can be categorized as funding, prioritizing, and resource allocation to several infrastructures. Some of the funding approaches are earmarks [118], pork-barrel [119], trust-fund [120], and block grants [121]. For resource allocation at a macro level, Hill *et al.* [122] suggested a method to reduce disaster impacts through systematic investments in which the socioeconomic risks associated with natural disasters is estimated. Graeden et. al. [57] proposed a rapid risk analysis that can be utilized to support risk-based investment prioritization at the community level. After the budget is assigned to a system, at the meso level, the system allocates resource to its components. For this purpose, one approach is to find the most critical components in the network and improve them within the limited budget. A resilience-based component importance (RCI) metric, which measures the extent to which individual component contributes to the network resilience [123], can be used for this purpose [34], [60], [124]. Component enhancement can result in a combination of less degradation in component functionality and rapid recovery of functionality in the face of a shock. This problem is handled at the micro level.

Literature has covered some specific issues and events regarding this subject, but there is more that needs to be taken into account. Some studies considered just a special system (transportation [125], power grid [58], [117], etc.), or a single event (e.g., cyber-attack [126], terrorist attacks [58], etc.), and they suggested a treatment for that specific system or event. Even so, a system is threatened by a pool of events, and preparing for only

one of them and neglecting the other can still be devastating if a second event strikes while attempting to recover from the first one. Moreover, if we consider the pool of potential events, the amount of investment to mitigate multiple risks is more efficacious than investing against each risk individually. The approaches based on RCI [34], [60], [124] do not provide the amount of the investment on the components. While RCI ranks the components based on their importance, it does not determine how much should be invested in each one. Moreover, the allotted resource to a component can be utilized in different ways to change the main resilience characteristics of that component, i.e., absorption and time to recovery. RCI does not determine which of these characteristics must be emphasized.

Therefore, the goal of this paper is to fill the identified gaps by proposing a method that can be applied to a general system. Specifically, this paper adds to the existing body of literature: a new formulation to maximize system resilience under budgetary constraint, an introduction of utility function into component enhancement, and a resilience-based component importance to map between an individual component functionality and its system functionality. The proposed method considers a set of possible events, their effects on the component functionality, and the component's enhancement alternatives. The alternatives employ a utility function to construct the set of alternatives for component enhancement. In the final step of the method, a mathematical programming model is introduced to optimize the system resilience of under a budget constraint using the information generated in the previous steps.

4.2. Model & Solution Methodology

The resource allocation problem has many applications in facility planning, job scheduling, buffer allocation, pollution control, and portfolio management. The investment on a system resilience can be translated into a resource allocation problem. In this section, we start with a tradeoff between absorption and recovery enhancements for a single component. Then, we propose an RCI followed by an integer programming formulation that optimally allocates budget to the components aiming at maximizing the system resilience.

4.2.1 Single component functionality and indifference curve

In order to develop a mathematical model and have a better understanding of the system behavior, we study the components individually. The functionality of a component is the level at which the component performs a task or function. For example, the functionality of a water transmission pipeline is the amount of flow that it carries. In a normal situation, the *target functionality* is the amount of water that the pipe is planned and expected to carry. Two component's characteristics that influence its functionality during and after an adverse event are absorbability and rapid recovery. After an event, the functionality degrades by A. Absorbability is the ability to reduce the negative effects of the event and have a smaller A. Rapid recovery or recovery is the time to recover (T) from a disruption. It is the length of the time from the moment that the event happens to the moment that the functionality returns to an acceptable level, usually the initial level. Keeping all other factors fixed, a component with a smaller A or a smaller T has a higher

resilience. In this section, we study different outcomes of enhancement activities on a single component. We will use the following notation.

A: The amount of degradation in the functionality
T: Recovery time of the component
a: Improvement in the absorption (in percent)
r: Improvement in the recovery time of the component (in percent)
f: Functionality of the component
Tf: Target functionality of the component
y: Amount of investment on the component
V: Value of the component

The functionality f here is normalized by dividing the real functionality by the target functionality, yielding a value between 0% and 100%. The 100% functionality occurs in the normal situation or for a system that is highly resilient. Different resilience enhancement activities can result in different outcomes for improving absorbability and recovery. Let a and r stand for the percent improvement in the absorption and recovery, respectively. The smallest value of a (or r) is 0, meaning that we do not improve the component's absorbability (recovery time), and the highest value is 1, for which the component will be intact by an event. For a given amount of investment, y, we may have different combinations of (a, r) (Figure IV.1). If we spend all the money on the robustness of the component, it will improve absorption by a percent (Figure IV.1-b) and A_{new} will be $A \times (1 - a)$. However, if we spend all the money on redundancy, it may just reduce time to recovery by r (i.e., $T_{new} = T \times (1 - r)$ as in Figure IV.1-c). Moreover, we may be able to improve both capabilities together (Figure IV.1-d). In an extreme case, if a is 100%,

then there is no degradation in the component functionality and, hence, there is no need to improve the time to recovery and vice versa.

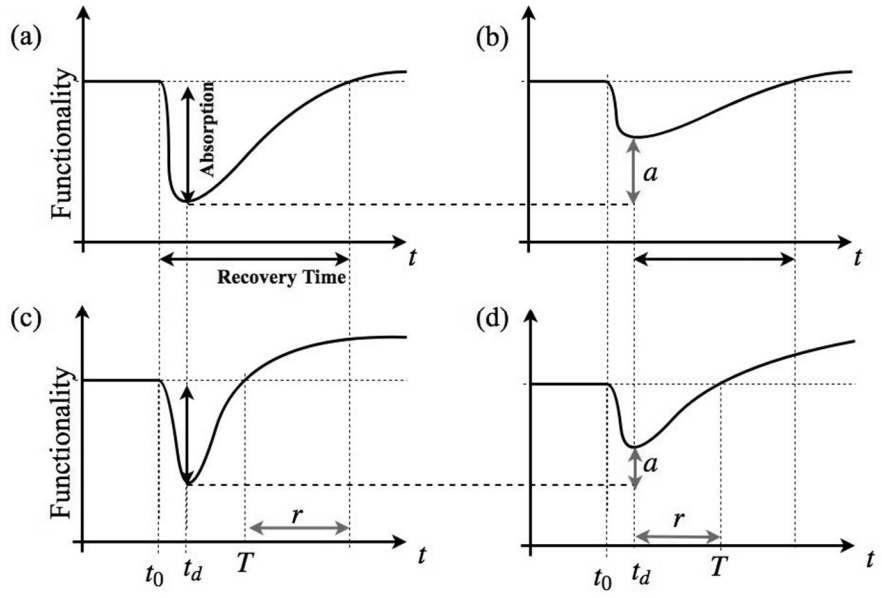

Figure IV.1: Component resilience enhancement scenarios for a fixed budget. System's functionality after disaster and a) before any enhancement, b) after enhancing absorbability, c) after reducing the recovery time, d) after improving both absorbability and recovery time.

The relationship between the investment amount and (a, r) can be established using the indifference curves. In economics, indifference curves represent different quantities of two goods for which a consumer has no preference for one combination of those goods over another combination on the same curve [127]. Using this concept, we define the component enhancement indifference curve (IC) to be all combinations of (a, r) for which we will have the same enhancement cost. It represents different types of improvements that we can perform for a fixed cost. Associated with indifference curves, there is a utility function $U(a, r)$ which relates the budget spent on a component and the improvements in

its absorption and recovery time (Equation 1). A utility function is mathematically represented as

$$U: [0,1] \times [0,1] \rightarrow R^{+} \quad (1)$$
$$(a, r) \rightarrow U(a, r)$$
$$y = U(a, r).$$

For example, in Figure IV.2, the cost of improving absorption and recovery corresponding to points $P1: (a_1, r_1)$ and $P2: (a_2, r_2)$ are $y(P_1) = U(a_1, r_1)$ and $y(P_2) = U(a_2, r_2)$. We assume that the ICs are *complete*, in a way that all points on the indifference curve cost the same amount, and the points not on the curve cost either more or less. Figure IV.2 shows three investment costs y_1, y_2, and y_3, where $y_1 < y_2 < y_3$. Since points P_1 and P_2 in Figure IV.2 are on the same indifference curve, they have the same cost of $y(P_1) = y(P_2) = y_1$. Another characteristic of the IC curves is that they have a negative slope. That is, if a is decreased, r should be increased to stay on the same IC. Linear [128], Cobb–Douglas [128], and Constant Elasticity Substitution (CES) [129] are examples of utility curves (Table 1). Value of the component (V_i) is the market value of the component. Consider two components with values of V_1 and V_2, where V_1 is much larger than V_2. To maintain the same enhancements for both components (i.e., $a_1 = a_2$ and $r_1 = r_2$), the amount of investment on the second component should be larger (i.e., $y_1(P_1) > y_2(P_1)$). It is assumed that y_i is proportionate to the V_i and it is incorporated into the model by scale factor k_i. We call the result of multiplication η by $U(a, r)$ the cost factor. Having the cost factor θ_i and the value V_i for the component i, the amount of investment on component will be

$$y_i = \theta_i V_i.$$

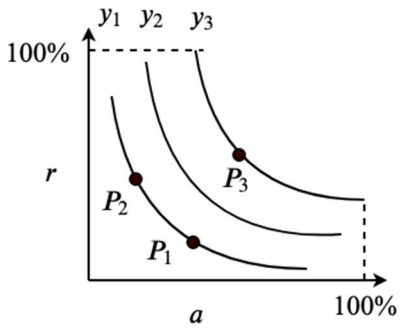

Figure IV.2: Indifference curve

Table IV-1: Utility functions and the relationship of a and r

name	formula	relationships
Linear [128]	$U(a,r)=\frac{\theta_1 a+\theta_2 r}{\eta}$	$r=\frac{\eta y-\theta_1 a}{\theta_2}$
Cobb–Douglas [128]	$U(a,r)=\frac{a^{\rho}r^{1-\rho}}{\eta},\rho<1$	$r=e^{\frac{\ln(\eta y)-\rho\ln(a)}{(1-\rho)}}$
CES [129]	$U(a,r)=\frac{C}{\eta}(\theta a^{\rho}+(1-\theta)r^{\rho})^{\frac{1}{\rho}}$	$r=\frac{((\eta y)^{\rho}-\theta a^{\rho})^{\frac{1}{\rho}}}{1-\theta}$

We will use the utility curve to formulate our mathematical model and to determine the optimal combination of a and r on the associated IC curve for a given budget.

4.2.2 Resilience-Based Component Importance (RCI)

In reliability component importance metrics like Fussell-Vesely, criticality importance measure, risk reduction worth (RRW), risk achievement worth (RAW), and Birnbaum measure the amount by which the failure of a component can affect the reliability of the system [61]. Based on the reliability context, the resilience-based component importance measure (RCI) is defined as the amount by which the resilience of a system is

reduced by a component's failure [34], [60]. A prerequisite for calculating the RCI is a resilience metric. . Several qualitative and quantitative resilience assessments have been proposed in the literature [24], [130]. Among the quantitative metrics, we need the one representing the essential characteristics of a resilient system (i.e., absorption and rapid recovery). Moreover, the metric must be simple enough to be utilized in the mathematical formulation. Therefore, this study uses the resilience metric suggested by Najarian and Lim [131]. It consists of a convex combination of three sub-metrics; absorption ($я_1$), adaptation ($я_2$), and rapid recovery ($я_3$). They can be calculated using the following formulas:

$$я_1 = \frac{\int_{t_o}^{t_d} F(t)dt}{\int_{t_o}^{t_d} TF(t)dt}, я_2 = \frac{\int_{t_d}^{T} F(t)dt}{\int_{t_d}^{T} TF(t)dt}, \text{and } я_3 = f(T) = \begin{cases} 1, & T \le T_0 \\ \frac{T_0}{T}, & otherwise' \end{cases}$$

where, $F(t)$ is the functionality of the system at time *t*, $TF(t)$ is the target functionality at time *t*, t_d is the time that functionality of the system reaches to its minimum, T_0 is the desired recovery time of the system which , and T is the recovery time of the system. The system resilience metric Я it lies in the closed interval [0, 1] and is calculated as

$$я = \alpha_1 я_1 + \alpha_2 я_2 + \alpha_3 я_3, \alpha_1 + \alpha_2 + \alpha_3 = 1, \alpha_1, \alpha_2, \alpha_3 \ge 0. \quad (2)$$

Let $я^{+c}$ be the resilience of the system when the component c is operable and $я^{-c}$ when it is not. Then the RCI of the component *i* is the difference between these two values. The following algorithm explains the steps to take to obtain the value of RCI.

Algorithm 1 Resilience-Based Critical Indexing Algorithm

Input the component index $i \in E \cup V$
Calculate the resilience of the system ($я^{+i}$)
Set $f_i = 0$
Calculate the resilience of the system ($я^{-i}$)
$я^i$ =($я^{+i} - я^{-i}$)
Return 1-$я^i$

Since $я^{+i} \geq я^{-i}$, the value of $я^{i}$ will be within the interval [0,1]; hence, the impact of the component i on the system resilience, $RCI_i = (1 - я^{i})$, assumes values between 0 and 1, inclusive.

4.2.3 Resilience Optimization under Budget Constraint

In a complex system, each component has its own absorption and recovery capabilities in the face of an adverse event. For example, in a power grid, even if two components are the same, the environment and the facility that supports them may be different. As a result, their absorptions and recovery times differ, and possible modifications, associated costs, and the effect of enhancement on the whole system must be calculated separately for each component. Consider a power generation unit with possible characteristics to be modified such as elevation, surrounding building and structure, redundancy, source of generation storage (e.g., coal), and environment (e.g., drainages). By improving each or a subset of these characteristics, we can enhance the absorption and/or reduce the recovery time of the generator. This enhancement will differ for different events; a higher elevation or drainage may keep a generator safe against a certain level of the flood, i.e., a better absorption against the flood, but it may not improve it against a hurricane. However, having a backup generator that can immediately become operable in the case of failure in the original generator, shortens the time to recover. Due to the budget limit, a subset of the set of all options should be selected in such a way that a higher resilience level for the system can be achieved. In this section, we are to formulate this problem as and optimization model, and we use the following notation.

Notations:

Sets:

$\Gamma = \{\gamma_1 \dots \gamma_K\}$: Set of k events (including attacks)

$\mathbb{Q} = \{q_1 \dots q_N\}$: Set of N components

$\mathbb{C} = \{c_{i,1} .. c_{i,M_i}\}$: The set of M_i possible investments on component i

Indices:

i: Index for component, $i \in \{1, \dots, N\}$

t: Index for time

j: Index for investment option, $j \in \{1..M_i\}$

k: Index for event option, $k \in \{1..K\}$

Variables:

$x_{i,j}$: A binary variable that is 1 if the investment option j, is selected for component q_i

$f_{i,j,t,k}$: Functionality of component i with investment $c_{i,j}$ at time t against γ_k

$f_{i,t}$: Functionality of component i at time t

B: Budget limit for enhancement against γ_k

A_i: A_{ij}: The drop in the functionality of the component i in face of event j

F_t: Functionality of system at time t, $F_t = F(t)$

Parameters:

$c_{i,j}$: The jth investment option of component i

RCI_i: Resilience-based component importance of q_i

T_i: Time to recovery of component i before investment

$T_{i,j,k}$: Time to recovery of component i after investment j against event k

Lf_i: Lowest functionality acceptable for a component

β_k: Weight of attack impact on resilience

$a_{i,j,k}$: Improvement in the absorption of component i in face of event k due to investment j.

$r_{i,j,k}$: Improvement in the recovery of component i in face of event k due to investment j.

ξ_{il}: Coefficients of the objective function $l = 1 \dots 5$

Proper functionality of a system depends on the seamless functionality of its components. If the relationship between the functionality of a component and functionality of a system is given, then it may facilitate the measurement of the effect of component enhancement on the overall system resilience. However, it is very difficult to find such a straightforward relationship because the effect is a function of many unknown variables. To simplify the problem, it is assumed that functionality of the component at time *t*, $f_{i,t}$, has a *linear influence* on the functionality of the system, F_t, proportional to its resilience-based importance, RCI_i. That is

$$F(t) = F_t = \frac{1}{N}\sum_{i}^{N} RCI_i \times f_{i,t}. \quad (3)$$

Moreover, it is assumed that the component indifference curve for a given budget is known. The degradation time, t_d, is assumed to be the same for all of the components before and after the event. We start developing the mathematical model based on a piecewise linear function, and then move on to a more general model.

4.2.4 Linear functionality and linear utility curve for a single event

Assume that components have functionality (f_t) that consists of or can be estimated by two line segments l_1 and l_2 (Figure IV.3). To calculate the resilience using Equation

(2), the integral is converted into the summation of the areas R_t captured by the trapezoid under the functionality curve in the interval $[t, t+1]$.

$$R_t = \int_t^{t+1} f(t)dt = \frac{f_{t+1} + f_t}{2}$$

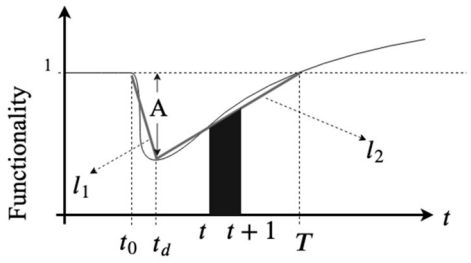

Figure IV.3: Estimation of the functionality of a component using two straight lines

At any time *t*, the functionality of a component is

$$f_{i,t} = \begin{cases} 1 - \dfrac{A_i}{t_{i,d}} t, & 0 \le t \le t_{i,d} \\ 1 - \dfrac{A_i}{T_i - t_d}(T_i - t), & t_{i,d} \le t \le T_i \\ 1, & t \ge T_i \end{cases}.$$

The sub-metrics absorption ($я_1$), adaptation ($я_2$), and recovery ($я_3$) sub-metrics can be calculated using $f_{i,t}$. In Appendix V, we have derived formulas to calculate $я_1$ and $я_2$. If T_0 is small enough that $T \ge T_0$ is true, then the resilience of the system will be

$$\begin{aligned} я &= \alpha_1 я_1 + \alpha_2 я_2 + \alpha_3 я_3 \\ &= \alpha_1 \frac{1}{N} \sum_{i=1}^{N} RCI_i\left(-\frac{1}{2}A_i + 1\right) + \alpha_2 \frac{1}{N} \sum_{i=1}^{N} RCI_i \left(\frac{-A_i}{2} \frac{(T_i - t_d)}{(T - t_d)} + 1\right) \\ &\quad + \alpha_3 \frac{T_0}{T}. \end{aligned} \tag{4}$$

Equation (4) can be described visually using Figure IV.3. In this figure, the expression $-\frac{1}{2}A_i + 1$ is the area enclosed by the trapezoid with the corner points of $(0,0), (0,1), (t_d, 0), (t_d, 1 - A_i)$ over the area enclosed by the rectangle $(0,0), (0,1), (t_d, 0), (t_d, 1)$. The weighted average of these areas, where weights are RCI, yields $я_1$. A similar intuition holds for $\frac{-A_i}{2}\frac{(T_i - t_d)}{(T - t_d)} + 1$ and $я_2$. For a linear utility function and investment y_i, the new degradation and recovery time for component *i* are as:

$$A_{i,new} = A_i(1 - a), \text{and}$$

$$T_{i,new} = T_i(1 - r_i).$$

In Appendix VI, Equation (4) is modified to include the enhancements resulted from the investments as explained. Then we formulated the problem as a nonlinear optimization model described as in Equations (5-1) to (5-5).

$$\max \quad я = \frac{1}{N}\sum_{i=1}^{N}\left(\frac{\xi_{i1}\, a_i + \xi_{i2}\, a_i r_i + \xi_{i3}\, r_i + \xi_{i4} T + \xi_{i5} a_i T + \xi_{i6}}{T - t_d}\right) + \frac{T_0}{T}, \tag{5-1}$$

s.t.

$$\sum_{i,j} y_i \le B, \tag{5-2}$$

$$\theta_{i1} a_i + \theta_{i2} r_i = k_i y_i, \forall i, \tag{5-3}$$

$$T \ge T_i(1 - r_i), \forall i, \tag{5-4}$$

$$y_i, T \ge 0, 0 \le a_i, r_i \le 1. \tag{5-5}$$

Decision variables are the budget allocated to component *i* (y_i), the percentage improvement in absorption and recovery time of the *component i* (a_i and r_i), and the *system*'s recovery time (T). Parameters include coefficients ξ_{ij}, which are calculated from parameters $\alpha_1, \alpha_2, RCI_i, A_i, T_i,$ and t_d in Appendix F; B the total system's budget limit;

utility function parameters (θ_{i1}, θ_{i2}, and η_i); and time to recovery T_i for component *i* before an investment is made. The objective is to maximize the resilience of the system, Equation. (5-1), which is a function of component enhancements (a_i, r_i) and system's recovery time (T). Equation (5-2) restricts the total spending on the system to be less than the budget. Equation (5-3) relates the investment on component *i* (i.e., y_i) to different possibilities of enhancements in a_i and r_i via an indifference curve. As we discussed in Section 2.1, the scale factor k_i accounts for the value of the component. Recovery time of the system is the latest recovery time of the components (Equation (5-4)). Finally, all the variables are continuous and non-negative (Equation (5-5)), and a_i and r_i are less than 1. Solving this problem will determine how much we will spend on each component and what absorption and recovery enhancement combination will yield a higher resilience.

4.2.5 A General model

In this section, we extend the linearity assumption in Section 2.3.1 to general functionality and propose a mathematical programming model to optimize the system's resilience within a budget constraint. The goal is to allocate the budget to the components and to determine the component absorption and recovery enhancements in a such way that a maximum resilience is achieved. Drawing an analytical relationship between investment and system resilience is far reaching. To tackle this problem, we discretized the investment options and components' functionality through the following steps. In the first step, for each component q_i, m_i possible improvements $p_{i,j,k} = (a_{i,j,k}, r_{i,j,k})$ and their associated cost $c_{i,j}$ is prepared. It is possible to have two different improvement scenarios $p_{i,j,k}$ and $p_{i,j\prime,k}$ associated with the same cost (i.e., $p_{i,j,k}$ and $p_{i,j\prime,k}$ lie on the same indifference

curve). An improvement on q_i has different absorption and recovery enhancement outcomes against different events; shown by index k. All these data will be summarized in a set of options $O_{i,j,k} = (c_{i,j}, a_{i,j,k}, r_{i,j,k})$ among which the optimization problem chooses the subset of optimal options. For all the components, option $O_{i,0,k} = (0,0,0)$ is included so that it can be selected if no enhancement for component i is in optimal set. Using indifference curves, the construction of $O_{i,j,k}$ can be done either by finding different enhancement points $p_{i,j,k}$ for a given investment amount, or by finding the cost $c_{i,j}$ for a $p_{i,j,k}$.

In the second step, by considering $a_{i,j,k}$ and $r_{i,j,k}$, we obtain the discrete system functionality for each $O_{i,j,k}$ after a disruption. Let $f_{i,j,t,k}$ be the normalized functionality of q_i at time t after investment j in the face of the adversarial event $\gamma_k \in \Gamma$. The normalized functionality is calculated by dividing the actual functionality over the target functionality so that $f_{i,j,t,k}$ assumes a value between 0 and 1. Based on the linear influence assumption made at the beginning of Section 2.3, the influence of q_i on the total system's functionality is $CPI_i \times f_{i,j,t,k}$. Now, we use Equations (2) and (3) to construct the objective function in Equation (6-1), which is an indicator of resilience against the set of events. Equations (6-1) to (6-5) compose our general budget allocation model.

$$\max \quad \sum_{k} \beta_k \left[\begin{array}{c} \dfrac{\alpha_1 \sum_{t=0}^{t_{d,k}-1} \left(1 - \dfrac{1}{N} \sum_{i,j} CPI_i \times \dfrac{f_{i,j,t,k} + f_{i,j,t+1,k}}{2} \times x_{i,j} \right)}{t_{d,k} - t_0} + \\ \dfrac{\alpha_2 \sum_{t=t_d}^{T-1} \left(1 - \dfrac{1}{N} \sum_{i,j} CPI_i \times \dfrac{f_{i,j,t,k} + f_{i,j,t+1,k}}{2} \times x_{i,j} \right)}{T - t_{d,k}} + \\ \alpha_3 \dfrac{T_0}{T} \end{array} \right], \tag{6-1}$$

s.t.

$$\sum_{i,j} c_{i,j}\, x_{i,j} \leq B, \tag{6-2}$$

$$\sum_{j} x_{i,j} = 1, \forall i, \tag{6-3}$$

$$T \geq T_{i,j,k}\, x_{i,j}, \forall i, \tag{6-4}$$

$$x_{i,j} \in \{0,1\}. \tag{6-5}$$

The objective function (Equation (6-1)) is the weighted sum of the resilience of the system for the set of events Γ. The binary variable $x_{i,j}$ assumes 1 if the j^{th} investment option for q_i is selected. The weights β_k are parameters to show the importance of the corresponding event. They can be calculated using multi-criteria decision methods (MCDM) with criteria such as the possibility of event occurrence, cost of the devastation caused by the event, and cost of making the system resilient against that event. The budget constraint, Equation (6-2), limits the total cost of chosen options to be less than the budget. In the optimal solution, we just choose one investment option (Equation (6-3)) for each component. The key point in this equation is that we have designed the cost scenarios in such a way that we do not need to select two options for the same component for different events. Equation (6-4) calculates the system's time to recovery (T), which is the largest time to recovery of all the components. The steps for constructing the mathematical model is demonstrated in Algorithm 2.

Algorithm 2 Constructing the mathematical programming for general model

1. Input the set of components, simulation model to calculate functionality in different situations
2. For each component $i \in V \cup E$ do:
3. Determine the value k_i of the component from the V_i
4. Choose S values for the investments on component i $(c_i^s, s = 1, \dots, S)$
5. Choose the utility function
6. $j = 0$
7. For each s in S:
    a. Determine P points on the indifference curve associated with C_i^s
    b. For each p in P:
        i. j =j+1
        ii. $c_{i,j} = c_i^s$
        iii. For k in events:
            a. Obtain $a_{i,j,k}$ and $r_{i,j,k}$ corresponding to point p on the IC of $c_{i,j}$ or find the cost associated with $(a_{i,j,k}, r_{i,j,k})$
            b. Calculate $f_{i,j,t,k}$ associated $a_{i,j,k}$ and $r_{i,j,k}$
8. Calculate the RCI_i using Algorithm 1
9. Insert these parameters into the model in Equations (6-1) to (6-5)

4.3. Numerical results

We perform our numerical studies on the power grid system using the security constrained unit commitment. We apply the SUSC model on a 6-bus IEEE standard test case. As shown in Figure IV.5, the grid comprises the generation units N0, N1, and N2; the electricity lines E3 to E9; and the demand nodes D4, D5, and D6 with share of total demand of 20%, 40%, and 40%, respectively. The 6-Bus data are available in Appendix F.

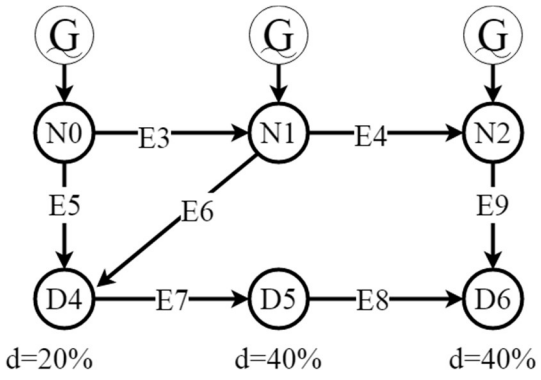

Figure IV.4: Network of IEEE 6-Bus test system

By following the steps in Algorithm 2, we construct the data for our investment optimization problem for a single event ($k = 1$). For convenience, we drop the index x from our parameters (e.g., we use $O_{i,j}$ instead of $O_{i,j,k}$). For a component, say generator $N1$ ($i = 1$), we find the values of $O_{i,j}, j = 1, \dots, m_i$ and related functionalities $f_{i,j,t}$. The calculations for the rest of the components will be similar. We choose the scale factor k_i to be the ratio $1/V_i$, which indicates that te investment will be proportionate to the value of the component. If we assume that the value of a brand new generator $N1$ is \$30,000 ($V_1 = 30000$), the value of k_1 will be 1/30000. If we invest \$7,500 on this generator (i.e., $y_1 = 7500$), then the cost factor τ_1 will be 0.25 ($\tau_1 = \eta_1 y_1 = 0.25$). In case both θ_i and V_i are given, then we can simply calculate the investment cost by $y_i = \tau_i V_i$. Associated with \$7,500 investment and a linear utility curve with $\gamma_{1,1}$ and $\gamma_{1,2}$ both equal to 0.5, the indifference curve in Figure IV.5 is constructed. Now we can choose as many points $p_{1,j} = (a_{1,j}, r_{1,j})$ on this curve as we need (e.g., $p_{1,1} = (0.5,0), p_{1,2} = (0,0.5)$, and $p_{1,3} = (0.25,0.25)$ with corresponding options of $O_{1,1} = (7500, 0.5,0), O_{1,2} = (7500,0,0.5)$, and $O_{1,3} = (7500,0.25,0.25)$). For a higher investment amount, say \$22,500, the cost factor θ_1 is 0.75 which provides better options such as $O_{1,4} = (22500,1.0,0.5)$ and $O_{1,5} = (22500,0.5,1.0)$. The above process constructs $p_{i,j}$ for a given $c_{i,j}$ (another way is to find the $c_{i,j}$ associate for a $p_{i,j}$ by first obtaining the θ_i using the utility function, and then multiplying it by V_i.) No matter whether we construct costs from enhancements or enhancements from cost, the goal in this step is to construct the investment options $O_{i,j}$, among which the decision maker will choose.

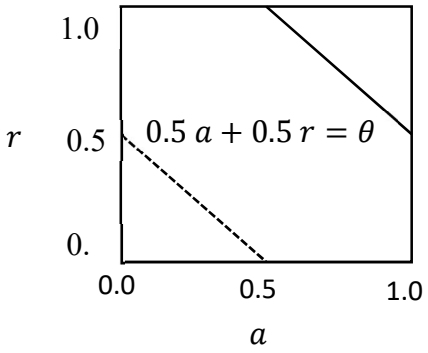

Figure IV.5: Change in the absorption and recovery of component *i* against event *k* for a) cost factor of 0.25 and b) cost factor of 1.5

Following the second way, we chose $p_{i,j}$ as in Figure IV.6Figure IV.6. For each component, the scenario $p_{i,0} = (0,0)$ is added and it stands for no enhancement option. The associated cost of these enhancement for a linear utility with γ_{i1} and γ_{i2} of 0.5 is summarized in the heat-map chart in Figure IV.7. In this figure darker cells indicates a higher investment (e.g., the cost of enhancing the component N1 by $(\mathrm{a}, \mathrm{r}) = (1,0.75)$ is 60). For each option $O_{i,j}$, we obtain the resulted functionality $f_{i,j,t}$ by considering the corresponding absorption and recovery.

r \ a	0	0.25	0.5	0.75	1
1		(0.25,1)	(0.5,1)	(0.75,1)	(1,1)
0.75		(0.25,0.75)	(0.5,0.75)	(0.75,0.75)	(1,0.75)
0.5		(0.25,0.50)	(0.5,0.5)	(0.75,0.5)	(1,0.5)
0.25		(0.25,0.25)	(0.5,0.25)	(0.75,0.25)	(1,0.25)
0	(0,0)				

Figure IV.6: Scenarios for $p_{i,j}$

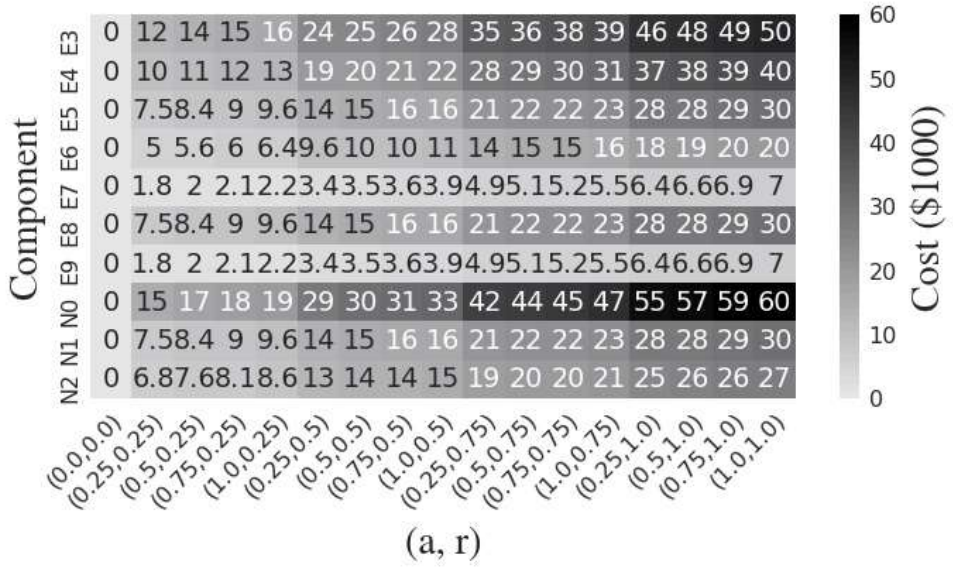

Figure IV.7: Heat-map of component investment options for a linear utility function with parameters γ_{i1} and γ_{i2} of 0.5 and 0.5 respectively. N1, N2, and N3 are nodes and E3 to E10 are electricity lines between the nodes. The color bar in the right shows the value cells in the heat map.

Utilizing the SCUC and the resilience metric in [131], Algorithm 1 outputs the RCI as in Figure IV.8. A failure in the component E9 has a higher impact on the resilience of the system and the component N2 disruption has the lowest effect. Now, the parameters $c_{i,j}, f_{i,j,t}, RCI_i,$ and $t_{i,j}$ for the problem Equations (6-1) to (6-5) are ready. Applying these parameters and optimizing the budget allocation for a budget limit of \$50,000 yields the solution in Table IV-2. We calculate the resilience metric for the optimal $P_{i,j}$. Let the initial resilience level of the system be $я = 0.73$, which happens when the absorption of all the components drop to 50% after an event and the recovery time is the same as mean time to repair of the component. The optimal investment in Table IV-2 with a total cost of \$49,500 improves the resilience level to $я = 0.84$.

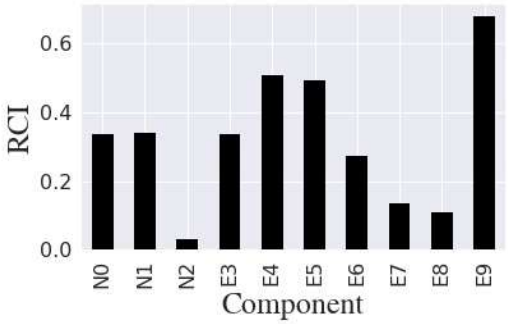

Figure IV.8: Component importance for IEEE 6-bus

Table IV-2: Optimal investments for linear utility with both parameters of 0.5 and budget limits of $50,000. The resulting total cast is $49,500 and the resulted objective is 0.372.

	N0	**N1**	**N2**	**E3**	**E4**	**E5**	**E6**	**E7**	**E8**	**E9**
$c_{i,j}^*$ **($1000)**	0	11.4	0	12.5	0	11.4	7.6	2.7	0	4.3
$a_{i,j,k}^*$	0	0.25	0	0.25	0	0.25	0.25	0.25	0	1
$r_{i,j,k}^*$	0	0.5	0	0.25	0	0. 5	0.5	0. 5	0	0.25

To find out the effect of different budget limits, further experiments are made on different budget scenarios. Considering that the value of the existing system is $301,000 ($\sum_{i=1}^{N} V_i$), we chose the values of $10,000, $50,000, $100,000, $150,000, and 300,000 for the budget limit. Following the steps for all these budgets, we will find the corresponding improvement in the resilience of the system (Figure IV.9Figure IV.9). For the budget of $150,000 and $300,000 the optimal solution yields the same amount of investment ($103,800) and the optimal solution remains the same. Hence, the highest budget that is needed to enhance the resilience of the 6-bus system with linear utility whose parameters are $(\gamma_{i1}, \gamma_{i2}) = (0.5, 0.5)$ is $103,800.

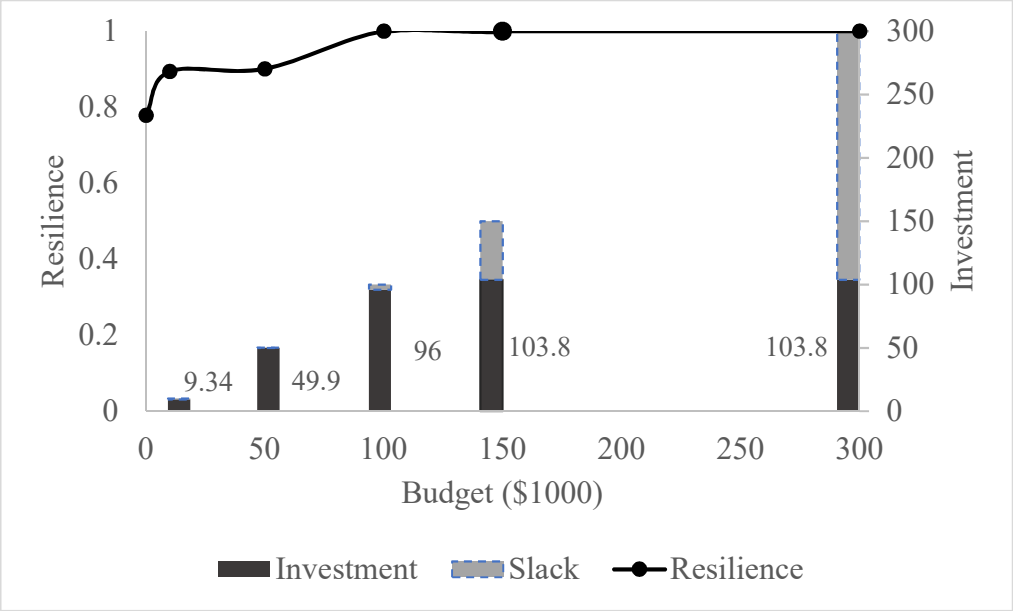

Figure IV.9: Resilience improvement within budget limits of \$10,000, \$50,000, \$100,000, \$150,000, and 300,000 and a linear utility function with $(\gamma_{1,1}, \gamma_{1,2}) = (0.5, 0.5)$.

The utility function and its parameters are inherent characteristics of a component. Knowing a utility function can help us to decide about the type of improvement in the component. Table 3 summarizes the $\theta_{i,j}$ for utility functions introduced in Table IV-1 with different parameters and $p_{i,j}$. Assuming that all the components have the same utility function, Algorithm 2 is applied for each utility function and budget limits of \$10,000, \$50,000, \$100,000, \$150,000, and 300,000. After obtaining the optimal allocation, the resulted resiliency measure is obtained as in Figure IV.*11*-13. The linear utility functions with parameters (γ_1, γ_2) of $(0.7, 0.3)$ and $(0.5, 0.5)$ show a higher cost and a lower resilience for budgets of \$10,000 and \$50,000. However, the amount of investment in the components can change this behavior. Figure IV.*13* shows the changes in the area under the functionality curves for different coefficients and cost factor θ. As θ increases the utility function shifts to the upper right (left-hand side plots in Figure IV.*13*), meaning that better absorption and recovery combinations are possible. The area under the functionality

curve, as a sub-metric of the resilience metric, shows highest value for the a to be 1. For an investment of 90% of the total value of the component (i.e., $\theta = 0.9$), the area under the utility curve approaches to 1, which means that the component is close to its highest functionality after an event. Based on Figure IV.*11*, the cost of enhancing resilience of a system whose components have a linear utility function with parameters of (0.9,0.1) is lower.

The Cobb-Douglas utility (Figure IV.*13*) with $\rho = 0.3$ and $\rho = 0.5$ resulted in similar resilience and investment costs. A $\rho = 0.1$ has a resilience similar to $\rho = 0.3$ and $\rho = 0.5$ but with lower costs for budget limits over $\$100{,}000$. The other two parameters ($\rho = 0.7$ and $\rho = 0.9$) resulted in a lower cost and a higher resilience. If components have a CES utility with parameters (γ, ρ) of (0.5,1), then system will reach to its highest resilience level for a budget greater than $\$100{,}000$, while this budget limit is $\$50{,}000$ for other parameters. If the goal is to increase the resilience of the system from $я = 0.73$ to a resilience around $я = 0.9$, then CES with parameters (0.3, 0.1) would need a more budget.

Table IV-3: Cost factor $\theta_{i,j}$ of absorption and recovery scenarios for utility functions

		$p_{i,j,k} = (a_{i,j,k}, r_{i,j,k})$																
Utility function	**parameters**	**(0,0)**	**(0.25,0.25)**	**(0.25,0.5)**	**(0.25,0.75)**	**(0.25,1)**	**(0.5,0.25)**	**(0.5,0.5)**	**(0.5,0.75)**	**(0.5,1)**	**(0.75,0.25)**	**(0.75,0.5)**	**(0.75,0.75)**	**(0.75,1)**	**(1,0.25)**	**(1,0.5)**	**(1,0.75)**	**(1,1)**
Linear (γ_1, γ_2)	**(0.1, 0.9)**	0	0.25	0.48	0.7	0.92	0.28	0.5	0.73	0.95	0.3	0.52	0.75	0.98	0.32	0.55	0.78	1
	(0.3, 0.7)	0	0.25	0.42	0.6	0.77	0.32	0.5	0.68	0.85	0.4	0.57	0.75	0.92	0.48	0.65	0.82	1
	(0.5, 0.5)	0	0.25	0.38	0.5	0.62	0.38	0.5	0.62	0.75	0.5	0.62	0.75	0.88	0.62	0.75	0.88	1
	(0.7, 0.3)	0	0.25	0.32	0.4	0.48	0.42	0.5	0.57	0.65	0.6	0.68	0.75	0.82	0.77	0.85	0.92	1
	(0.9, 0.1)	0	0.25	0.28	0.3	0.32	0.48	0.5	0.52	0.55	0.7	0.73	0.75	0.78	0.92	0.95	0.98	1
Cobb-Douglas ρ	**0.1**	0	0.25	0.47	0.67	0.87	0.27	0.5	0.72	0.93	0.28	0.52	0.75	0.97	0.29	0.54	0.77	1
	0.3	0	0.25	0.41	0.54	0.66	0.31	0.5	0.66	0.81	0.35	0.56	0.75	0.92	0.38	0.62	0.82	1
	0.5	0	0.25	0.35	0.43	0.5	0.35	0.5	0.61	0.71	0.43	0.61	0.75	0.87	0.5	0.71	0.87	1
	0.7	0	0.25	0.31	0.35	0.38	0.41	0.5	0.56	0.62	0.54	0.66	0.75	0.82	0.66	0.81	0.92	1
	0.9	0	0.25	0.27	0.28	0.29	0.47	0.5	0.52	0.54	0.67	0.72	0.75	0.77	0.87	0.93	0.97	1
CES (β, ρ)	**(0.1, 0.5)**	0	0.25	0.47	0.69	0.9	0.27	0.5	0.72	0.94	0.29	0.52	0.75	0.97	0.3	0.54	0.77	1
	(0.3, 0.1)	0	0.25	0.41	0.55	0.67	0.31	0.5	0.67	0.82	0.35	0.57	0.75	0.92	0.39	0.62	0.82	1
	(0.5, 1)	0	0.25	0.38	0.5	0.62	0.38	0.5	0.62	0.75	0.5	0.62	0.75	0.88	0.62	0.75	0.88	1
	(0.7, 0.3)	0	0.25	0.31	0.36	0.4	0.41	0.5	0.57	0.63	0.56	0.67	0.75	0.82	0.7	0.82	0.92	1
	(0.9, 0.4)	0	0.25	0.27	0.29	0.3	0.47	0.5	0.52	0.54	0.69	0.72	0.75	0.77	0.9	0.94	0.97	1

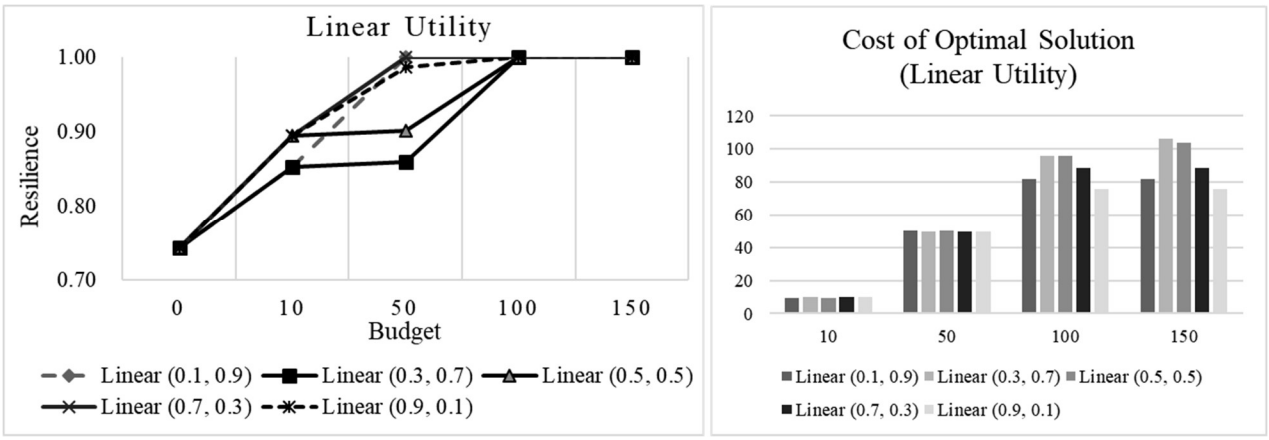

Figure IV.10: Resilience for linear utility functions achieved by applying the enhancement in the optimal solution for different budgets for linear utility functions.

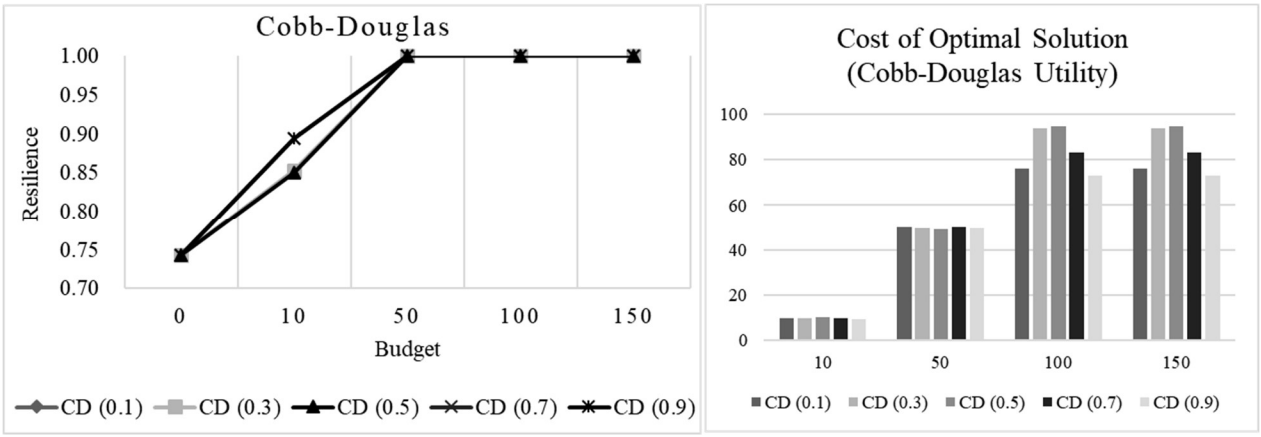

Figure IV.11: Resilience for Cobb-Douglas utility functions achieved by applying the enhancement in the optimal solution for different budgets for Cobb-Douglas utility functions.

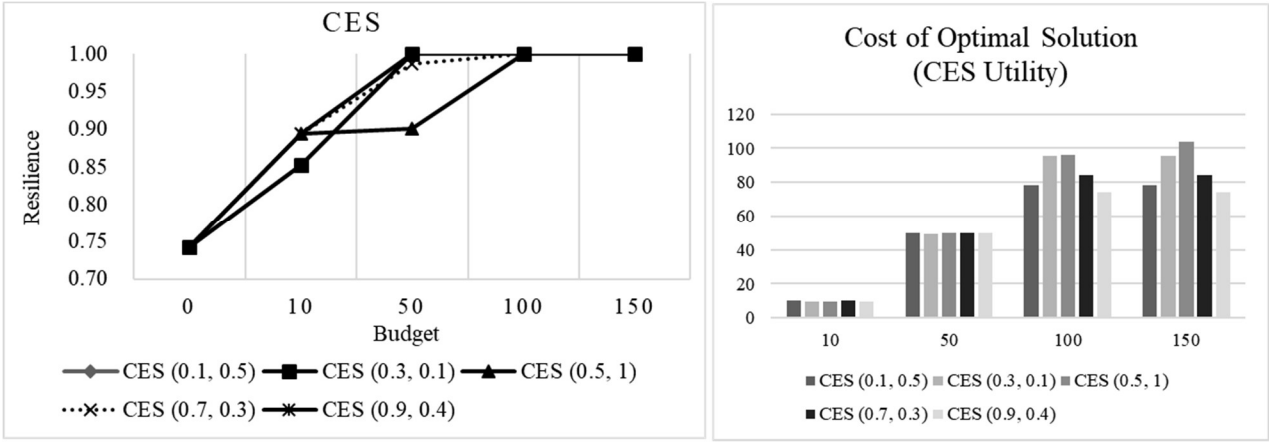

Figure IV.12: Resilience for CES utility functions achieved by applying the enhancement in the optimal solution for different budgets for CES utility functions.

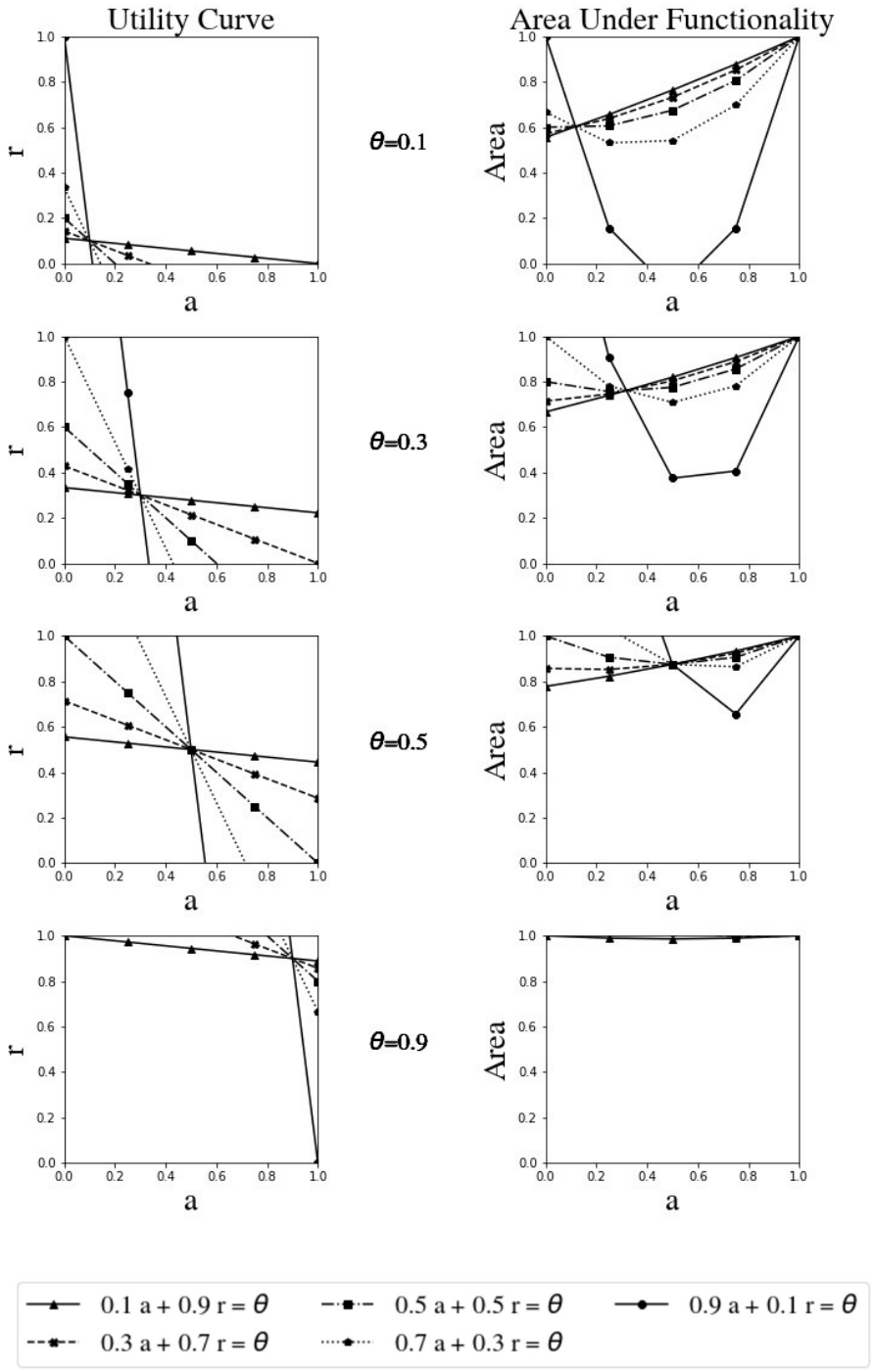

Figure IV.13: Linear utility curves: charts on the left are linear utility curves for different values of investment and parameters. Charts on the right are the area under utility function for the utility functions on the left.

In summary, if components of the system we considered in our numerical analysis, all have a Cobb-Douglas utility curve with $\rho = 0.9$, then the system will become more

resilient with a lower investment comparing to other utility functions. If we have two components with the same functionality and cost, but with two different utility curves, we can use similar analysis to choose one them. For a budget limit and known utility functions, Algorithm 2 can give the optimal budget allocation to maximize the resilience.

4.4. Conclusion

This study introduced a quantitative method to enhance system resilience under the budgetary constraint. Different states of enhancements for component's absorption and recovery were elaborated and a metric was introduced to measure the resilience-based component importance. A mathematical programming formulation was developed to optimally allocate budget to components while maximizing the resilience within the limited budget. Due to the difficulty of drawing an analytical relationship between investment and system resilience, we have developed an algorithm consisting of two steps, in which the investment options and components' functionality were discretized; hence, it overcomes the computational difficulty. The proposed optimization model determines how much to invest to each selected component, and optimal levels of enhancement in the component's absorption and recovery time. The proposed approach was tested on the IEEE 6-bus and the effects of different utility curves were discussed on the cost of enhancement and system's resilience level. Using the test case, we have demonstrated how optimally allocate budget to enhance the system resilience. Moreover, we have observed that the resilience of a system may be enhanced with a lower budget if the components follow a Cobb-Douglas utility function.

CHAPTER 5

V. MULTI-ARC DISRUPTION WITH MAXIMUM IMPACT ON NETWORK FLOW

In a network flow problem, critical arcs can be defined as arcs in which a failure occurrence results in maximum impact on the network flow. The problem of multi-arc disruption with maximum impact (MADP) aims to find multiple critical arcs whose simultaneous disruptions result in the maximum flow disruption of the network. This problem can be formulated as a mixed-integer programming (MIP) model. The MIP problem is computationally expensive; hence, this paper aims to reduce computational time. The contributions are a) a new problem formulation is presented following a pattern generation approach to provide a near optimal solution, and b) a fast heuristic is developed to find a good initial feasible solution for warm-start MIP. For this heuristic, a new centrality measure is developed. Our numerical results show that the initialization heuristic reduces the computational time for MIP drastically (between 10% to 90% percent). Moreover, the proposed pattern generation reduces the CPU time considerably while the gap between optimal objective value and the pattern generation approach is small and in in 70% of the cases the gap is zero.

5.1. Introduction

Disrupting an adversarial network is of interest in many domains. The adversarial network can be an enemy infrastructure, such as transportation system [132] of a drug,

weapon, or human trafficking network [133]; or an information network [132]. From a game theoretical perspective, an interdictor (attacker) has limited resources to disrupt an adversarial network while an adversary (defender) aims to maximize the flow through the disrupted network (residual network) [133]. In many cases, the resource limit can be translated into the number of arcs in the network to be disrupted (ϑ). For example, resources can be a limited number of missiles available to strike enemy's transportation system. Another example is the number of checkpoints in the supply chain of precursor chemicals for drug production [134]. In this case, the attacker is interested in selecting ϑ arcs whose disruption will have the highest impact on the defender's network [135], i.e., it minimizes the maximum flow in the residual network. Another application of the problem is to predict a terrorist's potential targets and reduce the impact caused by the terrorist attack on the network [136]. For example, a terrorist sets fire in a place and tries to maximize the shortest path of fire trucks to prevent them from reaching to the fire on time. The goal of the terrorist is to find the most vital arcs whose failure will result in the greatest increase in the length of the shortest path [137]. Therefore, one might be interested in protecting those arcs from such attacks to mitigate the resulting impact.

Different approaches can be used to find ϑ arcs to be disrupted. One approach can be based on some network measures. If the attacker has enough resources and the goal is to shut down the whole network, node and arc connectivity measures can be utilized. The *node connectivity* is the smallest number of nodes whose removal results in a disconnected or single-node graph. It is the smallest number of node-distinct paths between any two nodes [138]. Similarly, the *arc connectivity* is the smallest number of links whose removal results in a disconnected graph. Another group of metrics include *centrality measures*,

which are commonly described as indices of prestige, prominence, importance, and power [139]. The shortest-path-betweenness centrality is a measure of the extent to which a component is located on the paths between two other components [140]. It indicates how much a component has control over the flow between the components. Hence, their removal can have a negative impact on the network. The *eigenvector centrality* measures the influence of a node in a network and it depends on both the centrality of the component and the centrality of its neighbors [141]. Google's PageRank algorithm is a variant of eigenvector-centrality and is used to rank web pages in the search engine results. Eigenvector-centrality is Katz centrality and it measures the relative degree of influence of a node in a social network [142]. Freeman and Borgatti [139] introduced a *flow-betweenness centrality* (φ) that incorporates the strength of the linkage between nodes into the metric. Flow can be physical (e.g., used goods and money) or it can be non-physical (e.g., gossip, attitude). In an *s-t* network flow [143], arcs can be ranked based on their relative contribution to the flow in the network, i.e., based on their φ value. This metric can be useful when we are interested in a single vital arc; if the single arc with the highest φ is disrupted, the decrease in the network output will be high. However, for the problem of multiple-arc failure with maximum impact on network flow, these metrics may not provide the best solution, as they do not consider the effect of simultaneous disruption of arcs on the network flow.

An approach to solve MADP is to formulate the problem as a bilevel (attacker-defender) model, where in the upper level the attacker selects ϑ arcs to disrupt and in the lower level, the defender maximizes the flow through the residual network. The upper level objective is to minimize the maximum flow in the lower level. When the attacker has

enough resource to disrupt one arc ($\vartheta = 1$), the problem of finding a single vital arc in a network flow can be solved using the Newton algorithm [144]. The bilevel problem of finding ϑ arcs is NP-hard [133]. Some efforts were made in the literature to reduce the computational cost [133] by using a binary programming model that maximizes the sum of the arc capacities under attack; however, solving this model is still computationally expensive [134]. A Lagrangian-relaxation based heuristic has also been explored to provide a local optimum [134].

The goal of this study is to present methods to reduce the computational burden for solving the MADP. The contributions are twofold. First, a mathematical programming model is presented, and a pattern generation algorithm is proposed to solve it. Second, a new centrality measure and a heuristic are introduced to provide a good initial solution for the MIP formulation. The heuristic utilizes the path-based network flow problem. This initial solution is also used in the proposed pattern generation. The organization of the rest of this paper is as follows. Chapter 2 describes the path-based mathematical programming model for MADP. Chapter 3 presents the solution methodology which includes two algorithms. The first algorithm provides an initial solution generation strategy and the second is a pattern generation algorithm to solve the MADP. Section 4 provides the numerical results. The conclusion is drawn in Chapter

5.2. Multiple-Arc Failure Maximum Impact (MADP) Mathematical Formulation

Let $G = (V, E)$ be a directed graph or digraph where V is a set of vertices (nodes) and $A \subseteq V \times V$ is a set of arcs. Let G have two special nodes *s* and *t* (called the source and

the sink, respectively). Each arc is an ordered pair $e_{uv} = (u, v), u, v \in V$. A path $(P_{v_1 v_l})$ between nodes v_1 and v_l is a sequence of adjacent nodes v_i, $1 \leq i \leq l$, such that $(v_i, v_{i+1}) \in E$. In this study, the networks are assumed to be directed acyclic graph (DAG), or in other words, a directed graph with no cycles. Suppose an arc e_{uv} has a capacity of c_{uv}. A flow is a function which assigns the amount of flow f_{uv} to arc e_{uv}.

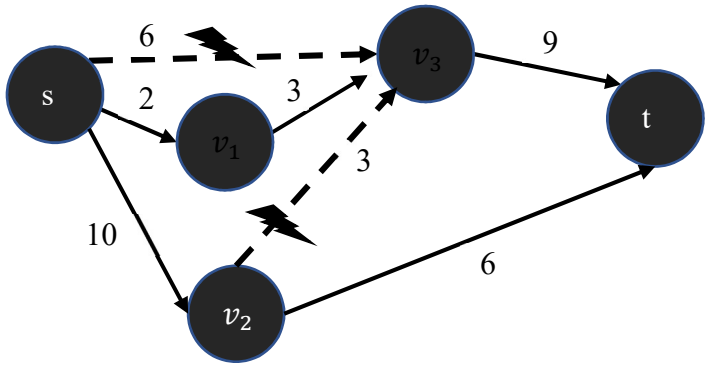

Figure V.1: MADP in a network flow

The MADP can be formulated as a bilevel programming model [145]. Prior to a disruption, an adversary (defender) flows the maximum commodity or information possible through a network from a source vertex (s) to a terminal vertex (t) (Figure V.*1*). In the upper level, the attacker disrupts a predetermined number (ϑ) of arcs in the adversarial network (e.g., arcs (s, v_3) and (v_2, v_3) in Figure V.*1* with $\vartheta = 2$). The defender notices the damages to the network and acts accordingly, i.e., in the lower level problem he changes its operations to maximize the flow through the residual network (the network excluding the disrupted arcs). The attacker is aware of the defender's goal and tries to choose ϑ arcs in a way that the adversary's maximum flow is minimized. Let y_{uv} be a binary variable that shows the attacker's decision, where

$$y_{uv} = \begin{cases} 1 & if\ arc\ (u,v) is\ selected, \\ 0 & otherwise \end{cases}$$

shows the attacker's decision. In the upper level, the attacker selects ϑ arcs. In the upper level the attacker selects ϑ arcs (Equation (1-2)), whose disruption will drop the flow through those arcs to 0 (Equation (1-4)). The flow through each arc is limited by its capacity (Equation (1-4)). Moreover, the flow is conserved (Equation (1-5)), and it does not flow into the source or out of the sink (Equation (1-6)). After disruption, the defender maximizes the flow in the residual network. The goal of the attacker is to minimize the maximum flow of the defender (Equation (1-1).

$$\min_{y} z_y \tag{1-1}$$

s.t.
$$\sum_{(u,v)\in E} y_{uv} = \vartheta, \tag{1-2}$$

$$z_y = \max_{f} \sum_{v\in V} f_{sv}\,, \tag{1-3}$$

s.t.
$$f_{uv} \le c_{uv}(1 - y_{uv}) \forall u, v \in V, \tag{1-4}$$

$$\sum_{u:(u,v)\in E} f_{uv} = \sum_{w:(v,w)\in E} f_{vw}, \tag{1-5}$$

$$f_{us} = f_{tu} = 0, \forall u, \tag{1-6}$$

$$f_{uv} \ge\ 0, y_{uv} \in \{0,1\}, \forall u, v \in V. \tag{1-7}$$

5.3.1. A path-based model formulation

The path-based formulation [146], [147] of Problem (1) is used in the literature to reduce the problem size. Let $\wp$ be a set of all distinct paths that contain at least one unique arc. For brevity, instead of denoting an arc with e_{uv}, it is shown as j, where j is a unique number assigned to an arc. Hence, a path-arc incidence matrix (P) can be defined as

$$P = \begin{matrix} \\ \text{Paths} \end{matrix} \begin{matrix} \text{Arcs} \\ \begin{bmatrix} p_{11} & \cdots & p_{1m} \\ \vdots & \ddots & \vdots \\ p_{h1} & \cdots & p_{hm} \end{bmatrix} \end{matrix}$$

where

$$p_{ij} = \begin{cases} 1 & \text{if arc } j \text{ is an incident in path } i, \\ 0 & \text{otherwise.} \end{cases}$$

One should note that this matrix does not show the sequence of incidences. Moreover, if arc e_j is incident to more than one path, then the aggregation of flows in all paths passing through e_j should be less than the arc's capacity (i.e., $\sum_i p_{ij} f_i \leq c_j$). Let $f = (f_1 \dots f_h)$ be the vector of the defender decision variables and $y = (y_1 \dots y_m)$ be the vector of the attacker decisions. Equations (2-1) through (2-5) construct the path-based bilevel MADP. In the upper level (Equations (2-1) and (2-2)), the attacker decides which arcs to attack. These arcs must meet the resource limitation (Equation (2-2)). In the lower level (Equations (2-3) through (2-5)), the defender maximizes the network flow in the residual network.

$$\min z \tag{2-1}$$

$$\text{s.t.} \quad \mathbf{1}^T y = \vartheta, \tag{2-2}$$

$$z = \max \mathbf{1}^T f, \tag{2-3}$$

$$P^T f \leq C(\mathbf{1} - y), \tag{2-4}$$

$$f \geq 0, y \in \{0,1\}^{|E|}. \tag{2-5}$$

5.3. Solution Approach

To reduce the computational burden for solving Problem (2), we provide two different solution approaches. The first one is a warm-start approach for the MIP model in which a heuristic method is used to initialize values of y so that the MIP model can be

solved much faster than the MIP model with default values provided by a commercial solver. The second approach is based on a model reformulation, followed by a pattern generation algorithm to solve it.

5.3.2. MIP formulation

Problem (2) is reformulated as an MIP model through the following process. After the attacker has made the decision on which arcs ($\hat{y}$) to disturb, the $\hat{y}$ remains constant for the defender in the lower level, in a way that the Equations (2-3) through (2-5) construct a linear programming. Hence, it can be replaced by its dual problem.

Let $w = (w_1 \dots w_m)$ be the dual variable corresponding to constraints (2-4), the dual of the subproblem for a fixed $\hat{y}$ is

$$z = \min_{w} C(\mathbf{1} - \hat{y})w, \tag{3-1}$$

$$\text{s.t.} \quad Pw \geq \mathbf{1}, \tag{3-2}$$

$$w \geq 0. \tag{3-3}$$

Problem (4) is an LP formulation of the minimum cut problem [148]. By applying these changes in the subproblem of Problem (4), the MADP becomes as:

$$\min_{\mathrm{y}} z, \tag{4-1}$$

$$\text{s.t.} \quad e^T y = \vartheta, \mathrm{y} \in \{0,1\}^{|E|}, \tag{4-2}$$

$$z = \min_{w} C(\mathbf{1} - \hat{y})w, \tag{4-3}$$

$$Pw \geq \mathbf{1}, \tag{4-4}$$

$$w \geq 0. \tag{4-5}$$

By replacing z in Equation (4-1) with Equation (4-3), the problem becomes

$$\min_{\mathrm{y}} \min_{w} C(\mathbf{1}-y)w\,, \tag{5-1}$$

$$\text{s.t.} \quad \mathbf{1}^T y = \vartheta, \tag{5-2}$$

$$Pw \geq \mathbf{1}, \tag{5-3}$$

$$\mathrm{w} \geq 0, \mathrm{y} \in \{0,1\}^{|E|}. \tag{5-4}$$

The objective (5-1) then can be changed to

$$\min_{w,y} \sum_{j\in E} c_j(1-y_j)w_j = \sum_{j\in E} c_j(w_j - y_j w_j). \tag{6}$$

The objective function in Equation (6) is non-convex, and the optimality is not guaranteed. Therefore, we linearize it by setting $x_j = y_j w_j$ and exploiting a sufficiently large number M. As a result, the new formulation is:

$$\min C(w-x) \tag{7-1}$$

$$-M\mathrm{y} \leq x \leq M\mathrm{y}, \tag{7-2}$$

$$M(\mathbf{1}-y) \leq w - x \leq M(\mathbf{1}-\mathrm{y}), \tag{7-3}$$

$$Pw \geq \mathbf{1}, \tag{7-4}$$

$$\mathbf{1}^T\mathrm{y} = \vartheta \tag{7-5}$$

$$w, x \geq 0, \mathrm{y} \in \{0,1\}^{|E|}. \tag{7-6}$$

Equation (7-1) and the variable linearization equations (Equations (7-2) and (7-3)) minimize the minimum cut capacity. This is equivalent to minimizing the maximum flow in the network. Equation (7-4) is the dual constraint in the path based minimum cut problem [148]. Equation (7-5) sets the limit on the number of arcs to be disrupted.

5.3.3. Initialization

This section introduces an initialization heuristic for variable vector y to solve the MIP model faster. A new metric, min-flow-betweenness centrality (φ), is developed, which is an integral part of the heuristic. The maximum-flow-betweenness (MFB) centrality introduced in [139] evaluates the maximum possible flow that can pass through an arc. The MFB of an arc is less than or equal to the arc capacity. For example, in Figure V.*1*, the arc (v_2, t) with capacity 6 has a an MFB equal to 4 which implies that the network set up doesn't allow it to utilize more than 4 units of its capacity. However, if an arc with high MFB is disrupted, other paths may have the capacity to carry a large portion of that flow (i.e., there can be an arc with high MFB but with low impact). Instead, our metric considers the minimum flow φ_j that can pass through arc j and does not decrease the maximum flow. The network in Figure 1 has four paths, delivered as $p_1: s \to v_3 \to t$, $p_2: s \to v_1 \to v_3 \to t$, $p_3: s \to v_2 \to v_3 \to t$, and $p_4: s \to v_2 \to t$ Assume that in the optimal solution, the flow along p1, p2, p3, and p4 are 6, 2, 1, and 4, respectively; these values are combined to create a maximum flow of 15. The maximum flow that can pass through the arc (v_1, v_3) is 2. However, if we choose to flow 3 units through p_3, the flow in p_2 will drop to 0 while the maximum flow of the network remains 15. The value of φ for the arc (v_1, v_3) is zero.

Let $1'$ and $2'$ represent the new indices such that $\varphi_{1'} \geq \varphi_{2'}$. When the problem refers to finding a single arc with the highest impact on the maximum flow, the solution is to select arc $e_{1'}$. However, in the case of $\vartheta \geq 2$ components, removing $e_{1'}, e_{2'}, \dots, e_{\vartheta'}$ may not result in the highest impact. Consider the simple network in Figure V.*2*. In this network $\varphi_1 = \varphi_2 = 5$, and $\varphi_3 = \varphi_4 = 2$, and the network has a maximum flow of 7. For $\vartheta = 1$, the solution to MADP is either e_1 or e_2, and the residual network maximum flow will be

2. If $\vartheta = 2$ and we choose the two components with highest values of φ_j (i.e., e_1 and e_2), then two units can still flow through the rest of the network. However, if we choose e_1 and e_3, then no flow can pass through the network.

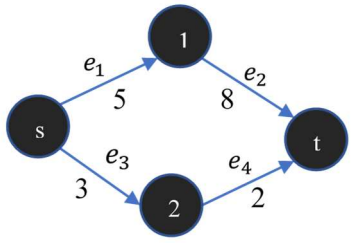

Figure V.2: A simple network. The numbers on the arcs are arc capacities.

In neuroscience, the functional connectivity is a matrix that captures the change in the level of activation regions of the brain in response to specific experimental conditions [149]. We define the functional connectivity of arcs similarly.

Definition: For two arcs e_l and e_j in E, *functional connectivity* is defined as the possible amount of change in the *MFB* of e_j if the functionality of e_l is disrupted.

$$\Gamma_l = [\gamma_{lj}]_{j \in E}$$

The vector Γ_l constructs the rows of the functional connectivity matrix Γ. Using the functional connectivity, we propose an algorithm that determines ϑ arcs (i.e., vector y) that serves as an initial solution. Let l be the index of the arc with the largest φ_j. Algorithm 1 begins by selecting arc e_l which reduces the maximum flow the most significantly, i.e., by $\varphi_l = \max_i \varphi_i$. The value of φ_j for the residual network after removing arc e_l will be decreased by γ_{lj} ($\varphi_{new} = \varphi - \gamma_{lj}$). Then, we choose the arc with largest φ_{new} as the second arc. In this algorithm, matrix P is collocated with the paths' capacity in the last

column, φ_j in the last row, and two, the number of arcs of to be disrupted in the last entry of the matrix. The tableau matrix will look like the Figure V.3:

$$M = \begin{array}{c} \\ Paths \\ \\ \varphi \end{array} \begin{array}{c} \begin{array}{cccc} Arcs & & & Q \end{array} \\ \left[\begin{array}{cccc:c} p_{11} & \cdots & p_{1m} & q_1 \\ \vdots & \ddots & \vdots & \vdots \\ p_{h1} & \cdots & p_{hm} & q_h \\ \hdashline \varphi_1 & \ldots & \varphi_m & \vartheta \end{array}\right] \end{array}$$

Figure V.3: Collocated matrix P, Q, φ_j, and k.

This algorithm also removes the redundant paths, thus drastically reducing the problem size at each iteration.

Algorithm 1

Input: A set of paths $\wp$

Output: $\mathbb{Q}$:= list of arcs to be disrupted

Step 1. Set counter =1; $\mathbb{Q} = \{\}$.
Step 2. Calculate/update φ_j.
Step 3. Select the arcs with highest φ_j.
Step 4. Delete the rows in which column j entry is 1.
Step 5. Delete column j and add j to the set $\mathbb{Q}$.
Step 6. If counter is equal to k or the maximum flow is 0 then
go to Step 6
else
go to Step 2
Step 7. Set counter=counter +1.
Step 8. Output the $\mathbb{Q}$

5.3.4. Pattern Generation Approach

The number of variables in Problem (2) and Problem (7) grow exponentially as the number of arcs grows. To address this challenge, a pattern generation (PG) is proposed by

reformulating Problem (2) to Problem (8). In PG, a master problem and corresponding subproblems are constructed [150]. The PG process starts with an initial pattern $\hat{y}$, finds the dual solution of the master problem, and uses them in the pricing subproblem to generate a new pattern. A difference between PG and the column generation [151] is that in column generation, the constructed pattern in the subproblem is appended to the technical coefficients, whereas in PG the current pattern is replaced with the new pattern. We propose a new formulation for Problem (2) and solve it using the pattern generation. A pattern $\hat{y} \in \{0,1\}^{|E|}$ has exactly ϑ entries where value 1 (i.e., $e^T\hat{y} = \vartheta$) indicates which arc is disrupted and as a result the flow in all the paths passing through them is stalled (Equation (8-2)).

$$z = \max \mathbf{1}^T f, \tag{8-1}$$

$$\text{s.t.} \quad p^T f + C\hat{y} \leq c, \tag{8-2}$$

$$f \geq 0. \tag{8-3}$$

In each iteration, the subproblem generates a new pattern that provides a better solution to Problem (8). Consider the general maximization problem in the form of

$$\max d^T x, \tag{9-1}$$

$$Ax \leq b, \tag{9-2}$$

$$x \geq 0, \tag{9-3}$$

where $d = (d_1 \dots d_n)$ is the cost coefficient, $X = (x_1 \dots x_n)$ is the non-negative decision variable, b is the resource constraint, and $A = [y_{ij}], i = 1..h,\ j = 1..m,$ is the technological coefficient. The current objective expression [152] for a feasible solution is

$$z = d_B A_B^{-1} b - \sum_{j \in NBV} \left(d_B A_{Basis}^{-1} y^j - d_j \right) x_j, \tag{10}$$

in which variables are divided into two groups: basic (BV) and non-basic (NBV) variables. Matrix A_{Basis}^{-1} consists of the columns of A corresponding to BVs, and y^j is the jth column of A. If a variable with negative $d_B A_{Basis}^{-1} y^j - d_j$ enters the basis, then the objective value will be increased; if a variable with positive value enters, then the objective value will be decreased. We are interested in the latter. The subproblem for the PG algorithm is

$$z^{sub} = \max \pi^{*T} C y, \tag{11-1}$$

$$\text{s.t} \quad \mathbf{1}^T y = \vartheta, \tag{11-2}$$

$$y \in \{0,1\}^{|E|}. \tag{11-4}$$

in which $\pi^{*T} C y$ equals $d_B A_{Basis}^{-1} y^j - d_j$. Problem (11) attempts to find a pattern that can decrease the current maximum flow. The pattern y must satisfy the constraint in Equation (5-2), i.e., this pattern has exactly ϑ non-zero variables. If the object value of Problem (11) is positive and it is different from the previous solution, then the new pattern will replace the current pattern. Algorithm 2 summarizes the PG process for MADP. It starts with generating an initial solution using Algorithm 1; then, it finds the dual values of the master problem. Using the dual values, Problem (11) finds a new pattern, and the process continues until the stopping criteria are met.

Algorithm 2 Pattern Generation for MADP

Input: the network

Output: The optimal solution to MADP

Step 1. Create an initial plan using Algorithm 1

Step 2. Set the current pattern to the initial pattern.

Step 3. Run the master problem (Problem (6)) for the current pattern.

Step 4. Use the optimal dual solution of the master problem and solve the subproblem

a. If the optimal objective value of the subproblem is positive and the current pattern is different from the previous pattern, set the current pattern to the pattern generated in the subproblem and go to 3.

b. Else go to 5

Step 5. Output the current pattern as optimal.

5.4. Numerical Results

We start the numerical example with a simple network presented by Freeman [139] (Figure V.4); we name it Net 1 for future reference. This network has four paths; the first path (p_1) begins at node s, passes through node 3, and ends at node t. Equivalently, path p_1 passes through arcs e_3 and e_7 (shown as $p_1: e_3 \rightarrow e_7$). Similarly, the other paths are $p_2: e_1 \rightarrow e_4 \rightarrow e_7$, $p_3: e_2 \rightarrow e_6 \rightarrow e_7$, and $p_4: e_2 \rightarrow e_5$. Figure V.5 shows the incident matrix P associated with these four paths. Suppose that the attacker has sufficient resources to attack two arcs (i.e., $\vartheta = 2$). The attacker then has $\binom{7}{2} = 21$ options to choose from (Figure V.6). Step 1 in Algorithm 1 starts with an empty set $\mathbb{Q}$ and sets the counter to 1. In Step 2, vector φ is calculated (Figure V.7). The arc with the highest value of φ (i.e., e_7 with $\varphi_7 = 4$ for Net 1) is selected in Step 3. Removing e_7 will disrupt the flows from paths p_1, p_2, and p_3. Hence, in Step 4, these paths are removed from the incidence matrix. Then e_7 column is removed, and it is added to set $\mathbb{Q}$ (i.e., $\mathbb{Q} = \{e_7\}$). Sine the counter is 1, being less than $\vartheta = 2$, we go to Step 2 for the second iteration. We can easily find the functional

connectivity for e_7, which is the updated φ after the removal of e_7; updating the functional connectivity $\Gamma_7 = (3,0,1,3,0,1)$ from φ results in

$$\varphi_{new} = \varphi - \Gamma_7 = (3,2,1,3,2,0,4) + (-3,0,-1,-3,0,0,-4) = (0,2,0,0,2,0,0). \quad (10)$$

Based on the φ_{new}, two options e_2 and e_5 will provide the same result. We select e_2 arbitrarily and update $\mathbb{Q} = \{e_7, e_2\}$. The resulting initial solution is $y = (0,1,0,0,0,0,1)$. Removing these two arcs will drop the maximum flow to 0. So, in this case, we do not need to run the MIP model.

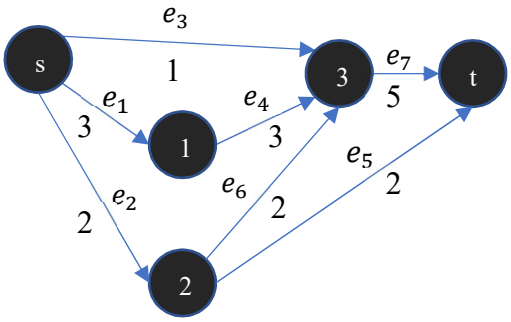

Figure V.4 Network of Net 1 [139]

Arc

	e_1	e_2	e_3	e_4	e_5	e_6	e_7
p_1	0	0	1	0	0	0	1
p_2	1	0	0	1	0	0	1
p_3	0	1	0	0	0	1	1
p_4	0	1	0	0	1	0	0

$A =$

Figure V.5 Path arc incidence matrix

	1	2	3	4	5	6	7	8	9	10	11	12	13	14	15	16	17	18	19	20	21
a_1	1	1	1	1	1	1	0	0	0	0	0	0	0	0	0	0	0	0	0	0	0
a_2	1	0	0	0	0	0	1	1	1	1	1	0	0	0	0	0	0	0	0	0	0
a_3	0	1	0	0	0	0	1	0	0	0	0	1	1	1	1	0	0	0	0	0	0
a_4	0	0	1	0	0	0	0	1	0	0	0	1	0	0	0	1	1	1	0	0	0
a_5	0	0	0	1	0	0	0	0	1	0	0	0	1	0	0	1	0	0	1	1	0
a_6	0	0	0	0	1	0	0	0	0	1	0	0	0	1	0	0	1	0	1	0	1
a_7	0	0	0	0	0	1	0	0	0	0	1	0	0	0	1	0	0	1	0	1	1

Figure V.6: Possible options to select two arcs from Net 1

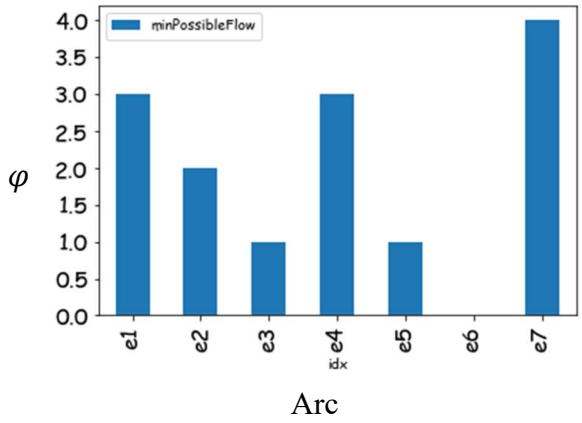

Figure V.7: The MFB for network of net1

The PG process begins with the initial pattern obtained using Algorithm 1. The master problem is solved after fixing y to the initial pattern. The duals of the constraints of the master problem then are used in the pricing subproblem to generate a new pattern y. To validate the PG approach, 200 randomly generated graphs are used for numerical experiments (see Appendix I). Figure V.*8* shows the histogram of the number of arcs for the generated networks, detailing a near-normal distribution with a mean of 100 and a standard deviation of 47 arcs. For each network, the optimal solution of the MADP problem using the PG is compared to the exact solution obtained from the MIP model. The gap between the two objective values resulting from the two approaches is measured as

$$gap = \frac{z^*_{PG} - z^*_{MIP}}{z^*_{MIP}}. \quad (11)$$

Figure V.*9* shows the histogram of the gap in the generated networks. The MADP is solved for each network for $\vartheta = 1, \ldots, 6$. This histogram shows that the MADP found an optimal solution (i.e., gap = 0) in 71% of the problems, while the gap ranged between 0 and 0.15 for 20% of the cases. Although the PG does not guarantee optimality, it finds a good solution at a small fraction of time to solve the optimization model. Hence, it can be a

decent way to generate an initial starting solution for the MIP model from which it can start its Branch-and-Bound process to speed up the convergence.

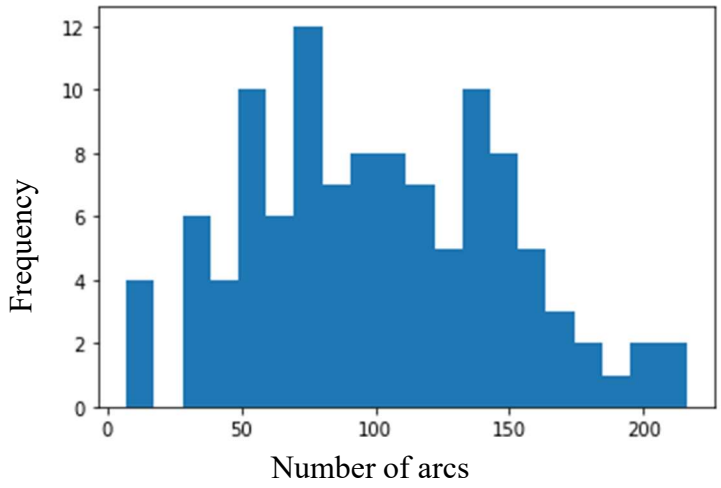

Figure V.8: Histogram of number of arcs

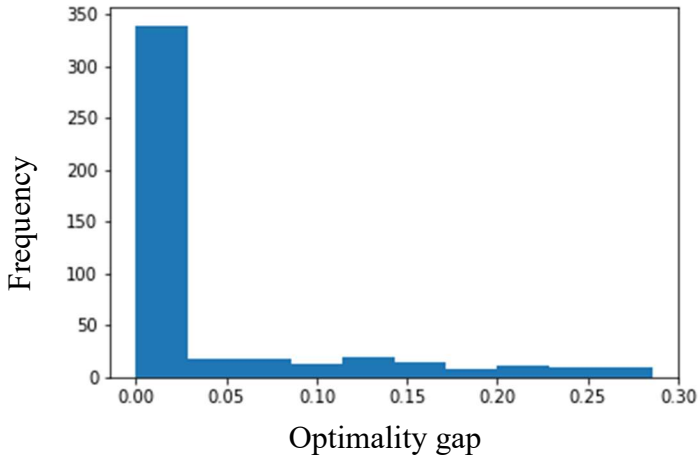

Figure V.9: Histogram of the objective gap between optimal CG and objectives

To illustrate the effectiveness of the proposed solution approach, a subset of networks is randomly selected from the previously generated networks; they are labeled as Net 2, …, Net 5. The network in Figure V.4 with 5 nodes and 7 arcs is also included and is named Net 1. All computational experiments are made on a personal computer with Core i5-3470S 2.9 GHz CPU and 8 Gigabyte of RAM. To account for the effect of the

performance of the PG on the CPU time, each experiment is run 10 times, and the average time is used in the analysis. Table V-1 summarizes the effect of the initialization on the CPU time for the selected networks and for values $1, \ldots, 6$ for ϑ. For Net 1 and $\vartheta = 1$, the initialization heuristic provides a feasible solution to the MIP problem with a flow of two in 0.0020 seconds. This solution is used as the initial solution (i.e., a warm-start) to the MIP model. After 0.0130 seconds, the MIP model yielded an optimal objective value of 2. In this case, the initialization heuristic happened to find the optimal solution. Similar results for some other cases are marked with a "*" in column (ϑ) of Table V-1. For Net 1 and $\vartheta = 2$, the initialization provided a solution with a flow of zero in 0.0030 seconds. The flow of 0 means that the disrupted arcs have produced the maximum impact on the network that disrupting more arcs will not disturb the network flow. Hence, the initial solution is optimal, and the algorithm stops. Similar results were observed for Net 3 and $\vartheta = 6$, in which the initialization heuristic resulted in an objective value of 0. Thus, there is no need to proceed to solving the MIP model.

Table V-1: The effect of a warm-start strategy on the MIP model

ID (N, E)	ϑ	Objective Value		Solution Time (Seconds)	
		Initialization Heuristic	MIP with Warm-Start	Initialization Heuristic	MIP with Warm-Start
Net 1 (5, 7)	**1***	2	2	0.0020	0.013
	2	0	-	0.0030	0.000
Net 2 (14, 32)	**1***	17	17	0.0040	0.175
	2	12	10	0.0060	0.160
	3	9	5	0.0060	0.237
Net 3 (25, 89)	**1***	21	21	0.003	3.909
	2	16	14	0.007	3.815
	3	11	9	0.010	3.751
	4	4	4	0.011	4.540
	5*	2	2	0.018	4.779
	6	0	-	0.014	0.000
Net 4 (32, 166)	**1***	26	26	0.007	81.28
	2	22	18	0.011	85.59
	3	21	14	0.023	114.08
	4	13	10	0.026	115.02
	5	11	7	0.031	128.40
	6	11	5	0.030	206.31
Net 4 (38, 216)	1*	65	65	0.0424	165.42
	2	56	55	0.0749	175.92
	3	55	46	0.0514	191.43
	4	48	39	0.0938	190.27
	5	46	32	0.1408	198.28
	6	39	25	0.1338	193.35

Now we examine the computational performance of three solution approaches: a) MIP formulation without warm-start, where the initial solution is provided by the solver; b) MIP formulation with warm-start, in which the initial solution is provided by Algorithm 1; and c) PG. The computational time of finding a solution to the MADP for the test networks are summarized in Table V-2.

Table V-2: Computational performance comparison of three solution approaches

	ϑ	CPU time MIP	MIP with warm-start		PG		
			CPU time	Reduction in CPU time due to initialization	CPU time	Gap	Reduction in CPU time comparing to MIP
Net 1 (5,7)	1	0.025	0.015	40%	0.02	0%	20%
	2	0.018	0.003	83%	0.017	0%	6%
Net 2 (14, 32)	1	0.200	0.179	10%	0.129	0%	36%
	2	0.184	0.166	10%	0.143	0%	22%
	3	0.263	0.243	8%	0.117	0%	56%
Net 3 (25, 89)	1	4.19	3.91	7%	2.88	0%	31%
	2	4.96	3.82	23%	4.73	0%	5%
	3	4.00	3.76	6%	3.9	0%	3%
	4	5.62	4.55	19%	2.78	0%	51%
	5	5.20	4.80	8%	5.01	0%	4%
	6	3.84	0.01	99%	2.77	0%	28%
Net 4 (32, 166)	1	93.05	81.28	13%	68.95	0%	26%
	2	97.87	85.60	13%	89.58	0%	8%
	3	163.43	114.10	30%	139.16	0%	15%
	4	137.63	115.04	16%	132.12	0%	4%
	5	149.36	128.42	14%	130.92	0%	12%
	6	230.64	206.34	11%	111.82	0%	52%
Net 5 (38, 216)	1	217.64	165.46	24%	133.92	0%	38%
	2	232.75	176.00	24%	136.63	0%	41%
	3	258.37	191.48	26%	128.61	0%	50%
	4	260.94	190.37	27%	131.81	0%	49%
	5	269.33	198.42	26%	127.76	0%	53%
	6	375.60	193.48	48%	124.96	4%	67%

These results show that the MIP with the proposed initialization heuristic reduced the computational time by a range of 6% to 99% when compared to the MIP without the warm-start. Especially, the reduction in CPU time was over 24% for Net 5 with 216 arcs. The PG also improved the computational time over the MIP without the warm-start. Moreover, the outperformance of the PG was more pronounced for larger-sized problems

(e.g., Net 5). For example, for Net 5 and $\vartheta = 6$, the initialization reduced the CPU time of MIP by 48%, while PG reduces it by 67%.

5.5. Conclusion

In this study, we have developed solution approaches to reduce the computational time of the multi-arc disruption with maximum impact on network flow problem (MADP). Our approaches include a pattern generation (PG) process and a warm-start heuristic to solve the MADP. The subproblem of the PG is designed to find a new pattern for an arc failure that can result in the highest reduction of the maximum flow in the network. The PG performed very well and provided the optimal solution in 71% of the test networks attempted in this paper. A minimum-flow-betweenness centrality metric is introduced for the warm-start heuristic. The warm-start strategy reduced the number of iterations as well as the computational time. In several cases, the initial solution was found to be the optimal solution. The performance comparison on the CPU time for solving the MIP model with-and-without the warm-start heuristic revealed that the initialization approach significantly reduced the computational time by a range of 6% to 99%.

Our approach in this paper for the initialization heuristic and the pattern generation relies on the network paths. Finding network paths is computationally extensive; many researchers try to develop path generation algorithms that generate a portion of paths which solving the problem using those paths can provide an objective value close to the objective value of the original problem (i.e., the problem in which all the paths are included). Future work to consider includes developing an enhanced functional connectivity for the initialization heuristic. Functional connectivity is used to show the effect of one edge

disruption on the other edges and on the network paths. A good functional connectivity can result in a better initial solution for warm-start strategy.

CHAPTER 6

VI. LEVELIZED RESILIENCY ASSESSMENT OF INTERDEPENDENT NATURAL GAS AND ELECTRIC POWER SYSTEMS

6.1. Introduction

Critical infrastructures serve as the pillars of nations' economy and security. Electricity power system, communication system, natural gas delivery system, water and wastewater systems, and transportation system are examples of critical infrastructures. Unprecedented disasters like tornado, flood, hurricane, earthquake, and explosion are destructive to infrastructures, and they incur billions of dollars of economic loss. Moreover, the infrastructure's interdependence and cascading effects compound the gravity of the consequences of these disasters.

The concept of resilience has been developed to mitigate the effects of these extreme events. Resilience means to bounce back after a shock. Several metrics have been presented to measure the resilience of systems. These metrics can be utilized to evaluate the current state of infrastructure resilience, determine the components and processes to be improved, select and prioritize the investments on resilience, and to measure the effect of the investment and actions. However, few studies have addressed the resilience of interdependent infrastructures. Natural gas is one of the primary sources for electricity generation in the U.S., and the number of gas-fired generators has been increasing (

Figure VI.1). As a result, disruption of gas supply may cause unsatisfied electricity demand. In this study, we are to measure the effect of the resilience of natural gas system on the resilience of Electric power systems. In section 2 a literature review on the resilience

is presented. In section 3 the methodology to assess the effect of the resilience of gas infrastructure on the resilience of electric power system is discussed. Section 4 describes the mathematical model. Finally, the numerical results and conclusion are the provided in sections 5 and 6.

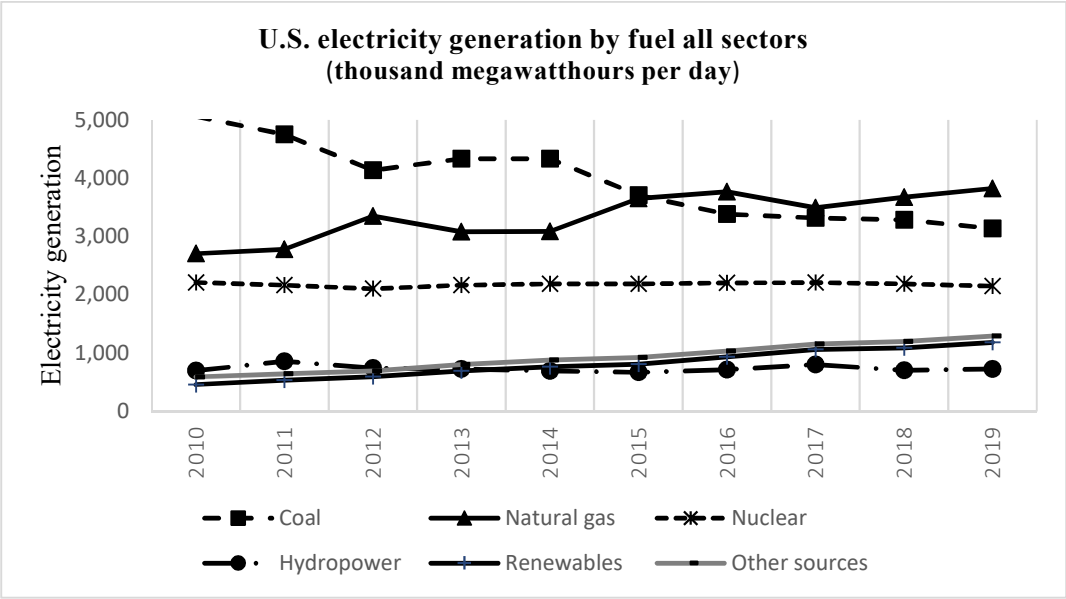

Figure VI.1: Annual share of total U.S. electricity generation by source (including forecasts for 2018 and 2019)

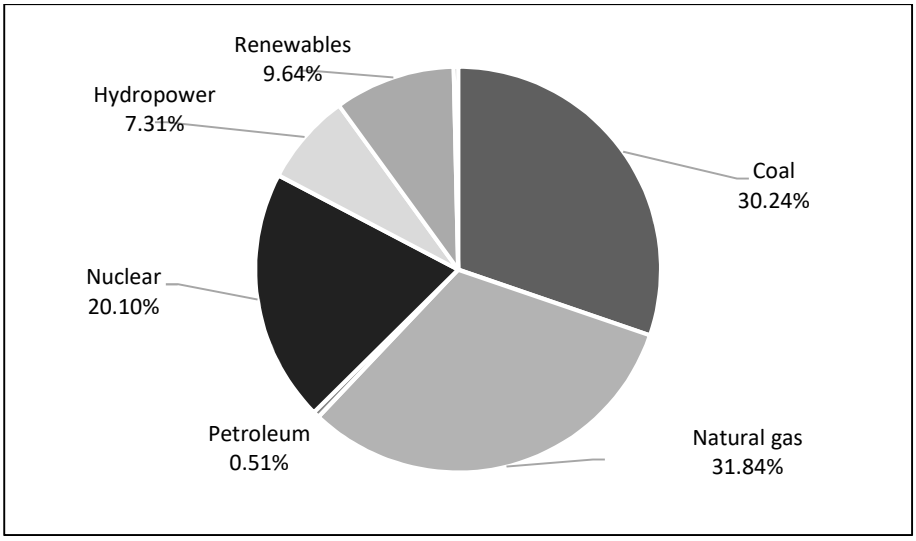

Figure VI.2: Share energy sources of total U.S. electricity generation in 2017

6.2. Literature Review

Resilience can be traced back to the work of Holling [11], who mentioned the features of a resilient ecological system. Five years later Gordon [12] referred to the "ability of woods to accommodate sudden and severe loads without breaking" as resilience. In fact, the concept of resilience emphasizes the unavoidability of extreme events. While it has been studied for decades, there isn't consensus on the definition of resilience and different disciplines developed their definition. The goals of resiliency are to reduce failure, the hazard consequences, and time to recovery [10]. Resilience has a multi-dimensional nature [30], [153]. Most of the researchers have focused on the conceptual framework. There are two approaches to a resilience framework: the strategic approach in which resources are being planned and utilized for an anticipated outcome; and the operational approach in which management considers outcomes satisfactory considering the available resources [154]. Conceptual frameworks emphasize that a resilient system be capable of anticipation, absorption, adaptation, and rapid recovery. Anticipate is the ability of a system to plan and prepare the system to face an extreme event. Resist/absorb is the ability to mitigate the seventy or consequences. Respond/adapt is the ability to employ the current resources and ongoing activities, tasks, and programs to manage the adverse effects of the unfavorable event. Rapid recovery is the ability to effectively and efficiently change the functionality to a level that is acceptable to the stakeholders.

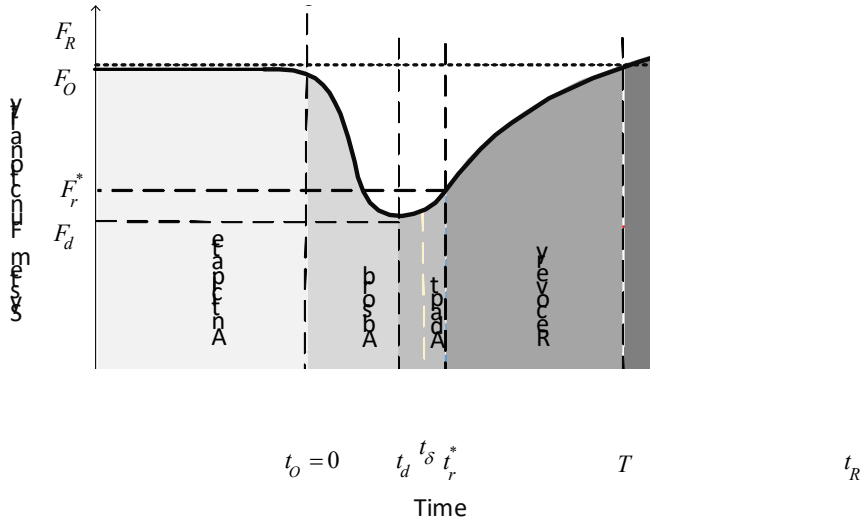

Figure VI.3: Functionality of a system during a resilience evaluation

These capacities can also be thought of as phases that a system may undergo in the face of hazard (Figure VI.3). In each of these phases, different improvements can be employed to enhance the resilience of the system. For example, in the planning phase design of the system and also forecasts are included [23] in the absorption phase robustness plays a crucial role in the resilience [93], in the adaptability phase resourcefulness can improve the resilience, and in the rapid recovery phase, agility is vital[89].

Quantification is an essential tool for resilience management. Molyneaux et al. [155] discuss the ways that disciplines try to measure resilience. A system may have different levels of resilience to different disruptions, and the resilience of a system is assessed against a specific disruption [156]. Resilience is a multi-dimensional measure. However, most of the developed metrics have just considered one or a few of the dimensions. The measures may be infrastructure specific (water, transportation, power, natural gas) or for a general system or network. The quantitative assessment of resilience dimensions is based on the measure of performance. Examples of such measures are demand not served, percent of

the nodes in the network that are inoperable, and time to full recovery. A resilience matrix can be used to assess the performance of complex systems [157] at global, technical, and organizational levels.

It is unrealistic to think of an isolated system. There are a few studies on the importance of interdependence, and several studies [158]–[161] have addressed the interdependence of natural gas and power system. In this study, we measure the effect of interdependence on the resilience of power systems. Due to complexity, it is not feasible to prepare a mathematical model that incorporates the dynamics of the system. Hence we utilized a levelized approach. Also, the gas supply during an adverse event is not deterministic. We used Monte Carlo simulation with several gas supply scenarios to incorporate this stochastic in our model. For each scenario, we obtained a measure of performance using the SCUC and the resilience.

6.3. Methodology

One of the widely used resilience metrics is the real functionality (F) over targeted functionality (TF)

$$я = \frac{\int_{t_e}^{t_r} F(t)\,dt}{\int_{t_e}^{t_r} TF(t)\,dt}. \tag{1}$$

We used this metric to generate scenarios for gas resilience at a given resilience level and finally to determine the natural gas supply to the gas-fired generation units. To calculate the performance of power grid we used the SCUC [103], [162], [163] and incorporated the dependency of the gas in the constraints [164]. It is supposed that extreme events will disrupt electricity generation until the recovery action brings the generators

back to generation. A full 2^3 factorial experiment was designed to test for any significant differences among three factors to the resilience of the power grid. The factors consist of generation capacity (GC), repair time (RT), and severity (SE), which indicated by percent inoperable of total generators. summarizes the treatments.

Table VI-1 Treatments of the factorial design

Factor	Level Low (-)	Level High (+)
Recovery Time (RT)	9	24
Generation Capacity (GC)	<30 MW	>500 MW
Severity (SE)	# of Gen. Out. <6 (~10%)	# of Gen. Out. >27 (~50%)

Table VI-2: Experiment design

	A	B	C
1	-	-	-
a	+	-	-
b	-	+	-
ab	+	+	-
c	-	-	+
ac	+	-	+
bc	-	+	+
abc	+	+	+

To examine the resiliency of the gas network, the resiliency of the gas system, we fixed the gas system resilience at six distinct levels, including 100%, 90%, 80%, 70%, 60%, and 0%. For the scenarios, we supposed the following assumptions: 1) the gas facility system has enough adequacies to provide the natural resiliency more than 60%. 2) The functionality of the system after recovery will be retained to the initial target functionality

(100%) of the system. The decision tree of the proposed model consisting the levelized gas resilience and electric power system is shown in the following figure.

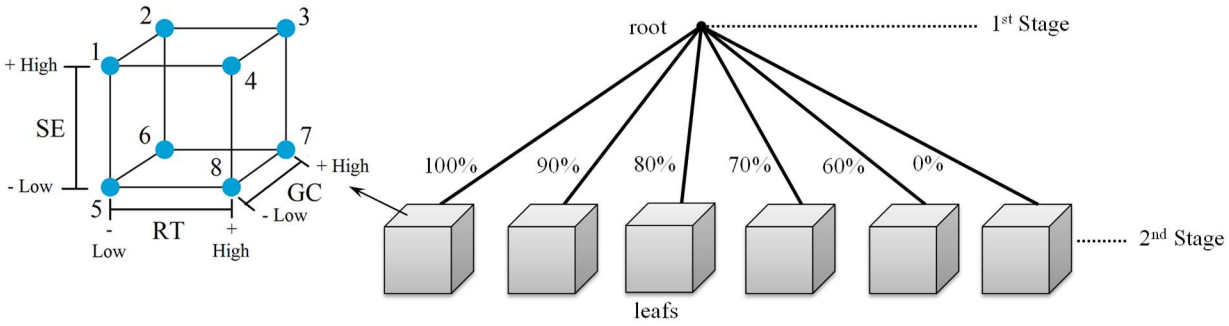

Figure VI.4 Decision tree of combine gas and power system infrastructure

6.4. Numerical Result

An integrated IEEE 118-bus system with the Belgian high-calorific gas network [22] is used to illustrate the effect of gas supply constraint into the hourly SCUC. All test data and network diagrams are available online on the provider's website [22]. The power network includes 54 thermal units, 186 branches, and 91 demand sides. The gas system has 21 pipelines, three compressors, 20 nodes, nine non-electrical loads, two wells and four storages. These networks are linked through 12 gas units: U1, U2, U5, U10 and U11 consume gas from node 16; U16, U19, and U29 consume gas from node 5; and U40, U47, U48, and U52 consume gas from node 10. The result of the simulation for each treatment is calculated separately. We assumed different resilience levels for natural gas five different supply scenarios for each of these levels were generated. For each gas scenario (100%, 90%, 70%, 60%, and 0%) and each treatment (Table VI-3). We ran the SCUC using CPLEX 12.6 and Java API. The loss of load was calculated for each of the 198 runs of SUSC and then 100,000 iterations for Monte Carlo simulation per gas resilience level

generated. The summary is presented in Table VI-3. Although the model was to generate the events and the generators' inoperability based on experiments, the result shows a range of 1% to 9% decrease as the effect of gas resilience on the resilience of the power system. One can compare it to 15% drop in the resilience if the gas is not supplied to any generator and there is not a contingency. A high correlation between the gas resilience and power resilience observed.

Table VI-3: The summary of the Monte Carlo simulation for each experiment treatment

		Electric Resilience							
		1	**a**	**ab**	**abc**	**ac**	**b**	**bc**	**c**
Natural Gas Resilience	**90%**	97%	96%	78%	44%	93%	93%	74%	96%
	80%	95%	94%	76%	43%	91%	91%	73%	94%
	70%	94%	93%	75%	43%	90%	90%	73%	93%
	60%	93%	92%	74%	42%	89%	89%	72%	92%
	0%	84%	83%	65%	36%	80%	81%	63%	83%
Correlation		**93%**	**92%**	**93%**	**97%**	**91%**	**93%**	**98%**	**92%**

6.5. Conclusion

In this study, we presented a formulation for SCUC which includes gas supply constraints. The model was run using CPLEX 12.6 and Java Eclipse. Four levels of gas resilience and five scenarios for each of these levels were developed. For each treatment of the experiment and each of the gas scenarios, we ran the SCUC and the loss of load obtained. The results show a high correlation between power system resilience and natural gas system resilience. In some cases, the low resilience of gas supply can reduce the resilience of power system to 9%.

CHAPTER 7

VII. CONCLUSIONS AND FUTURE WORK

In this dissertation, we focused on the resilience enhancement. As a first step, we provided a resilience metric. There have been several approaches reported in the literature to quantify resilience of a system. However, they were often designed for a specific system and there is a they may not be suitable for a given resilience conceptual framework. Therefore, we have developed a statistical assessment method for a resilient metric to be valid according to the concept of resilience. The design of experiments and ANOVA are utilized.

Then we introduced a quantitative method to enhance system resilience under the budgetary constraint. Different states of enhancements for component's absorption and recovery were elaborated and a metric was introduced to measure the resilience-based component importance. A mathematical programming formulation was developed to optimally allocate budget to components while maximizing the resilience within the limited budget. Due to the difficulty of drawing an analytical relationship between investment and system resilience, we have developed an algorithm consisting of two steps, in which the investment options and components' functionality were discretized; hence, it overcomes the computational difficulty. The proposed optimization model determines how much to invest to each selected component, and optimal levels of enhancement in the component's absorption and recovery time. The proposed approach was tested on the IEEE 6-bus and

the effects of different utility curves were discussed on the cost of enhancement and system's resilience level. Using the test case, we have demonstrated how optimally allocate budget to enhance the system resilience. Moreover, we have observed that the resilience of a system may be enhanced with a lower budget if the components follow a Cobb-Douglas utility function.

The impact of multi-arc failure on system output is considered from the prospect of attacker. The problem is a bilevel programming problem; to tackle the computational intensity, we developed an MIP problem that solves the original bilevel problem and reduce the solving time drastically. We also provided an initialization heuristic that can be used in the MIP problem to reduce the computational time. This heuristic is based on our new minimum-flow-betweenness centrality. The combination of initializing and MIP can solve the problems rather fast.

For future work the following extensions of the problems studied is suggested. Although the relationship between the change in the component absorption and recovery and the change in the system functionality was assumed to be linear in this paper, one can study further to find a system specific relationship between different enhancement scenarios and the change in the functionality of the system in the face of adverse events. This can help estimate the projected benefit of an investment on the system resilience. The behavior of more utility curve can be studied to find the one with better resilience traits. Finally, finding a path generation algorithm for the MADP that generates a portion of all the paths, but retains the important paths that are in the optimal solution can enhance our approach in this research. Moreover, finding functional connectivity will be utilized in the

initialization process. With good functional connectivity, Algorithm 1 can provide a very good solution in a short time

REFERENCES

[1] "The Cost of September 11," *IAGS*. [Online]. Available: http://www.iags.org/costof911.html. [Accessed: 21-Jul-2017].

[2] W. Safire, "Opinion | The Farewell Dossier," *The New York Times*, 02-Feb-2004.

[3] NOAA National Centers for Environmental Information (NCEI), "U.S. Billion-Dollar Weather and Climate Disasters," National Oceanic and Atmospheric Administration, 2018.

[4] "Fukushima Accident - World Nuclear Association." [Online]. Available: http://www.world-nuclear.org/information-library/safety-and-security/safety-of-plants/fukushima-accident.aspx. [Accessed: 06-Dec-2017].

[5] R. B. Corotis, "Robustness versus Resilience: Hurricanes and Other Natural Hazard Risks," 2012, pp. 900–911, doi: 10.1061/9780784412626.078.

[6] D. R. Kiran, "Chapter 27 - Reliability Engineering," in *Total Quality Management*, Butterworth-Heinemann, 2017, pp. 391–404.

[7] J. Tolk, S. Fritts, J. Cantu, and A. Gharehyakheh, "Deriving Quantitative Measures for High Reliability Organizations," in *International Annual Conference of the American Society for Engineering Management*, Huntsville, AL, 2017.

[8] E. Jen, "Stable or robust? What's the difference?," *Complexity*, vol. 8, no. 3, pp. 12–18, Jan. 2003, doi: 10.1002/cplx.10077.

[9] J. P. G. Sterbenz, D. Hutchison, E. K. Çetinkaya, A. Jabbar, J. P. Rohrer, M. Schöller, P. Smith, "Resilience and survivability in communication networks:

Strategies, principles, and survey of disciplines," *Computer Networks*, vol. 54, no. 8, pp. 1245–1265, Jun. 2010, doi: 10.1016/j.comnet.2010.03.005.

[10] M. Omer, A. Ali Mostashari, and R. Nilchiani, "Assessing resilience in a regional road-based transportation network," *International Journal of Industrial and Systems Engineering*, vol. 13, no. 4, 2013.

[11] C. S. Holling, "Resilience and Stability of Ecological Systems," *Annu. Rev. Ecol. Syst.*, vol. 4, no. 1, pp. 1–23, Nov. 1973, doi: 10.1146/annurev.es.04.110173.000245.

[12] J. E. Gordon, *Structures or Why Things Don't Fall Down*. UK: Penguin Books, 1978.

[13] L. H. Gunderson, C. Holling, and S. S. Light, "Barriers & Bridges to the Renewal of Ecosystems & Institutions," *Environments*, vol. 23, no. 3, p. 113, 1996.

[14] "resiliency - Dictionary Definition," *Vocabulary.com*. .

[15] M. Wallace and A. R. Berkeley III, "A Framework for Establishing Critical Infrastructure Resilience Goals," National Infrastructure Advisory Council, Oct. 2010.

[16] C. Folke, S. Carpenter, T. Elmqvist, L. Gunderson, C. S. Holling, and B. Walker, "Resilience and Sustainable Development: Building Adaptive Capacity in a World of Transformations," *AMBIO: A Journal of the Human Environment*, vol. 31, no. 5, pp. 437–440, Aug. 2002, doi: 10.1579/0044-7447-31.5.437.

[17] W. N. Adger, "Social and ecological resilience: are they related?," *Progress in Human Geography*, vol. 24, no. 3, pp. 347–364, Sep. 2000, doi: 10.1191/030913200701540465.

[18] N. Sahebjamnia, S. A. Torabi, and S. A. Mansouri, "Building organizational resilience in the face of multiple disruptions," *International Journal of Production Economics*, vol. 197, pp. 63–83, Mar. 2018, doi: 10.1016/j.ijpe.2017.12.009.

[19] R. J. Standish, R. J. Hobbs, M. M. Mayfield, B. T. Bestelmeyer, K. N. Suding, "Resilience in ecology: Abstraction, distraction, or where the action is?," *Biological Conservation*, vol. 177, pp. 43–51, Sep. 2014, doi: 10.1016/j.biocon.2014.06.008.

[20] S. Chanda and A. K. Srivastava, "Defining and Enabling Resiliency of Electric Distribution Systems with Multiple Microgrids," *IEEE Transactions on Smart Grid*, vol. PP, no. 99, pp. 1–1, 2016, doi: 10.1109/TSG.2016.2561303.

[21] S. Kaplan and B. J. Garrick, "On The Quantitative Definition of Risk," *Risk Analysis*, vol. 1, no. 1, pp. 11–27, 1981, doi: 10.1111/j.1539-6924.1981.tb01350.x.

[22] J. Wilder, "Operationalizing the Pressure and Release Theoretical Framework Using Risk Ratio Analysis to Measure Vulnerability and Predict Risk from Natural Hazards in the Tampa, FL Metropolitan Area," *Graduate Theses and Dissertations*, Mar. 2018.

[23] Saeedeh Abbasi, Masoud Barati, and Gino Lim, "A Multi-objective MPEC Model for Disaster Management of Power System Restoration," in *Proceedings of the 2017 Industrial and Systems Engineering Conference*, Pittsburgh, PA, 2017.

[24] S. Hosseini, K. Barker, and J. E. Ramirez-Marquez, "A review of definitions and measures of system resilience," *Reliability Engineering & System Safety*, vol. 145, pp. 47–61, Jan. 2016, doi: 10.1016/j.ress.2015.08.006.

[25] B. M. Ayyub, “Systems Resilience for Multihazard Environments: Definition, Metrics, and Valuation for Decision Making,” *Risk Analysis*, vol. 34, no. 2, pp. 340–355, Feb. 2014, doi: 10.1111/risa.12093.

[26] M. Ouyang and L. Dueñas-Osorio, “Time-dependent resilience assessment and improvement of urban infrastructure systems,” *Chaos: An Interdisciplinary Journal of Nonlinear Science*, vol. 22, no. 3, p. 033122, Sep. 2012, doi: 10.1063/1.4737204.

[27] G. P. Cimellaro, A. M. Reinhorn, and M. Bruneau, “Framework for analytical quantification of disaster resilience,” *Engineering Structures*, vol. 32, no. 11, pp. 3639–3649, Nov. 2010, doi: 10.1016/j.engstruct.2010.08.008.

[28] A. A. Ganin, E. Massaro, A. Gutfraind, N. Steen, J. M. Keisler, “Operational resilience: concepts, design and analysis,” *Scientific Reports*, vol. 6, p. 19540, Jan. 2016.

[29] J. P. Watson, R. Guttromson, C. Silva-Monroy, R. Jeffers, K. Jones, “Conceptual Framework for Developing Resilience Metrics for the Electricity, Oil, and Gas Sectors in the United States,” Sandia National Laboratories, SAND2014-18019, Sep. 2014.

[30] M. Ouyang and L. Dueñas-Osorio, “Multi-dimensional hurricane resilience assessment of electric power systems,” *Structural Safety*, vol. 48, pp. 15–24, May 2014, doi: 10.1016/j.strusafe.2014.01.001.

[31] Cimellaro G. P., Villa O., and Bruneau M., “Resilience-Based Design of Natural Gas Distribution Networks,” *Journal of Infrastructure Systems*, vol. 21, no. 1, p. 05014005, Mar. 2015, doi: 10.1061/(ASCE)IS.1943-555X.0000204.

[32] D. C. Montgomery, “Design and analysis of experiments,” 1991.

[33] G. Enderlein, “Finney, D. J.: An introduction to the theory of experimental design. The University of Chicago Press, Chicago 1960; 223 S., $ 7,—,” *Biometrische Zeitschrift*, vol. 4, no. 1, pp. 69–70, 1962, doi: 10.1002/bimj.19620040112.

[34] K. Barker, J. E. Ramirez-Marquez, and C. M. Rocco, “Resilience-based network component importance measures,” *Reliability Engineering & System Safety*, vol. 117, pp. 89–97, Sep. 2013, doi: 10.1016/j.ress.2013.03.012.

[35] “Hurricane Harvey Event Analysis Report,” North American Electric Reliability Corporation, Mar. 2018.

[36] C. N. June 1, 2018, and 7:38 Am, “As hurricane season begins, 11,000 customers in Puerto Rico still without power.” [Online]. Available: https://www.cbsnews.com/news/puerto-rico-hurricane-maria-despair-11000-still-without-power/. [Accessed: 31-Jul-2018].

[37] N. H. Center, “National Hurricane Center.” [Online]. Available: https://www.nhc.noaa.gov/. [Accessed: 31-Jul-2018].

[38] R. Francis and B. Bekera, “A metric and frameworks for resilience analysis of engineered and infrastructure systems,” *Reliability Engineering & System Safety*, vol. 121, pp. 90–103, Jan. 2014, doi: 10.1016/j.ress.2013.07.004.

[39] M. Kamalahmadi and M. M. Parast, “A review of the literature on the principles of enterprise and supply chain resilience: Major findings and directions for future research,” *International Journal of Production Economics*, vol. 171, Part 1, pp. 116–133, Jan. 2016, doi: 10.1016/j.ijpe.2015.10.023.

[40] Z. A. Collier, M. Panwar, A. A. Ganin, A. Kott, and I. Linkov, “Security Metrics in Industrial Control Systems,” in *Cyber-security of SCADA and Other Industrial Control Systems*, Springer, Cham, 2016, pp. 167–185.

[41] L. Carlson, G. Basset, W. Buehring, M. Collins, S. Folga, “Resilience Theory and Applications,” Argonne National Laboratory, Decision and Information Sciences Division, 2012.

[42] J. Phillips, M. Finster, J. Pillon, F. Petit, and J. Trail, “State Energy Resilience Framework,” Argonne National Laboratory, Global Security Sciences Division, 2016.

[43] A. Sharifi and Y. Yamagata, “Principles and criteria for assessing urban energy resilience: A literature review,” *Renewable and Sustainable Energy Reviews*, vol. 60, pp. 1654–1677, Jul. 2016, doi: 10.1016/j.rser.2016.03.028.

[44] The National Academy, *Disaster Resilience: A National Imperative*. Washington, DC: The National Academies Press, 2012.

[45] M. C. Hamilton, J. H. Lambert, E. B. Connelly, and K. Barker, “Resilience analytics with disruption of preferences and lifecycle cost analysis for energy microgrids,” *Reliability Engineering & System Safety*, vol. 150, pp. 11–21, Jun. 2016, doi: 10.1016/j.ress.2016.01.005.

[46] N. Ahmadian, G. J. Lim, J. Cho, and S. Bora, “A Quantitative Approach for Assessment and Improvement of Network Resilience,” *Reliability Engineering & System Safety*, p. 106977, Apr. 2020, doi: 10.1016/j.ress.2020.106977.

[47] A. Sharifi, “A critical review of selected tools for assessing community resilience,” *Ecological Indicators*, vol. 69, pp. 629–647, Oct. 2016, doi: 10.1016/j.ecolind.2016.05.023.

[48] M. Panteli and P. Mancarella, “The Grid: Stronger, Bigger, Smarter?: Presenting a Conceptual Framework of Power System Resilience,” *IEEE Power and Energy Magazine*, vol. 13, no. 3, pp. 58–66, May 2015, doi: 10.1109/MPE.2015.2397334.

[49] “Microsoft PowerPoint - QER Workshop June 10 2014 Posted - QER Workshop June 10 2014 Posted.pdf.” [Online]. Available: https://energy.gov/sites/prod/files/2015/01/f19/QER%20Workshop%20June%2010%202014%20Posted.pdf. [Accessed: 01-Jan-2017].

[50] A. Molavi, G. J. Lim, and B. Race, “A framework for building a smart port and smart port index,” *International Journal of Sustainable Transportation*, vol. 0, no. 0, pp. 1–13, May 2019, doi: 10.1080/15568318.2019.1610919.

[51] A. Kwasinski, “Quantitative Model and Metrics of Electrical Grids’ Resilience Evaluated at a Power Distribution Level,” *Energies*, vol. 9, no. 2, p. 93, Feb. 2016, doi: 10.3390/en9020093.

[52] United States. Federal Emergency Management Agency, “National Mitigation Investment Strategy,” Washington, DC: FEMA, Aug. 2019.

[53] A. Ghosh and K. Meagher, “The politics of infrastructure investment: The role of product market competition,” *Journal of Economic Behavior & Organization*, vol. 119, pp. 308–329, Nov. 2015, doi: 10.1016/j.jebo.2015.08.017.

[54] S. Ben Ammar and M. Eling, “Common risk factors of infrastructure investments,” *Energy Economics*, vol. 49, pp. 257–273, May 2015, doi: 10.1016/j.eneco.2015.01.021.

[55] A. Yazdani, R. A. Otoo, and P. Jeffrey, “Resilience enhancing expansion strategies for water distribution systems: A network theory approach,” *Environmental Modelling & Software*, vol. 26, no. 12, pp. 1574–1582, Dec. 2011, doi: 10.1016/j.envsoft.2011.07.016.

[56] S. Mukhopadhyay and M. Hastak, “Public Utility Commissions to Foster Resilience Investment in Power Grid Infrastructure,” *Procedia - Social and Behavioral Sciences*, vol. 218, pp. 5–12, May 2016, doi: 10.1016/j.sbspro.2016.04.005.

[57] D. E. Graeden, D. J. Kerr, and A. Aziz, “Linking Risk to Resilience: A Quantitative Method for Communities to Prioritize Resilience Investments,” p. 9.

[58] Y. Fang and G. Sansavini, “Optimizing power system investments and resilience against attacks,” *Reliability Engineering & System Safety*, vol. 159, pp. 161–173, Mar. 2017, doi: 10.1016/j.ress.2016.10.028.

[59] H. Baroud, K. Barker, J. E. Ramirez-Marquez, and C. M. Rocco S., “Importance measures for inland waterway network resilience,” *Transportation Research Part E: Logistics and Transportation Review*, vol. 62, pp. 55–67, Feb. 2014, doi: 10.1016/j.tre.2013.11.010.

[60] H. Baroud and K. Barker, “A Bayesian kernel approach to modeling resilience-based network component importance,” *Reliability Engineering & System Safety*, vol. 170, pp. 10–19, Feb. 2018, doi: 10.1016/j.ress.2017.09.022.

[61] J. F. Espiritu, D. W. Coit, and U. Prakash, “Component criticality importance measures for the power industry,” *Electric Power Systems Research*, vol. 77, no. 5, pp. 407–420, Apr. 2007, doi: 10.1016/j.epsr.2006.04.003.

[62] S. M. Rinaldi, J. P. Peerenboom, and T. K. Kelly, “Identifying, understanding, and analyzing critical infrastructure interdependencies,” *IEEE Control Systems*, vol. 21, no. 6, pp. 11–25, Dec. 2001, doi: 10.1109/37.969131.

[63] Rocco Claudio M., Barker Kash, Moronta Jose, and Ramirez-Marquez Jose E., “Multiobjective Formulation for Protection Allocation in Interdependent Infrastructure Networks Using an Attack-Diffusion Model,” *Journal of Infrastructure Systems*, vol. 24, no. 1, p. 04018002, Mar. 2018, doi: 10.1061/(ASCE)IS.1943-555X.0000415.

[64] E. E. Lee, J. E. Mitchell, and W. A. Wallace, “Assessing vulnerability of proposed designs for interdependent infrastructure systems,” in *37th Annual Hawaii International Conference on System Sciences, 2004. Proceedings of the*, 2004, pp. 8 pp.-, doi: 10.1109/HICSS.2004.1265182.

[65] M. Gil, P. Dueñas, and J. Reneses, “The interdependency of electricity and natural gaas markets: Coupling of models,” in *2013 10th International Conference on the European Energy Market (EEM)*, 2013, pp. 1–6, doi: 10.1109/EEM.2013.6607276.

[66] A. B. Smith and R. W. Katz, “US billion-dollar weather and climate disasters: data sources, trends, accuracy and biases,” *Natural Hazards*, vol. 67, no. 2, pp. 387–410, Jun. 2013, doi: 10.1007/s11069-013-0566-5.

[67] “Hurricane Katrina in the Gulf Coast Mitigation Assessment Team Report,” FEMA, FEMA 549, Jul. 2006.

[68] “Costliest U.S. tropical cyclones tables update,” National Hurricane Center, Jan. 2018.

[69] FEMA, “FEMA Fact Sheet: Mitigation Assessment Team Results – Hurricane Sandy,” 01-Nov-2017. [Online]. Available: https://www.fema.gov/MAT-results-hurricane-sandy. [Accessed: 11-Feb-2018].

[70] R. B. Corotis, .

[71] D. E. Alexander, “Resilience and disaster risk reduction: an etymological journey,” *Nat. Hazards Earth Syst. Sci.*, vol. 13, no. 11, pp. 2707–2716, Nov. 2013, doi: 10.5194/nhess-13-2707-2013.

[72] A. H. Kwok, E. E. H. Doyle, J. Becker, D. Johnston, and D. Paton, “What is ‘social resilience’? Perspectives of disaster researchers, emergency management practitioners, and policymakers in New Zealand,” *International Journal of Disaster Risk Reduction*, vol. 19, pp. 197–211, Oct. 2016, doi: 10.1016/j.ijdrr.2016.08.013.

[73] A. Z. Rose, “Defining and measuring economic resilience to disasters,” *Disaster Prev and Management*, vol. 13, no. 4, pp. 307–314, Sep. 2004, doi: 10.1108/09653560410556528.

[74] R. Brown, “Building children and young people’s resilience: Lessons from psychology,” *International Journal of Disaster Risk Reduction*, vol. 14, pp. 115–124, Dec. 2015, doi: 10.1016/j.ijdrr.2015.06.007.

[75] N. Yodo and P. Wang, “Engineering Resilience Quantification and System Design Implications: A Literature Survey,” *Journal of Mechanical Design*, vol. 138, no. 11, pp. 111408–111408, Sep. 2016, doi: 10.1115/1.4034223.

[76] H. R. Heinimann and K. Hatfield, “Infrastructure Resilience Assessment, Management and Governance – State and Perspectives,” in *Resilience and Risk*, Springer, Dordrecht, 2017, pp. 147–187.

[77] C. Ji and Y. Wei, “Dynamic resilience for power distribution and customers,” in *2015 IEEE International Conference on Smart Grid Communications (SmartGridComm)*, 2015, pp. 822–827, doi: 10.1109/SmartGridComm.2015.7436403.

[78] Y. Liu, Q. H. Wu, and X. X. Zhou, “Co-Ordinated Multiloop Switching Control of DFIG for Resilience Enhancement of Wind Power Penetrated Power Systems,” *IEEE Transactions on Sustainable Energy*, vol. PP, no. 99, pp. 1–11, 2016, doi: 10.1109/TSTE.2016.2524683.

[79] “Critical Infrastructure Resilience, Final Report and Recommendations,” National Infrastructure Advisory Council, Sep. 2009.

[80] A. Molavi, J. Shi, Y. Wu, and G. J. Lim, “Enabling smart ports through the integration of microgrids: A two-stage stochastic programming approach,” *Applied Energy*, vol. 258, p. 114022, Jan. 2020, doi: 10.1016/j.apenergy.2019.114022.

[81] E. Goodykoontz, A. Taylor, B. Jackson, E. Jones, S. Nashed, S. Reichow, A. Smith, “Measuring for Results: Application of Key Concepts to Resilience Measurement,” Homeland Security Studies and Analysis Institute, 2015.

[82] E. D. Vugrin, K. Stamber, M. Baca, G. Kao, H. Le, “A mission resilience assessment methodology for infrastructure disruptions,” in *Security Technology (ICCST), 2012 IEEE International Carnahan Conference on*, 2012, pp. 53–58, doi: 10.1109/CCST.2012.6393537.

[83] H. H. Willis and K. Loa, “Measuring the Resilience of Energy Distribution Systems,” *Santa Monica, CA: RAND Corporation*, 2015.

[84] “Resilience Metrics and Measurements: Technical Report,” ENISA, Feb. 2011.

[85] J. W. Wang, F. Gao, and W. H. Ip, “Measurement of resilience and its application to enterprise information systems,” *Enterprise Information Systems*, vol. 4, no. 2, pp. 215–223, May 2010, doi: 10.1080/17517571003754561.

[86] S. Abbasi, M. Barati, and G. J. Lim, “A Parallel Sectionalized Restoration Scheme for Resilient Smart Grid Systems,” *IEEE Transactions on Smart Grid*, vol. PP, no. 99, pp. 1–1, 2017, doi: 10.1109/TSG.2017.2775523.

[87] W. Zhang and N. Wang, “Resilience-based risk mitigation for road networks,” *Structural Safety*, vol. 62, pp. 57–65, Sep. 2016, doi: 10.1016/j.strusafe.2016.06.003.

[88] A. Khayatian, M. Barati, and G. J. Lim, “Market-based and resilient coordinated Microgrid planning under uncertainty,” in *2016 IEEE/PES Transmission and Distribution Conference and Exposition (T D)*, 2016, pp. 1–5, doi: 10.1109/TDC.2016.7520030.

[89] Saeedeh Abbasi, Masoud Barati, and Gino Lim, “A GPP-Based Sectionalization Toward a Fast Power Transmission System Restoration,” presented at the International Conference on Applied Human Factors and Ergonomics, Los Angeles, California, USA, 2017, pp. 11–21.

[90] J. C. Whitson and J. E. Ramirez-Marquez, “Resiliency as a component importance measure in network reliability,” *Reliability Engineering & System Safety*, vol. 94, no. 10, pp. 1685–1693, Oct. 2009, doi: 10.1016/j.ress.2009.05.001.

[91] L. Shen and L. Tang, “A resilience assessment framework for critical infrastructure systems,” in *2015 First International Conference on Reliability Systems Engineering (ICRSE)*, 2015, pp. 1–5, doi: 10.1109/ICRSE.2015.7366435.

[92] C. W. Zobel and L. Khansa, “Characterizing multi-event disaster resilience,” *Computers & Operations Research*, vol. 42, pp. 83–94, Feb. 2014, doi: 10.1016/j.cor.2011.09.024.

[93] M. Bruneau, S. E. Chang, T. Ronald, G. C. Lee, T. D. O’rourke, “A Framework to Quantitatively Assess and Enhance the Seismic Resilience of Communities,” *Communities,” Earthquake Spectra*, vol. 19, pp. 733–752, 2003.

[94] J. G. Jin, L. C. Tang, L. Sun, and D.-H. Lee, “Enhancing metro network resilience via localized integration with bus services,” *Transportation Research Part E: Logistics and Transportation Review*, vol. 63, pp. 17–30, Mar. 2014, doi: 10.1016/j.tre.2014.01.002.

[95] F. Kadri and S. Chaabane, “Resilience-Based Performance Assessment of Strain Situations in Emergency Departments,” presented at the 6th IESM Conference, Seville, Spain, 2015.

[96] C. S. Renschler, A. E. Frazier, L. A. Arendt, G. P. Cimellaro, A. M. Reinhorn, and M. Bruneau, “Developing the ‘PEOPLES’resilience framework for defining and measuring disaster resilience at the community scale,” in *Proceedings of the 9th US national and 10th Canadian conference on earthquake engineering (9USN/10CCEE), Toronto*, 2010, pp. 25–29.

[97] D. Henry and J. Emmanuel Ramirez-Marquez, “Generic metrics and quantitative approaches for system resilience as a function of time,” *Reliability Engineering & System Safety*, vol. 99, pp. 114–122, Mar. 2012, doi: 10.1016/j.ress.2011.09.002.

[98] E. Calixto, “Chapter 4 - Reliability, Availability, and Maintainability (RAM Analysis),” in *Gas and Oil Reliability Engineering (Second Edition)*, Boston: Gulf Professional Publishing, 2016, pp. 269–470.

[99] “Capacity planning,” *Wikipedia*. 15-Feb-2018.

[100] T. L. Brink, “R.L. Keeney, H. Raiffa: Decisions with multiple objectives–preferences and value tradeoffs, Cambridge University Press, Cambridge & New York, 1993, 569 pages, ISBN 0-521-44185-4 (hardback), 0-521-43883-7 (paperback),” *Behavioral Science*, vol. 39, no. 2, pp. 169–170, 1994, doi: 10.1002/bs.3830390206.

[101] www.itl.nist.gov, “5.1.1. What is experimental design?” [Online]. Available: http://www.itl.nist.gov/div898/handbook/pri/section1/pri11.htm. [Accessed: 31-Mar-2017].

[102] A. Khodaei and M. Shahidehpour, “Transmission Switching in Security-Constrained Unit Commitment,” *IEEE Transactions on Power Systems*, vol. 25, no. 4, pp. 1937–1945, Nov. 2010, doi: 10.1109/TPWRS.2010.2046344.

[103] D. Bertsimas, E. Litvinov, X. A. Sun, J. Zhao, and T. Zheng, “Adaptive Robust Optimization for the Security Constrained Unit Commitment Problem,” *IEEE Transactions on Power Systems*, vol. 28, no. 1, pp. 52–63, Feb. 2013, doi: 10.1109/TPWRS.2012.2205021.

[104] ee.washington.edu, “57-bus test data.” [Online]. Available: https://www2.ee.washington.edu/research/pstca/pf57/pg_tca57bus.htm. [Accessed: 20-Feb-2018].

[105] M. Matos, R. Bessa, A. Botterud, and Z. Zhou, “11 - Forecasting and setting power system operating reserves,” in *Renewable Energy Forecasting*, G. Kariniotakis, Ed. Woodhead Publishing, 2017, pp. 279–308.

[106] S. Ahmadian, B. Vahidi, J. Jahanipour, S. H. Hoseinian, and H. Rastegar, “Price restricted optimal bidding model using derated sensitivity factors by considering risk concept,” *Transmission Distribution IET Generation*, vol. 10, no. 2, pp. 310–324, 2016, doi: 10.1049/iet-gtd.2015.0014.

[107] P. O’Connor, *Practical Reliability Engineering*, 4th ed. Wiley, 2002.

[108] Podofillini, L., Sudret, B., Stojadinovic, B., Zio, E., and Kröger, W., *Safety and Reliability of Complex Engineered Systems*. London: CRC Press., 2015.

[109] Janusz Buchta, Andrzej Oziemski, and Maciej Pawlik, “Probabilistic Issue of Reliability for Power Machinery Operating in Coal Fired Power Plants,” *Journal of Power and Energy Engineering*, vol. 2, 2014, doi: http://dx.doi.org/10.4236/jpee.2014.24020.

[110] Lee C. Cadwallader, “Review of Maintenance and Repair Times for Components in Technological Facilities,” Idaho National Laboratory Experimental Programs, Idaho Falls, Idaho, 2012.

[111] S. O. Oyedepo, R. O. Fagbenle, and S. S. Adefila, “Assessment of performance indices of selected gas turbine power plants in Nigeria,” *Energy Sci Eng*, vol. 3, no. 3, pp. 239–256, May 2015, doi: 10.1002/ese3.61.

[112] P. n S. T. says, “Applied Statistics Lesson of the Day – Choosing the Number of Levels for Factors in Experimental Design,” *The Chemical Statistician*, 08-Jan-2014. [Online]. Available: https://chemicalstatistician.wordpress.com/2014/01/07/statistics-lesson-of-the-day-choosing-the-range-of-levels-for-quantitative-factors-in-experimental-design/. [Accessed: 27-Mar-2018].

[113] “IBM Knowledge Center - Java tutorial,” 2018. [Online]. Available: https://www.ibm.com/support/knowledgecenter/en/SSSA5P_12.6.3/ilog.odms.cplex.help/CPLEX/GettingStarted/topics/tutorials/Java/Java_synopsis.html. [Accessed: 29-Mar-2018].

[114] Jack Williams and Bob Sheets, *Hurricane Watch: Forecasting the Deadliest Storms on Earth*, 1st ed. Vintage, 2001.

[115] S. Polefka and G. T. April, “Building Resilience to Climate Change Requires Investment in Nature,” p. 7.

[116] E. Kim, “Economic Gain and Loss from Public Infrastructure Investment,” *Growth and Change*, vol. 29, no. 4, pp. 445–469, Jan. 2006, doi: 10.1111/j.1468-2257.1998.tb00029.x.

[117] K. LaCommare, P. Larsen, and J. Eto, “Evaluating Proposed Investments in Power System Reliability and Resilience: Preliminary Results from Interviews with Public Utility Commission Staff,” LBNL--1006971, 1342947, Jan. 2017.

[118] R. Studart and K. Gallagher, “Guaranteeing sustainable infrastructure,” *International Economics*, vol. 155, pp. 84–91, Oct. 2018, doi: 10.1016/j.inteco.2018.03.003.

[119] O. Cadot, L.-H. Röller, and A. Stephan, “Contribution to productivity or pork barrel? The two faces of infrastructure investment,” *Journal of Public Economics*, vol. 90, no. 6, pp. 1133–1153, Aug. 2006, doi: 10.1016/j.jpubeco.2005.08.006.

[120] E. M. Gramlich, “Infrastructure Investment: A Review Essay,” *Journal of Economic Literature*, vol. 32, no. 3, pp. 1176–1196, 1994.

[121] E. Boyd, “Community Development Block Grant Funds in Disaster Relief and Recovery,” p. 19.

[122] H. Hill, J. Wiener, and K. Warner, “From fatalism to resilience: reducing disaster impacts through systematic investments,” *Disasters*, vol. 36, no. 2, pp. 175–194, Apr. 2012, doi: 10.1111/j.1467-7717.2011.01256.x.

[123] Y. Zhang, R. Kang, R. Li, C. Yang, and Y. Yang, “Resilience-based component importance measures for complex networks,” in *2016 Prognostics and System Health Management Conference (PHM-Chengdu)*, 2016, pp. 1–6, doi: 10.1109/PHM.2016.7819761.

[124] X. Zhang, S. Mahadevan, S. Sankararaman, and K. Goebel, “Resilience-based network design under uncertainty,” *Reliability Engineering and System Safety*, vol. 169, pp. 364–379, 2018, doi: 10.1016/j.ress.2017.09.009.

[125] J. Aarhaug and F. Gundersen, “Infrastructure investments to promote sustainable regions,” *Transportation Research Procedia*, vol. 26, pp. 187–195, 2017, doi: 10.1016/j.trpro.2017.07.019.

[126] J. Caulkins, E. Hough, N. Mead, and H. Osman, “Using Integer Programming to Optimize Investments in Security Countermeasures: A Practical Tool for Fixed Budgets,” p. 9.

[127] Geanakoplos, John, *Arrow-Debreu model of general equilibrium*, 1st ed. Springer, 1954.

[128] E. Silberberg and Wing Suen, *The Structure of Economics: A Mathematical Analysis*, 3rd ed. McGraw-Hill/Irwin, 2000.

[129] K. J. Arrow, H. B. Chenery, B. S. Minhas, and R. M. Solow, "Capital-Labor Substitution and Economic Efficiency," *The Review of Economics and Statistics*, vol. 43, no. 3, pp. 225–250, 1961, doi: 10.2307/1927286.

[130] I. Linkov, C. Fox-Lent, L. Read, C. Allen, J. Arnott, "Tiered Approach to Resilience Assessment," *Risk Analysis*, vol. 38, Apr. 2018, doi: 10.1111/risa.12991.

[131] M. Najarian and G. J. Lim, "Design and Assessment Methodology for System Resilience Metrics," *Risk Analysis*, vol. 0, no. 0, Feb. 2019, doi: 10.1111/risa.13274.

[132] Joint Force Development, "Joint Interdiction," Federation of American Scientists, Washington, DC, Sep. 2016.

[133] R. K. Wood, "Deterministic network interdiction," *Mathematical and Computer Modelling*, vol. 17, no. 2, pp. 1–18, Jan. 1993, doi: 10.1016/0895-7177(93)90236-R.

[134] L. Bingol, "A Lagrangian Heuristic for solving a network interdiction problem," p. 57.

[135] J. O. Royset and R. K. Wood, "Solving the Bi-Objective Maximum-Flow Network-Interdiction Problem," *INFORMS Journal on Computing*, vol. 19, no. 2, pp. 175–184, May 2007, doi: 10.1287/ijoc.1060.0191.

[136] R. L. Church, M. P. Scaparra, and R. S. Middleton, "Identifying Critical Infrastructure: The Median and Covering Facility Interdiction Problems," *Annals of*

the Association of American Geographers, vol. 94, no. 3, pp. 491–502, Sep. 2004, doi: 10.1111/j.1467-8306.2004.00410.x.

[137] K. Malik, A. K. Mittal, and S. K. Gupta, "The k Most Vital Arcs in the Shortest Path Problem," *Operations Research Letters*, vol. 8, no. 4, p. 5, 1989.

[138] A. H. Dekker and B. D. Colbert, "Network Robustness and Graph Topology," in *ACSC*, 2004.

[139] L. C. Freeman, S. P. Borgatti, and D. R. White, "Centrality in valued graphs: A measure of betweenness based on network flow," *Social Networks*, vol. 13, no. 2, pp. 141–154, Jun. 1991, doi: 10.1016/0378-8733(91)90017-N.

[140] M. E. J. Newman, "A measure of betweenness centrality based on random walks," *Social Networks*, vol. 27, no. 1, pp. 39–54, Jan. 2005, doi: 10.1016/j.socnet.2004.11.009.

[141] S. P. Borgatti and M. G. Everett, "A Graph-theoretic perspective on centrality," *Social Networks*, vol. 28, no. 4, pp. 466–484, Oct. 2006, doi: 10.1016/j.socnet.2005.11.005.

[142] M. J. Park, O. M. Kwon, and J. H. Ryu, "A Katz-centrality-based protocol design for leader-following formation of discrete-time multi-agent systems with communication delays," *Journal of the Franklin Institute*, vol. 355, no. 13, pp. 6111–6131, Sep. 2018, doi: 10.1016/j.jfranklin.2018.06.022.

[143] Y. P. Aneja, R. Chandrasekaran, and K. P. K. Nair, "Maximizing residual flow under an arc destruction," *Networks*, vol. 38, no. 4, pp. 194–198, Dec. 2001, doi: 10.1002/net.10001.

[144] S. H. Lubore, H. D. Ratliff, and G. T. Sicilia, “Determining the most vital link in a flow network,” *Naval Research Logistics Quarterly*, vol. 18, no. 4, pp. 497–502, 1971, doi: 10.1002/nav.3800180408.

[145] R. K. Wood, “Bilevel Network Interdiction Models: Formulations and Solutions,” in *Wiley Encyclopedia of Operations Research and Management Science*, American Cancer Society, 2011.

[146] D. Mount, “CMSC 451: Lecture 14 Network Flows: Basic Definitions,” p. 4, 2017.

[147] M. Rungta, G. Lim, and M. Baharnemati, “Optimal egress time calculation and path generation for large evacuation networks,” *Annals of Operations Research*, vol. 201, no. 1, pp. 403–421, 2012.

[148] J.-P. W. Kappmeier, “Generalizations of Flows over Time with Applications in Evacuation Optimization,” 2015, doi: 10.14279/depositonce-4358.

[149] B. P. Rogers, V. L. Morgan, A. T. Newton, and J. C. Gore, “Assessing Functional Connectivity in the Human Brain by FMRI,” *Magn Reson Imaging*, vol. 25, no. 10, pp. 1347–1357, Dec. 2007, doi: 10.1016/j.mri.2007.03.007.

[150] M. E. Lübbecke and J. Desrosiers, “Selected Topics in Column Generation,” *Operations Research*, vol. 53, no. 6, pp. 1007–1023, Dec. 2005, doi: 10.1287/opre.1050.0234.

[151] G. B. Dantzig and P. Wolfe, “Decomposition Principle for Linear Programs,” *Operations Research*, vol. 8, no. 1, pp. 101–111, Feb. 1960, doi: 10.1287/opre.8.1.101.

[152] Mokhtar S. Bazaraa, John J. Jarvis, Hanif D. Sherali, *Linear Programming and Network Flows*, 4th ed. Wiley, 2011.

[153] S. L. Cutter, K. D. Ash, and C. T. Emrich, "The geographies of community disaster resilience," *Global Environmental Change*, vol. 29, pp. 65–77, Nov. 2014, doi: 10.1016/j.gloenvcha.2014.08.005.

[154] D. Ahmad and C. K. Chanda, "A framework for resilience performance analysis of an electrical grid," in *2016 2nd International Conference on Control, Instrumentation, Energy Communication (CIEC)*, 2016, pp. 392–396, doi: 10.1109/CIEC.2016.7513735.

[155] L. Molyneaux, C. Brown, L. Wagner, and J. Foster, "Measuring resilience in energy systems: Insights from a range of disciplines," *Renewable and Sustainable Energy Reviews*, vol. 59, pp. 1068–1079, Jun. 2016, doi: 10.1016/j.rser.2016.01.063.

[156] E. D. Vugrin, D. E. Warren, and M. A. Ehlen, "A resilience assessment framework for infrastructure and economic systems: Quantitative and qualitative resilience analysis of petrochemical supply chains to a hurricane," *Process Safety Progress*, vol. 30, no. 3, pp. 280–290, 2011, doi: 10.1002/prs.10437.

[157] I. Linkov, T. Bridges, F. Creutzig, J. Decker, C. Fox-Lent, "Changing the resilience paradigm," *Nature Climate Change*, vol. 4, no. 6, pp. 407–409, Jun. 2014, doi: 10.1038/nclimate2227.

[158] A. Alabdulwahab, A. Abusorrah, X. Zhang, and M. Shahidehpour, "Coordination of Interdependent Natural Gas and Electricity Infrastructures for Firming the Variability of Wind Energy in Stochastic Day-Ahead Scheduling," *IEEE*

Transactions on Sustainable Energy, vol. 6, no. 2, pp. 606–615, Apr. 2015, doi: 10.1109/TSTE.2015.2399855.

[159] D. Peng, R. Poudineh, and Oxford Institute for Energy Studies, *A holistic framework for the study of interdependence between electricity and gas sectors*. 2015.

[160] "Gas-Power Interdependence: Knock-on Effects of the Dash to Gas." [Online]. Available: http://www.scottmadden.com/wp-content/uploads/userFiles/misc/800c2313571d34853cc26c3200ab9ec7.pdf. [Accessed: 04-Jan-2017].

[161] "The Interdependence of Electricity and Natural Gas: Current Factors and Future Prospects." [Online]. Available: http://www.sciencedirect.com/science/article/pii/S1040619012000899. [Accessed: 04-Jan-2017].

[162] Y. Fu, M. Shahidehpour, and Z. Li, "Security-Constrained Unit Commitment With AC Constraints*," *IEEE Transactions on Power Systems*, vol. 20, no. 3, pp. 1538–1550, Aug. 2005, doi: 10.1109/TPWRS.2005.854375.

[163] C. M. Correa-Posada and P. Sánchez-Martín, "Security-constrained unit commitment with dynamic gas constraints," in *2015 IEEE Power Energy Society General Meeting*, 2015, pp. 1–5, doi: 10.1109/PESGM.2015.7285943.

[164] M. Qadrdan, J. Wu, N. Jenkins, and J. Ekanayake, "Operating Strategies for a GB Integrated Gas and Electricity Network Considering the Uncertainty in Wind Power Forecasts," *IEEE Transactions on Sustainable Energy*, vol. 5, no. 1, pp. 128–138, Jan. 2014, doi: 10.1109/TSTE.2013.2274818.

APPENDIX I : SECURITY CONSTRAINED UNIT COMMITMENT

The objective of the SCUC problem is to find a unit commitment schedule that minimizes the commitment and dispatch costs while meeting the forecasted system load. It takes into account various physical or intertemporal constraints of generating resources, transmission, and system reliability requirements [103]. The following notations will be used in the mathematical model:

- **Sets/indices**: GG stands for the number of gas generation units, NG the number of units, NT the number of periods, and NB the number of buses. Index b is for the buses, index i for units, l for lines, and t for the time.
- **Parameters**: The parameters in the mathematical formulation consist of, H for gas heating value (39 MJ/MBTU), $P_{D,t}$ for system demand at time t, $P_{L,t}$ for system losses at time t, $P_{\min}$ / $P_{\max}$ for the Lower / upper limit of the real power generation of the unit, $PL^{t}_{l,max}/PL^{t}_{l,min}$ for the maximum/minimum capacity of the line l, $R_{O,t}$ / $R_{S,t}$ for the system operating / spinning reserve requirement at time t, T_i^{off} / T_i^{on} for minimum down and up time of the unit i, UR_i/ DR_i for the maximum Ramp up/down, and finally η_i for the efficiency of the generator. Parameter Z_{it} and G_{it} are the control variables in our simulations that are designed specifically for each scenario.
- **Decision variables**. I_{it} is the commitment state of the unit i at time t , P_{it} is the generation of unit i at time t, PL_l^t is the real power flow on line l, $R_{O,it}$ and $R_{S,it}$ are the operating and spinning reserve of the unit i at time t respectively. X_{it}^{off} and X_{it}^{on} are the OFF and ON time of the unit i at time t, θ_{bi} is the phase angle, and Q_{it} the quantity of gas consumed by the (gas fired) generator i at time t.

Equation (7) is the objective function, which is the cost of generation and load shedding cost with a value of lost load (VOLL) $1000/MWh. The objective function is comprised of the fuel cost for producing electric power, the startup cost, and the shutdown cost. Originally the fuel cost is a quadratic and convex function, and we used a piecewise linear function to estimate it. Equation (8) is the generation limit. Constraint (9) indicates the capacity boundaries of each unit. The C problem must meet the required system spinning and operating reserves (10) which are defined by the independent system operator (ISO). The ramp up (11) and ramp down (12) constraints, minimum uptime and minimum down time (13) constraints have to satisfy in operation of the power system. Constraint (14) shows the static network security constraints, including power flow and transmission line flow. The constraint (15) reflects the dependency of power generation dispatch and natural gas supply as an input of a power plant. We extract load shedding from the last equation (16).

$$min \sum_{i=1}^{NG} \sum_{t=1}^{NT} [F_{ci}(P_{it}) + SU_{it} + SD_{it}] + \sum_{i=1}^{NB} \sum_{t=1}^{NT} Voll \times LS_{it}$$

s.t.

$$P_{min}\, I_{it} \leq P_{it} \leq P_{max} \quad I_{it}, \forall i, t \tag{1}$$

$$\sum_{i=1}^{NG} p_{it} = P_{D,t}, \forall t \tag{2}$$

$$\sum_{i=1}^{NG} R_{S,it} \times I_{it} \geq R_{S,t}\,, \forall s, t$$

$$\sum_{i=1}^{NG} R_{O,it} \times I_{it} \geq R_{O,t}\,, \forall s, t \tag{3}$$

$$P_{it} - P_{i(t-1)} \leq [1 - I_{it}\big(1 - I_{i(t-1)}\big)UR_i + I_{it}\big(1 - I_{i(t-1)}\big)P_{i,min}] \tag{4}$$

$$P_{i(t-1)} - P_{it} \leq [1 - I_{it}(1 - I_{i(t-1)})DR_i + I_{it}(1 - I_{i(t-1)})P_{i,min}] \quad (5)$$

$$[X^{on}_{i(t-1)} - T^{on}_i][I_{i(t-1)} - I_{it}] \geq 0, \forall \mathrm{i}, \mathrm{t}$$

$$[X^{off}_{i(t-1)} - T^{off}_i][I_{it} - I_{i(t-1)}] \geq 0, \forall i, t \quad (6)$$

$$-PL_{lt,\max} \leq PL_{lt} \leq PL_{lt,\max}, \forall \mathrm{i}, \mathrm{t}$$

$$PL_{lt} = \frac{\theta_{bi} - \theta_{bj}}{x_{bi,bj}} \quad (7)$$

$$p_{it} = \eta_i Q_{it} H, \forall \mathrm{i} \in \mathrm{GG}, \mathrm{t}$$

$$Q_{it} \leq QG_{it}, \forall \mathrm{i} \in \mathrm{GG}, \mathrm{t} \quad (8)$$

$$\sum_{l=1}^{NL} PL_{lt} = P_{bt} - PD_{bt} + LS_{bt}. \forall b, t \quad (9)$$

APPENDIX II: 57-BUS SYSTEM DATA

Table II.1: Demand data for the first 24 hours

Hour	demand	ssr	sor	Hour	demand	ssr	sor
1.	131.97	0	0	13.	183.43	0	0
2.	136.12	0	0	14.	188.41	0	0
3.	128.65	0	0	15.	189.24	0	0
4.	123.67	0	0	16.	193.39	0	0
5.	120.35	0	0	17.	199.2	0	0
6.	120.35	0	0	18.	199.2	0	0
7.	125.33	0	0	19.	191.73	0	0
8.	135.29	0	0	20.	191.73	0	0
9.	138.61	0	0	21.	185.09	0	0
10.	145.25	0	0	22.	185.09	0	0
11.	161.02	0	0	23.	180.94	0	0
12.	177.62	0	0	24.	152.72	0	0

Table II.2: Percent of total load at each bus

bus	percent load	bus	percent load	bus	percent load
1	0	20	65.82	39	87
2	24.42	21	18.05	40	17
3	37	22	25.48	41	17
4	0	23	45.65	42	18
5	21.23	24	62.63	43	23
6	24.42	25	24.42	44	113
7	24.42	26	62.63	45	63
8	49.89	27	35.03	46	84
9	36.09	28	32.91	47	12
10	14.86	29	27	48	12
11	95.54	30	20	49	277
12	26.54	31	37	50	78
13	11.68	32	37	51	77
14	63.69	33	18	52	39
15	47.77	34	16	53	28
16	19.11	35	53	54	66
17	14.86	36	28	55	68
18	10.62	37	34	56	47
19	7.43	38	20	57	68

Table II.3: Line data

start	**End**	**Max Flow**	**x**	**Start**	**End**	**Max Flow**	**x**
23	24	100	0.0492	30	31	500	0.127
25	27	500	0.163	31	32	100	0.4115
31	32	100	0.0985	32	33	100	0.0355
23	24	100	0.0492	34	32	100	0.196
1	3	100	0.0424	34	35	100	0.18
25	27	500	0.163	35	36	100	0.0454
25	27	500	0.163	36	37	100	0.1323
8	9	100	0.0605	37	38	100	0.141
9	10	100	0.0487	37	39	500	0.122
9	11	100	0.289	36	40	100	0.0406
9	12	100	0.291	22	38	100	0.148
9	13	100	0.0707	11	41	100	0.101
13	14	100	0.00955	41	42	100	0.1999
13	15	100	0.0151	41	43	100	0.0124
1	15	100	0.0966	38	44	100	0.0244
1	16	100	0.134	15	45	500	0.0485

start	End	Max Flow	x	Start	End	Max Flow	x
1	17	100	0.0966	14	46	500	0.105
3	15	100	0.0719	46	47	100	0.0704
4	18	100	0.2293	47	48	500	0.0202
4	18	100	0.251	48	49	500	0.037
5	6	100	0.239	49	50	100	0.0853
7	8	100	0.2158	50	51	100	0.03665
10	12	100	0.145	10	51	100	0.132
11	13	100	0.15	13	49	100	0.148
12	13	500	0.0135	29	52	100	0.0641
12	16	100	0.0561	52	53	500	0.123
12	17	100	0.0376	53	54	500	0.2074
14	15	500	0.0386	54	55	100	0.102
18	19	500	0.02	11	43	100	0.173
19	20	500	0.0268	44	45	500	0.0712
21	20	500	0.0986	40	56	500	0.188
21	22	500	0.0302	56	41	500	0.0997
22	23	500	0.0919	56	42	100	0.0836
23	24	500	0.0919	39	57	500	0.0505
24	25	100	0.218	57	56	500	0.1581
24	25	100	0.117	38	49	100	0.1272
24	26	500	0.037	38	48	100	0.0848
26	27	100	0.1015	9	55	100	0.158
27	28	500	0.016	28	29	100	0.2778
7	29	100	0.324	25	30	500	0.037

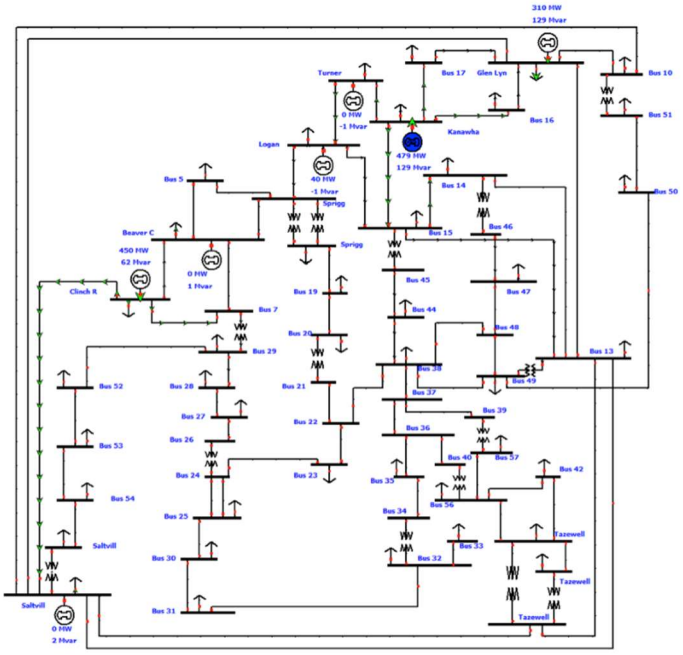

Figure II.1: Graph of 57-bus, source: http://icseg.iti.illinois.edu

Table II.4: unit data

bus	pmin	pmax	cnl	sdc	suc	mu	md	ru	rd	msr	qsc	laststt	mn	lastp	mf	pseg	cseg1	cseg2
1	30	80	74	0	0	4	4	40	40	3	0	1	4	30	96	40	17	52
2	5	20	18	0	0	1	1	10	10	1	0	1	1	5	96	10	38	114
3	20	50	59	0	0	1	1	50	50	1	0	1	1	20	96	25	23	70
6	30	80	74	0	0	4	4	40	40	3	0	1	4	30	96	40	17	52
8	5	30	32	0	0	1	1	30	30	1	0	1	1	5	96	15	27	82
9	5	20	18	0	0	1	1	10	10	1	0	1	1	5	96	10	38	114
12	5	20	18	0	0	1	1	10	10	1	0	1	1	5	96	10	38	114

APPENDIX III: α SCENARIOS

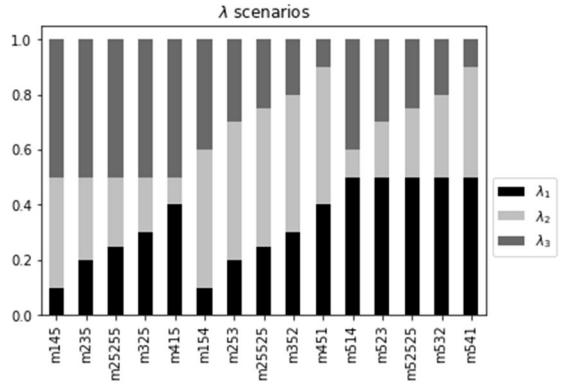

Figure III.1: Different λ combinations

APPENDIX IV: INTERACTION PLOTS

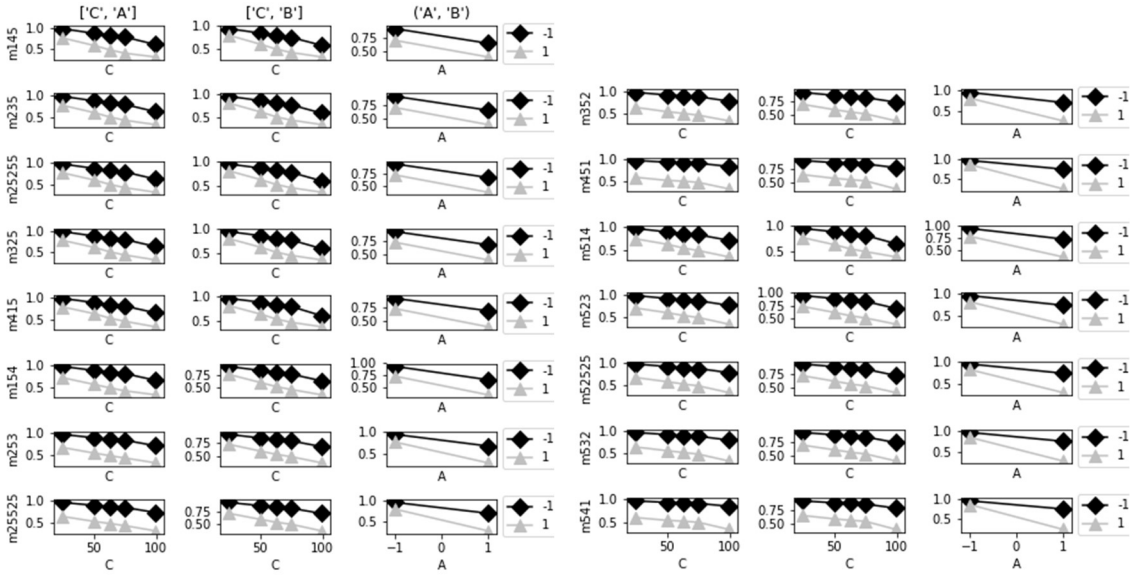

Figure IV.1: Interaction plots

APPENDIX V: CALCULATIONS OF $Я_1$ AND $Я_2$ BEFORE INVESTMENT

a) Calculations for $Я_1$

$$Я_1 = \int_0^{t_d} \frac{F(t)}{TF(t)}dt = \sum_{t=0}^{t_d-1} \frac{F(t)+F(t+1)}{2} = \frac{1}{2t_d}\sum_{t=0}^{t_d-1}\left(\frac{1}{N}\sum_{i=1}^{N} RCI_i\, f_{i,t} + \frac{1}{N}\sum_{1}^{N} RCI_i\, f_{i,t+1}\right)$$

$$\frac{1}{2Nt_d}\sum_{t=0}^{t_d-1}\left(\sum_{i=1}^{N} RCI_i\left(\left(1-\frac{A_i}{t_d}t\right)+\left(1-\frac{A_i}{t_d}(t+1)\right)\right)\right)$$

$$= \frac{1}{2Nt_d}\sum_{i=1}^{N}\left(RCI_i\sum_{t=0}^{t_d-1}\left(2-\frac{2A_i}{t_d}t-\frac{A_i}{t_d}\right)\right) = \frac{1}{Nt_d}\sum_{i=1}^{N} RCI_i(-\frac{1}{2}A_i t_d + t_d)$$

$$= \frac{1}{N}\sum_{i=1}^{N} RCI_i(-\frac{1}{2}A_i + 1)$$

b) Calculations for $Я_2$

$$Я_2 = \int_{t_d}^{T} \frac{F(t)}{TF(t)}dt = \frac{1}{T-t_d}\sum_{t=t_d}^{T-1}\frac{F(t)+F(t+1)}{2}$$

$$= \frac{1}{2(T-t_d)}\sum_{t=t_d}^{T-1}\left(\frac{1}{N}\sum_{i=1}^{N} RCI_i\, f_{i,t} + \frac{1}{N}\sum_{i=1}^{N} RCI_i\, f_{i,t+1}\right)$$

$$= \frac{1}{2N(T-t_d)}\sum_{i=1}^{N} RCI_i\left(\sum_{t=t_d}^{T-1} f_{i,t} + \sum_{t=t_d+1}^{T} f_{i,t+1}\right)$$

We calculate $\sum_{t=t_d}^{T-1} f_{i,t} + \sum_{t=t_d+1}^{T} f_{i,t+1}$ separately and plug it into the above formula.

$$\sum_{t=t_d}^{T-1} f_{i,t} = \sum_{t=t_d}^{T_i-1} \left(1 - \frac{-A_i}{T_i - t_d}(T_i - t)\right) + \sum_{t=T_i}^{T-1} 1$$

$$= \sum_{t=t_d}^{T_i-1} \frac{-A_i}{T_i - t_d} T_i + \sum_{t=t_d}^{T_i-1} \frac{A_i}{T_i - t_d} t + \sum_{t=t_d}^{T-1} 1$$

$$= -A_i T_i + \frac{A_i}{2}(t_d + T_i - 1) + (T - t_d),$$

and

$$\sum_{t=t_d+1}^{T} f_{i,t+1} = \sum_{t=t_d+1}^{T_i} \left(1 - \frac{A_i}{T_i - t_d}(T_i - t)\right) + \sum_{t=T_i+1}^{T} 1$$

$$= \sum_{t=t_d+1}^{T_i} \frac{-A_i}{T_i - t_d} T_i + \sum_{t=t_d+1}^{T_i} \frac{A_i}{T_i - t_d} t + \sum_{t=t_d+1}^{T} 1$$

$$= -A_i T_i + \frac{A_i}{2}(t_d + T_i + 1) + (T - t_d).$$

Hence

$$\sum_{t=t_d}^{T-1} f_{i,t} + \sum_{t=t_d+1}^{T} f_{i,t+1}$$

$$= -A_i T_i + \frac{A_i}{2}(t_d + T_i - 1) + (T - t_d) - A_i T_i + \frac{A_i}{2}(t_d + T_i + 1) + (T - t_d)$$

$$= -2A_i T_i + \frac{A_i}{2}(2t_d + 2T_i) + 2(T - t_d) = -A_i(T_i - t_d) + 2(T - t_d)$$

Replacing the $\sum_{t=t_d}^{T-1} f_{i,t} + \sum_{t=t_d+1}^{T} f_{i,t+1}$ in the $я_2$ yields

$$я_2 = \frac{1}{2N(T - t_d)} \sum_{i=1}^{N} RCI_i\big(-A_i(T_i - t_d) + 2(T - t_d)\big) = \frac{1}{N} \sum_{i=1}^{N} RCI_i \left(\frac{-A_i}{2} \frac{(T_i - t_d)}{(T - t_d)} + 1\right).$$

APPENDIX VI: CALCULATING Я AFTER INVESTMENT

The parameters $\alpha_1, \alpha_2, RCI_i, A_i, T_i, \gamma_{i,2}$, and t_d are inputs to the model and they are known prior to the optimization. Let $b_{i1} = \frac{\alpha_1 RCI_i A_i}{2}$, $b'_{i1} = -b_{i1} + \alpha_1 RCI_i t_d$, $b_{i2} = \frac{\alpha_2 RCI_i A_i}{2}$, and $b'_{i2} = b_{i2} T_i$, then $я_1$ and $я_2$ can be calculated as follows:

$$я_1 = \frac{1}{N}\sum_{i=1}^{N} RCI_i \left(-\frac{1}{2}A_i(1-a_i)+1\right) = \frac{1}{N}\sum_{1}^{N}(b_{i1}a_i + b'_{i1})$$

$$я_2 = \frac{1}{N}\sum_{i=1}^{N} RCI_i \left(\frac{-A_i(1-a_i)}{2}\frac{[T_i\,(1-r_i)-t_d]}{(T-t_d)}+1\right)$$

$$= \frac{1}{N}\sum_{i=1}^{N}\frac{-\alpha_2 RCI_i A_i}{2}\frac{[T_i\,(1-r_i)-t_d]}{(T-t_d)}$$

$$+\frac{1}{N}\sum_{i=1}^{N}\frac{\alpha_2 RCI_i A_i}{2}\frac{a_i[T_i\,(1-r_i)-t_d]}{(T-t_d)} + \alpha_2 RCI_i$$

$$= \frac{1}{N}\sum_{i=1}^{N}\left(\frac{[b'_{i2}\,r_i - b'_{i2} + b_{i2}t_d] + [\,b'_{i2}\,a_i - b'_{i2}\,r_i a_i + b_{i2}t_d a_i]}{T-t_d}\right) + \alpha_2 RCI_i$$

$$= \frac{1}{N}\sum_{i=1}^{N}\left(\frac{b'_{i2}\,r_i + (b'_{i2} + b_{i2}t_d)a_i - b'_{i2}\,r_i a_i + (b_{i2}t_d - b'_{i2})}{T-t_d}\right) + \alpha_2 RCI_i$$

$$я = \alpha_1 я_1 + \alpha_2 я_2 + \alpha_3\frac{T_0}{T} = \frac{1}{N}\sum_{i=1}^{N}\left(\frac{\xi_{i1}\,a_i + \xi_{i2}\,a_i r_i + \xi_{i3}\,r_i + \xi_{i4}T + \xi_{i5}a_i T + \xi_{i6}}{T-t_d}\right) + \frac{T_0}{T}$$

where $\xi_{i1} = b_{i1}t_d + b'_{i2} + b_{i2}t_d$, $\xi_{i2} = -b'_{i2}$, $\xi_{i3} = b'_{i2}$, $\xi_{i4} = b'_{i1}$, $\xi_{i5} = b_{i1}$ and $\xi_{i6} = b'_{i1}t_d + b_{i2}t_d - b'_{i2}$.

APPENDIX VII: IEEE BUS-6 DATA

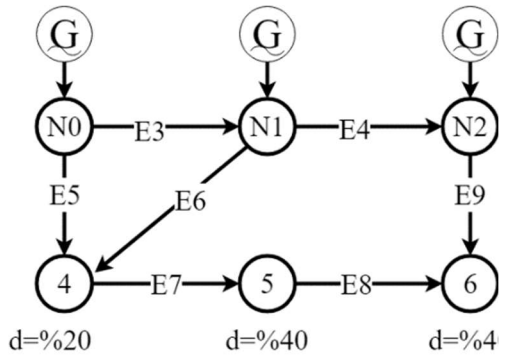

Figure VII.1: Bus-6 network diagram

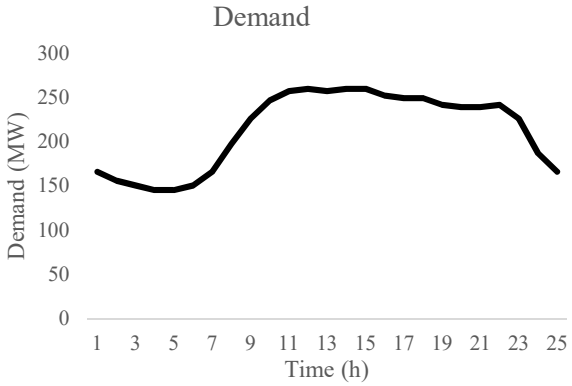

Figure VII.2: Bus-6 hourly total demand

Table VII.1: Bus-6 data for generation units

Name	bus	pmin	pmax	cnl	sdc	suc	mu	md	ru	rd	msr	qsc	laststat	mn	lastp	mf	psegmax1	psegmax2	cseg1	cseg2	genmttr	investment
N0	1	100	220	10.15	50	100	4	4	55	55	1	0	1	5	25	25	50	50	18.46	55.4	30	60
N1	2	10	100	39	100	200	3	2	50	50	1	0	1	11	50	25	100	100	13.73	41.2	68	30
N2	3	10	40	31.67	0	0	1	1	20	20	1	0	1	1	10	25	15	15	27.2888	81.9	68	27

Table VII.2:Bus-6 data for transmission lines.

Names	begin	end	phase	capacity	linemttr	investment
E3	1	2	0.17	200	12	10
E4	2	3	0.037	100	8	7
E5	1	4	0.258	100	8	7
E6	2	4	0.197	100	8	7
E7	4	5	0.037	100	8	7
E8	5	6	0.14	100	8	7
E9	3	6	0.018	100	8	7

APPENDIX VIII: COST FACTORS

Table VIII.1: Cost factors

	re	0	0.25				0.5				0.75				1			
	ab	**0**	**0.25**	**0.5**	**0.75**	**1**	**0.25**	**0.5**	**0.75**	**1**	**0.25**	**0.5**	**0.75**	**1**	**0.25**	**0.5**	**0.75**	**1**
Linear	**(0.75,0.25)**	0	0.25	0.31	0.38	0.44	0.44	0.5	0.56	0.62	0.62	0.69	0.75	0.81	0.81	0.88	0.94	1
	(0.6,0.4)	0	0.25	0.35	0.45	0.55	0.4	0.5	0.6	0.7	0.55	0.65	0.75	0.85	0.7	0.8	0.9	1
	(0.5,0.5)	0	0.25	0.38	0.5	0.62	0.38	0.5	0.62	0.75	0.5	0.62	0.75	0.88	0.62	0.75	0.88	1
	(0.4,0.6)	0	0.25	0.39	0.54	0.68	0.36	0.5	0.64	0.79	0.46	0.61	0.75	0.89	0.57	0.71	0.86	1
	(0.25,0.75)	0	0.25	0.41	0.56	0.72	0.34	0.5	0.66	0.81	0.44	0.59	0.75	0.91	0.53	0.69	0.84	1
CD	**0.1**	0	0.25	0.27	0.28	0.29	0.47	0.5	0.52	0.54	0.67	0.72	0.75	0.77	0.87	0.93	0.97	1
	0.3	0	0.25	0.31	0.35	0.38	0.41	0.5	0.56	0.62	0.54	0.66	0.75	0.82	0.66	0.81	0.92	1
	0.5	0	0.25	0.35	0.43	0.5	0.35	0.5	0.61	0.71	0.43	0.61	0.75	0.87	0.5	0.71	0.87	1
	0.9	0	0.25	0.47	0.67	0.87	0.27	0.5	0.72	0.93	0.28	0.52	0.75	0.97	0.29	0.54	0.77	1
CES	**(0.1, 0.1)**	0	0.25	0.27	0.28	0.29	0.47	0.5	0.52	0.54	0.68	0.72	0.75	0.77	0.88	0.94	0.97	1
	(0.3, 0.5)	0	0.25	0.36	0.45	0.54	0.36	0.5	0.62	0.72	0.45	0.62	0.75	0.87	0.54	0.72	0.87	1
	(0.5, 0.4)	0	0.25	0.34	0.42	0.49	0.39	0.5	0.59	0.68	0.52	0.64	0.75	0.85	0.64	0.78	0.9	1
	(0.9, 1)	0	0.25	0.5	0.75	1	0.25	0.5	0.75	1	0.25	0.5	0.75	1	0.25	0.5	0.75	1